

1999

Development of simulation models for HVAC systems using an icon-based method

Christopher T. Groszcyk
University of Iowa

Copyright © 1999 Christopher T. Groszcyk Posted with permission of the author.

This thesis is available at Iowa Research Online: <https://ir.uiowa.edu/etd/4556>

Recommended Citation

Groszcyk, Christopher T.. "Development of simulation models for HVAC systems using an icon-based method." MS (Master of Science) thesis, University of Iowa, 1999.
<https://doi.org/10.17077/etd.s4ve2c93>

Follow this and additional works at: <https://ir.uiowa.edu/etd>

Part of the [Mechanical Engineering Commons](#)

**DEVELOPMENT OF SIMULATION MODELS FOR HVAC
SYSTEMS USING AN ICON-BASED METHOD**

by

Christopher T. Groszcyk

A thesis submitted in partial fulfillment
of the requirements for the Master of
Science degree in Mechanical Engineering
in the Graduate College of
The University of Iowa

May 1999

Thesis supervisor: Professor Theodore F. Smith

Graduate College
The University of Iowa
Iowa City, Iowa

CERTIFICATE OF APPROVAL

MASTER'S THESIS

This is to certify that the Master's thesis of

Christopher T. Groszcyk

has been approved by the Examining Committee
for the thesis requirement for the Master of Science
degree in Mechanical Engineering at the May 1999 graduation.

Thesis committee: _____
Thesis supervisor

Member

Member

ACKNOWLEDGMENTS

I would like to acknowledge the following in aiding support throughout this study. Data and model parameters are obtained with the assistance of my colleague Mr. B. Andy Price through the Iowa Energy Center under grant 96-10. I would like to recognize the Department of Mechanical Engineering at The University of Iowa for allowing me to do my graduate work at this institution and providing financial support throughout my time here. I would also like to thank other colleagues, Mr. Adam J. Cannon of The University of Iowa and Larry Tietze of Boeing for technical support help in using the Easy5 software and implementation.

A special thanks goes to my advisor, Professor T. F. Smith, for his guidance and patience, his dedication and attention to detail has taught me a great deal through both undergraduate and graduate school. Finally, I would like to give special thanks to my close family and friends for their undying love and support.

“I can do all things through Christ who strengthens me.” Philippians 4:13

ABSTRACT

This study creates a model of a heating, ventilating, and air-conditioning system comprising of an air handling unit and four zones in an icon-based software package, couples the multi-zone thermal model with an indoor air quality model, introduces a control method to operate the entire system, and examines the behavior of the system for a range of operating conditions. An icon-based software tool is attractive because of the practicality of the graphical user interface that allows easily insertion and deletion of modules representing components of the system. Connection lines between the icons describe the exchange of information components. The software solves the system of equations that represents the thermal and indoor-air-quality models. Proportional-integral and feedforward controllers are used to maintain setpoints in the air handling unit and zones. Results from the cases examined in this study show that it is possible to create thermal and indoor-air-quality models using an icon-based software package. By proper selection of the gain coefficients, the control schemes provide a stable operation of the system. The feedforward controller dampens disturbances and allows the setpoints to be reached faster.

TABLE OF CONTENTS

	Page
LIST OF TABLES	vi
LIST OF FIGURES.....	vii
LIST OF SYMBOLS.....	ix
CHAPTER 1 INTRODUCTION	1
1.1 Motivation	1
1.2 Literature review.....	5
1.2.1 HVAC simulation models	5
1.2.2 Simulators.....	7
1.2.3 IAQ.....	8
1.3 Objective	9
1.4 Outline.....	10
CHAPTER 2 DESCRIPTION OF MULTI-ZONE SYSTEM.....	11
2.1 Introduction	11
2.2 Thermal Model	16
2.3 IAQ Model.....	18
2.4 Controllers.....	21
2.4.1 Introduction.....	21
2.4.2 Feedback control.....	21
2.4.3 Feedforward control.....	22
2.4.4 Feedback and feedforward control.....	24
2.4.5 Performance merits	24
2.5 Summary	26
CHAPTER 3 ICON-BASED SOFTWARE IMPLEMENTATION.....	27
3.1 Introduction	27
3.2 Basic operations.....	27
3.3 Model implementation	28

3.3.1 AHU representation	29
3.3.2 Zone representation.....	40
3.4 Numerical solution considerations.....	44
3.5 Summary	47
CHAPTER 4 RESULTS AND DISCUSSION.....	48
4.1 Introduction	48
4.2 Zone control.....	53
4.3 AHU control	55
4.3.1 Heating and cooling coil.....	55
4.3.2 Sensitivity to gain coefficients.....	61
4.4 System control	65
4.4.1 Heating mode.....	65
4.4.2 Cooling mode.....	75
4.5 Feedforward control.....	77
4.6 IAQ considerations	82
4.7 Summary	89
CHAPTER 5 CONCLUSIONS AND RECOMMENDATIONS.....	90
5.1 Conclusions	90
5.2 Future work	91
APPENDIX MASS TO CONCENTRATION CONVERSION.....	93
REFERENCES	96

LIST OF TABLES

	Page
Table 4.1 Numerical values of model parameters for AHU.....	49
Table 4.2 Numerical values of model parameters for Zones.....	50
Table 4.3 Numerical values of general model parameters.....	51
Table 4.4 Simulation cases.....	51
Table 4.5 Scheduled zone loads.....	71
Table 4.6 Cost function comparison.....	77
Table 4.7 Scheduled zone CO ₂ generation rates.....	85

LIST OF FIGURES

	Page
Figure 2.1 HVAC system model.....	13
Figure 2.2 Model of AHU in system.....	14
Figure 2.3 Model of a Zone.....	15
Figure 3.1 Easy5 representation of model.....	30
Figure 3.2 Easy5 representation of AHU.....	30
Figure 3.3 Icon representation of FM 1.....	32
Figure 3.4 Temperature mixer 1.....	32
Figure 3.5 Concentration mixer 1.....	33
Figure 3.6 Icon representation of HC.....	33
Figure 3.7 Easy5 schematic of HC conductance.....	34
Figure 3.8 Easy5 schematic of HC capacitance.....	34
Figure 3.9 Easy5 representation of the SF.....	35
Figure 3.10 Easy5 schematic of the FS 1.....	35
Figure 3.11 Easy5 schematic of FM 2.....	37
Figure 3.12 Easy5 schematic of combined temperature submodel.....	37
Figure 3.13 Easy5 representation of combined concentration submodel.....	38
Figure 3.14 Main control submodel.....	38
Figure 3.15 Feedforward submodel.....	39
Figure 3.16 Supply air merit calculation.....	41
Figure 3.17 Heating, cooling, and pollutant merit equations.....	41
Figure 3.18 Zone representation.....	42

Figure 3.19 Detailed zone representation.	42
Figure 3.20 Zone envelope representation.....	43
Figure 3.21 Zone pollutant concentration representation.	45
Figure 3.22 Zone merit representation.	45
Figure 3.23 Outdoor air parameters.	46
Figure 4.1 Case 1 setpoint temperature change within a zone.....	54
Figure 4.2 Case 2 zone load change.....	56
Figure 4.3 Case 3 AHU heating setpoint change.	58
Figure 4.4 Case 4 AHU heating ambient air change.....	59
Figure 4.5 Case 5 AHU cooling setpoint change.....	60
Figure 4.6 Case 6 AHU cooling ambient air change.....	62
Figure 4.7 Case 7 AHU coefficient sensitivity.	64
Figure 4.8 Case 8.0 System in all heating mode.....	66
Figure 4.9 Case 8.1 System in all heating mode improved controller.	68
Figure 4.10 Random number distribution.....	70
Figure 4.11 Case 8.2 simulated system.	72
Figure 4.12 Case 8.3 simulated system.	74
Figure 4.13 Case 9.0 system in all cooling mode.	76
Figure 4.14 Cases 10.0 and 10.1 without and with FF control.	79
Figure 4.15 Cases 11.0 and 11.1 without and with FF control using instability.	81
Figure 4.16 Case 12.0 effect of CO ₂ generation in Zone 1.	84
Figure 4.17 Case 12.1 CO ₂ distribution throughout zones.	86
Figure 4.18 Case 12.2 effect of increased outdoor air flow rate.....	88

LIST OF SYMBOLS

Symbol

A	area, ft ²
C	concentration, ppm
c	specific heat, Btu/lb _m -°F
e(t)	error
G	volumetric generation rate, ft ³ /h per million
h	heat transfer coefficient, Btu/h-ft ² -°F
J _c	comfort cost, °F ² -h
J _{clg}	energy cost, Btu ² /h
J _{htg}	energy cost, Btu ² /h
J _p	pollutant comfort, ppm-h
J _{sa}	supply air comfort cost, °F ² -h
K _p	proportional gain coefficient, 1/°F
K _i	integral gain coefficient, 1/°F-h
K ₁	proportional gain coefficient
K ₂	proportional gain coefficient
M	molecular mass, lb _m /lbmol
m	effectiveness
m _p	pollutant mass, lb _m
\dot{m}	mass flow rate, lb _m /h
P	pressure, lb _f /in ²

Q	volumetric flow rate, ft^3/h
q_c	cooling energy rate, Btu/h
q_h	heating energy rate, Btu/h
q_{rh}	reheating energy rate, Btu/h
q_x	total internal load, Btu/h
R_i	gas constant, $\text{ft}\cdot\text{lb}_f/\text{lbmol}\cdot\text{R}$
R_u	universal gas constant, $\text{ft}\cdot\text{lb}_f/\text{lbmol}\cdot\text{R}$
S_o	solar radiation, $\text{Btu}/\text{hr}\cdot\text{ft}^2$
T	temperature, $^\circ\text{F}$
T_i	integral time constant, h
t	time, h
V	volume, ft^3
$u(t)$	control signal
ρ	density, lb_m/ft^3
μ	mean, $^\circ\text{F}$
σ	standard deviation, $^\circ\text{F}$
τ	time, h
ω	phase, rad/h

Subscripts

a	air
amb	ambient
c	cooling
f	final time
fb	feedback
ff	feedforward

gen	generation
h	heating
max	maximum
i	incoming, inside, counter
i,0	initial value
o	outdoor, outgoing
oa	outdoor air
p	pollutant
sa	supply air
set	set point
sf	supply fan
ra	return air
rc	recirculated air
rf	return fan
w	wall
z	zone

Acronyms

AHU	Air handling unit
BCS	Boeing computer service
CAV	Constant-air-volume
CC	Cooling coil
CFD	Computational fluid dynamics
CO ₂	Carbon dioxide
EEM	Energy efficient measures
ERS	Energy Resource Station

FB	Feedback
FM	Flow Mixer
FF	Feedforward
FS	Flow Splitter
GUI	Graphical user interface
HC	Heating coil
HEX	Heat exchanger
HVAC	Heating, ventilating, and air-conditioning
IAQ	Indoor air quality
NIST	National Institute of Standards and Technology
OA	Outdoor air
PI	Proportional-integral
ppm	parts per million
PSD	Proportional summed derivative
RC	Recirculated air
RF	Return fan
RH	Reheat coil
SA	Supply air
SF	Supply fan
SPARK	Simulation Problem Analysis and Research Kernel
W	Wall
Z	Zone

CHAPTER 1

INTRODUCTION

1.1 Motivation

Energy-efficient measures (EEMs) to control the ever demanding processes of heating and cooling of buildings in the United States must be investigated to adapt them to current systems and future structures. With the number of buildings on the rise, and the demand for electricity during peak times approaching the maximum amount of electricity available, EEMs must be incorporated into the control systems that thermally condition air for a building. Along with thermal consideration, another critical factor regarding buildings is the fact that indoor air quality (IAQ) is sometimes degraded at peak times of the day. Hence, attention must be given to ventilating the building by exhausting stale indoor air and bringing in outdoor air. Heating, ventilating, and air conditioning (HVAC) systems must provide quality air at the right quantity to the thermal zones of the building. A Zone (Z) is a physical space of a building that is serviced by a single thermostat. HVAC systems are operated to control the zone to a specific temperature, called the setpoint temperature. Limitations exist on the maximum efficiency that can be achieved from modifying the equipment in the building and the amount of insulation that can be added to the structure. It was reported that buildings consume over 33 percent of all energy used annually in the United States and even more worldwide (Kelly, 1992). With this statistic in mind, the need to develop EEMs to control building HVAC systems is apparent.

To develop EEMs, two procedures could be undertaken. In one procedure, an idea for an EEM undergoes a series of tests to evaluate its effectiveness. For the second

procedure, theoretical simulation models of the building and HVAC systems are developed and EEMs are implemented in the models. In this day and age of computers and computer simulations, software tools are available to take advantage of the speed and cost effectiveness of the computers. However, questions arise about how good of a model can be developed and how complex of a model is required? Computer simulations use physically-based mathematical equations to model the systems and components, in this case the structure and air handling unit (AHU) of a building. These models then need to be verified and compared with a “real world” situation. This is done through comparisons with experimental data. Once model and the data are compared, a determination is made on how far the simulation model deviates from the experimental data. The developer then must return to the simulation model and modify it to achieve a closer agreement. However, once the simulation model proves to be a close enough representation of the experimental data, the model can be used to simulate a wide variety of changes in the system much easier and faster than an experiment of a real situation. This gives the developer a large advantage in evaluating the potential of EEMs much more quickly instead of doing solely experiments. Simulation models of HVAC systems, therefore, play an important role in developing and evaluating EEMs.

Computer simulators have grown over the years as the computational capabilities have increased. The ability to simulate more complex systems and to solve more equations at once is making this type of development more attractive and cost-effective to engineers. A wide variety of computer-based simulators are available, from the methods based on programming in a computer language, to mathematical equation solvers, and to icon driven software with a user friendly interface. Traditional methods of programming in languages, such as C or FORTRAN, can be laborious, but this is generally how HVAC models are initially developed. This is not to say that these methods are not successful,

as they have proven successful in the past and maybe needed to some degree for the other methods. Equation solvers such as MATLAB, Maple (Maple, 1998), and Mathematica (Mathematica, 1991) exist to simply solve a system of equations written by the user. These types of solvers still require models that describe the performance characteristics of HVAC systems, such as chillers, heat exchangers, fans, and building envelopes. Once the models are available for several building and HVAC components, it becomes necessary to assemble these models into a building HVAC system. This assembly has proven to be rather tedious in the past. The development of icon-based graphical packages has aided in development of models for systems. Library “add-ons” such as MATLAB’s SIMULINK (SIMULINK, 1992) provides graphical representation of the equations to be solved. SIMULINK simulates dynamics systems by using block diagrams to assemble components with necessary interconnections. Another icon-based software package that presents a convenient method of implementing simulation models is Easy5 (Easy5, 1996). SIMULINK and Easy5 are similar in functionality by connecting icons together with connection lines. Both also visually represent the physical model as an icon model. SIMULINK and Easy5 have a graphical user interface (GUI) to provide easy interaction between the program and user. This study develops a computer generated model for a multi-zone HVAC system using an icon-based software package. The icon-driven software package chosen for this study is Easy5 (Easy5, 1996), which is an analysis package that contains built in library icons to perform a variety of functions. These functions perform a number of different tasks, including addition and subtraction, integration and differentiation, simulating a single HEX in one icon, and various controllers. The complexity of the icon does not change how each icon is operated and used. Each icon is installed on the workspace and the icons are interconnected by drawing lines from one icon to another. Although there are many

advanced and complex icons in the software package, this study focuses on using elemental mathematical functions. These mathematical functions are in fact the basis for the more advanced icons. All of the components used in this study are available in the general library that is standard to the software package.

Two important areas in HVAC development are the thermal requirements for the system and a control methodology to govern the entire system. While the physical model of the thermal system is relatively consistent in its makeup, new control algorithms are being developed to better control these systems. An HVAC system is usually controlled using proportional integral (PI) feedback loops. Some recent advances have extended this control technology to use such methods as feedforward (Salsbury, 1998); (Ahemed et al., 1998a, 1998b, 1998c) and fuzzy logic (So et. al, 1994) to make systems “smarter” and efficient in their control schemes.

While programming and control methods are important subject matters in HVAC systems, research has lead to taking a closer look at the quality of air that flows through the system. The subject of IAQ is becoming an important factor as HVAC systems become more efficient and recycle air to reduce as much as possible the heating or cooling demands. A standard for the quality of air that a person breathes has been established (ASHRAE, 1991). However, many systems do not monitor the levels of pollutants in a system and only monitor temperature for comfort levels. While temperature levels are important to maintain comfort, the presence of airborne pollutants may in fact affect comfort level more than temperature. Hence, this investigation combines both thermal and IAQ factors into a single simulation model.

1.2 Literature review

A literature review of HVAC simulations consists of investigating the types of simulations in existence and current modeling methods that are being used and includes the types of HVAC models, types of simulators, and topics related to IAQ. In view of the number of studies and interest areas in HVAC, this literature review is not meant to be exhaustive but is focused on those topics relevant to this study.

1.2.1 HVAC simulation models

In the formulation process of developing simulation models related to HVAC systems and components, developers must be aware of the fact there may be many components to HVAC systems (Bundschuh and Smith, 1997). Along with this fact, the developers must be aware of the increasing computational requirement to simulate these types of systems for optimal control as the models become increasingly more complex. Several different approaches can be taken to derive the models. These approaches include (1) using a fundamental formulation based on computing detailed solutions of the three-dimensional, transient conservation equations for mass, momentum, and energy transfer within each component, (2) solving the first-order differential equations where the dependency of a variable in one spatial direction or on time is retained, (3) specifying the value of a single parameter related to the effectiveness or thermal efficiency of a component, and (4) developing curve fits of the manufacturer data for a particular component. Each of these approaches has a trade off in accuracy, the amount of information required to describe the thermal performance of a component, the capability of the model to accommodate changing conditions, and the amount of computational power required to calculate the result. In view of the complexity of buildings and HVAC systems, most simulation models are based on approaches (2) or (3).

HVAC simulation software has been in existence since the 1970's. Earlier attempts at a component-based simulation that allowed user definable connections between the components suffered from numerical instabilities and computing power requirements that were either time or cost prohibitive (Metcalf, 1994). Additionally, the steps required to set up, define a system, and to run simulations for the system have often been lengthy and awkward. These problems or stalling points have been remedied with advances in computational power and simulation techniques that warranted another look at generalized system simulations.

The development of HVAC simulation software started in the form of input from punch cards and evolved into menu driven software. The menu driven software works as the user inputs data for each question asked by the software. A program called TRACE (TRACE, 1990) is a menu driven interface that simulates building cooling and heating loads and computes the economic analysis of the designed system. Similar to TRACE, DOE-Plus (1992) is another menu drive simulation software package. User data are inserted into the given fields of a system and the model generates energy and economic analyses of the configured system. A menu driven interface such as TRACE and DOE-Plus provides a simpler interaction with the user, but visually does not allow the designer to see the system in a graphical visually-orientated environment. Because both DOE-Plus and TRACE are menu driven, but text based, they lack the visual representation in the interface to represent the system. The Building Loads Analysis and System Thermodynamics (BLAST) is a set of programs for predicting energy consumption and energy system performance (Building, 1998). Like DOE-Plus and TRACE, BLAST uses a menu driven interface. However, BLAST gives a visual representation of the system that is to be simulated. The preprogrammed component parameters, such as windows and walls, are then entered and the system is simulated. The menu based programs

provide many of the same functions, but still do not provide a component by component graphical method to combine components together via connection lines to form a system. This study examines an icon-based method where this type of connection is possible.

1.2.2 Simulators

New breeds of desktop computers and more aggressive software that takes advantage of the increased capabilities of these computers allow for more complex and realistic simulations to be undertaken. An example of the progress in computer simulation is given by the developments over the past ten years. In 1989, a group of researchers (Nungester, 1989) wished to perform a flow analysis on the duct work of a multi-zone HVAC unit. The program consisted of 450 lines of BASIC programming and a 80286-based computer and required between 30 to 60 s per iteration for a solution to converge. Even though this technique was successful, the designers were required to program and debug the 450 lines of computer code and wait for a solution to converge. Today's approach to solving this problem would be to use an icon driven software package to link up each object with a series of connecting lines. The user would then input the initial conditions and parameters for the system and allow the program to run. This technique provides a much faster result and could also generate more information than what was initially requested.

The use of icons can be viewed as a simplified method of looking at the governing equations for a system as well as adding an easy method for providing parameters, initial conditions, or inputs to the system. Once the developer has a general model, it is convenient to duplicate the various components to create a much larger system. At this level, the developer can choose to incorporate different aspects into the model. Because the subject of HVAC has so many topics and areas to consider, the developer may choose

to focus on certain main topics and leave less important or non-applicable topics out of the simulation. This is accomplished in an icon driven user interface, with a click of the mouse. Programs do exist that bridge the gap between menu driven and icon driven software. Such programs include TRNSYS (Bradley, 1999), where the interface uses both modular components on the screen to represent HVAC type components and a menu interface that uses inputs to configure the parameters for the components. A program such as this leads the trend to development of icon-based software.

At Berkeley National Laboratory in California, a graphical simulation software package, Simulation Problem Analysis and Research Kernel (SPARK), is being developed (Ellington, 1999). This simulation software works by linking component icons like walls, chillers, heaters, windows, and other types of component groups together via connecting lines. SPARK then creates a customized simulation program for the components linked together. Input parameters are then entered by the user. The main elements of the program are an interactive graphical editor, an object library containing components for building modules, and a solver for solving the set of algebraic and differential equations. The graphical interface allows the user to add their own components, modify existing components, and link the components together to create the network of the building system. Current work is aimed at developing more individual components to add to the HVAC library and to improve the speed and efficiency of the solver (Ellington, 1999).

1.2.3 IAQ

IAQ has been a concern since it gained its popularity in the late 1980's with more and more office building being constructed and being tightly insulated more emphasis is focussed on IAQ. Standard 62-1989 not only focuses on airborne particulates, but

airborne gas pollutants (ASHRAE, 1989). In most commercial structures, carbon dioxide (CO₂) gives rise to complaints by workers in the forms of the feelings of fatigue and “stiffness”. At level of 600 ppm and above, complaints from occupants in the zone will occur (Grot, 1991). Typical levels of background levels of CO₂ in the atmosphere are found to be approximately 300 ppm (Walsh, 1984). Fanger et al. (1989) presents an idea to quantify the actual comfort in a space. This comfort equation predicts the percentage of comfort level an occupant will have while in a certain space with a given flow rate of air, the quality of the incoming air to the space, and the pollution source strength (Fanger, 1989).

The National Institute of Standards and Technology (NIST) is responsible for a number of laboratories for research and development. One of these laboratories includes the building and fire research laboratory which is responsible for indoor air quality and ventilation. This particular group is working to develop a software package called CONTAM (Persily, 1999), to predict air flows and contaminant concentrations in multi-zone building systems. The GUI allows the user to select icons to represent airflow pathways and ventilation components. This type of design provides a graphical representation of the designed system and an easier method to enter system parameters of the designers choice. This study will focus on a similar method of design using an icon-based simulation combining both thermal and IAQ models to describe a building system.

1.3 Objective

The objectives of this study are (1) to develop a multi-zone thermal model using an icon-based software program, (2) to couple the multi-zone thermal model with an IAQ model, (3) to introduce a control method to operate the entire system, and (4) to analyze the output from the model given initial conditions and inputs to the system. Comparisons

are made on the different control methods that govern the system by analyzing the output from the system.

1.4 Outline

The outline of this study will follow the objectives mentioned in this report. Chapter 2 introduces the thermal and IAQ models as well as examines a control method to govern the entire model. Chapter 3 examines the implementation of the thermal and IAQ models into an icon-based software program. The analysis and discussion of the results occur in Chapter 4, while Chapter 5 summarizes the entire investigation with concluding remarks and recommendations.

CHAPTER 2

DESCRIPTION OF MULTI-ZONE SYSTEM

2.1 Introduction

This chapter describes the building HVAC system that is simulated in this study. The building HVAC system is made up of two major parts, an air handling unit (AHU) and the conditioned zones. A diagram showing both the AHU and the four zones is shown in Fig. 2.1. The main purpose of the AHU is to supply conditioned air to zones at a specified flow rate and at a specified and controlled temperature. The components within an AHU are shown in Fig. 2.2. The AHUs range in size and have varying capacities to meet the demands of different sizes of zones, number of zones, and load conditions throughout the zones.

The individual zones have different heating and cooling loads. Thermal loads due to people, equipment, lights, and heat exchanges within the zone envelope must be considered when selecting the air flow rate for the zone and the temperature of the air supplied to the zone. The system accounts for these zonal differences by adjusting the amount of cooling or heating allowed for a zone. The cooling capacity for a zone is varied by adjusting the amount of cooled air sent to a zone. The heating capability may be accomplished using a reheat coil (RH). In general, there are the same number of reheat coils as there are number of individual zones. The number of zones may vary, but for this study a four zone system is investigated. A four zone system is selected in anticipation of a future study that validates the findings of the current study using the Iowa Energy Center Energy Resource Station (ERS) (Price and Smith, 1998). The reheat

coil may either be electric or hydronic, where the latter is considered in this study. The presence of a pollutant in the air is described in the form of a concentration.

Figure 2.2 shows the components of the AHU. An AHU is comprised of, among other components, a heating coil (HC), cooling coil (CC), supply fan (SF), reheat coil (RH), return fan (RF), and dampers. Additionally, the AHU has a control unit that regulates the operation of the AHU so that set air flow rates and supply air temperatures are maintained. Recirculated air at a flow rate Q_{rc} , temperature T_6 , and concentration C_{rc} combines with outdoor air at a flow rate Q_{oa} , temperature T_{amb} , and concentration C_{oa} to form supply air with a flow rate Q_{sa} , temperature T_1 , and concentration C_{sa} . Dampers (not shown) control the amount of recirculated air that mixes with the outdoor air. The system air flows to the HC where it may be heated with energy q_h . The air then passes through to the CC where it may be cooled using energy q_c . The conditioned air then proceeds to the SF. After the SF, the air is divided and supplied to each of the four reheat (RH) coils where it may be heated with energy q_{rh} and then passes into each zone as shown in Fig. 2.3.

A zone consists of a RH coil, the zone volume, and an envelope (W). In each zone, air interacts with the zone envelope which has interior and exterior convection and exterior solar energy, S_o . There is also a thermal load, q_x , and a pollutant load, G_z , in each zone. The air leaves each zone and is combined with air from the other zones and flows through the RF.

The governing equations for each of the HVAC components are derived from statements of the conservation of mass and energy as applied to a control volume. The equations written to describe the system are assumed to satisfy the following conditions:

- Constant thermodynamic properties,
- No heat transfer or pollutant exchange as the air flows between components,

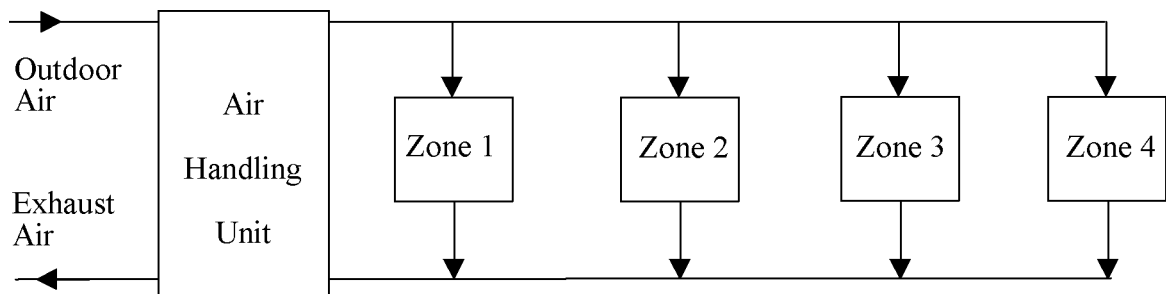
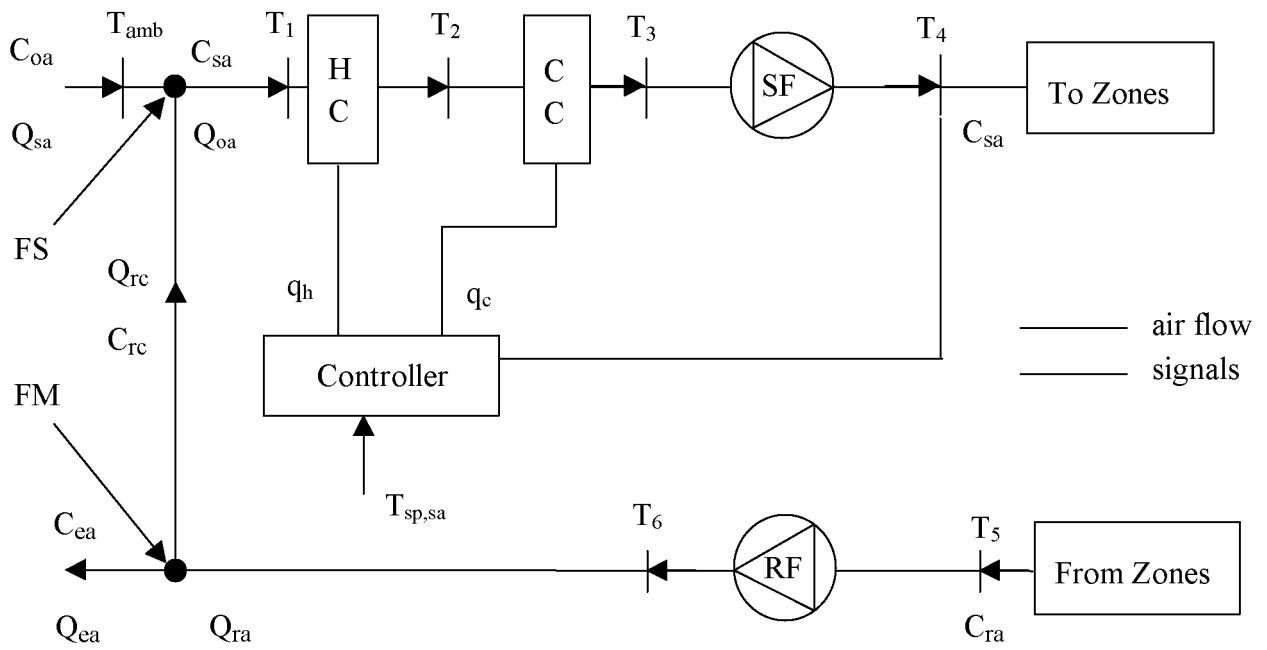


Figure 2.1 HVAC system model.



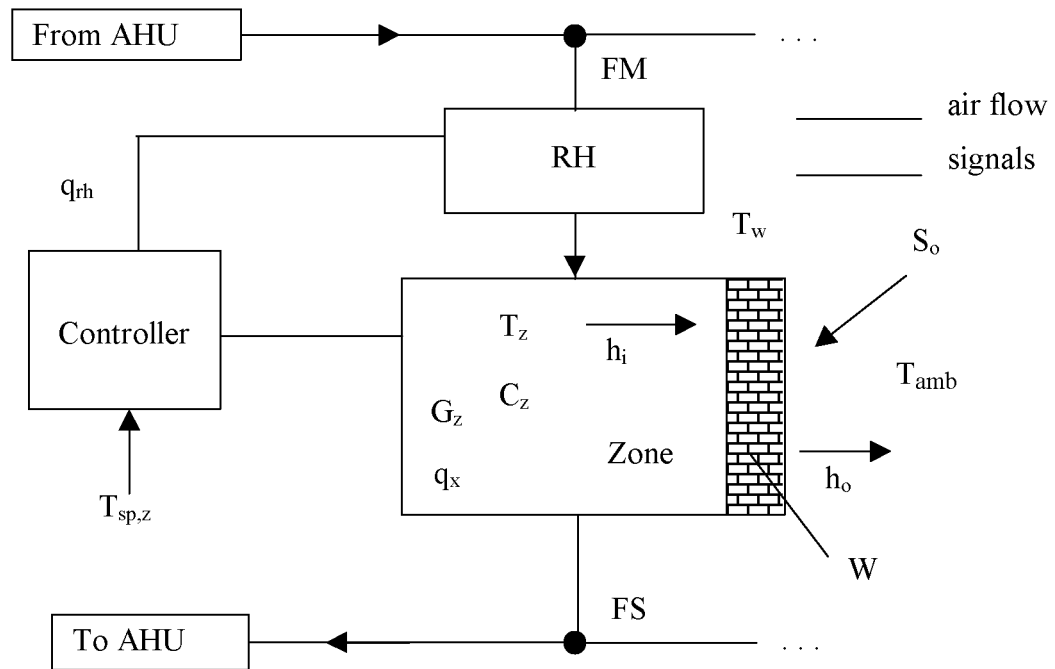
FM: flow mixer
 FS: flow splitter
 CC: cooling coil
 HC: heating coil

oa: outdoor air
 sa: outdoor air
 rc: recirculated air
 RF: return fan

ra: return air
 set,sa: setpoint supply air

T: temperature
 C: concentration
 Q: flow rate
 q: energy

Figure 2.2 Model of AHU in system.



rh: reheat coil
 W: wall
 S: solar energy
 Z: zone generation

h: convection term
 amb: ambient conditions
 set,z: setpoint zone air

T: temperature
 C: concentration
 G: generation
 q: energy

Figure 2.3 Model of a Zone.

- No interzonal exchange of pollutant or thermal energy,
- No exfiltration and infiltration in the ducts and zones,
- Zone envelope described by a single uniform temperature, and zone envelope is imperious to outdoor pollutant transport,
- No relative humidity effects,
- Kinetic and potential energies are neglected,
- Uniform temperature and pollutant concentration in each component,
- SF and RF and motors are within air streams,
- Fully air-mixed streams of both temperature and concentration of pollutant,
- No storage of air in flow mixers, splitters, and zones,
- No active removal mechanism of pollutant, and
- No time delay while operating HVAC equipment.

Once the equations are derived, they are coupled together to form a set of ordinary differential equations. A mathematical solver is introduced to solve the set of equations describing the system.

2.2 Thermal Model

Using the assumptions stated previously, mass and energy balances for the system components reduce to the following forms:

Flow mixer:

$$Q_{sa} T_1 = T_6 (Q_{sa} - Q_{oa}) + Q_{oa} T_{amb} \quad (2.1)$$

Heating coil:

$$\rho_h V_h c_h \frac{dT_2}{dt} = \rho_a Q_{sa} c_a (T_1 - T_2) + q_h \quad (2.2)$$

Cooling coil:

$$\rho_c V_c c_c \frac{dT_3}{dt} = \rho_a Q_{sa} c_a (T_2 - T_3) + q_c \quad (2.3)$$

Supply fan:

$$\rho_s V_s c_s \frac{dT_4}{dt} = \rho_a Q_{sa} c_a (T_3 - T_4) + q_{sf} \quad (2.4)$$

Reheat coil:

$$\rho_{rh,i} V_{rh,i} c_{rh,i} \frac{dT_{rh,i}}{dt} = \rho_a Q_{sa} c_a (T_4 - T_{rh,i}) + q_{rh,i} \quad (2.5)$$

Zone air:

$$\rho_a V_{z,i} c_a \frac{dT_{z,i}}{dt} = \rho_a Q_{sa} c_a (T_{rh,i} - T_{z,i}) + q_{x,i} + h_{z,i} A_{z,i} (T_{w,i} - T_{z,i}) \quad (2.6)$$

Zone envelope:

$$\rho_w V_w c_w \frac{dT_{w,i}}{dt} = h_{z,i} A_{z,i} (T_{z,i} - T_{w,i}) + S_{o,i} A_{o,i} - h_{o,i} A_{o,i} (T_{w,i} - T_{amb,i}) \quad (2.7)$$

Return air:

$$T_5 = \frac{1}{Q_{sa}} \sum_{i=1}^n Q_{z,i} T_{z,i} \quad (2.8)$$

Return fan:

$$\rho_r V_r c_r \frac{dT_6}{dt} = \rho_a Q_{sa} c_a (T_5 - T_6) + q_{rf} \quad (2.9)$$

Flow rate:

$$Q_{sa} = \sum_{i=1}^n Q_{z,i} \quad (2.10)$$

where $i = 1$ to n with n representing the number of zones, ρ_x , V_x , and c_x are the density, volume, and specific heat of a component (HC, CC, SF, RH, Z, W, and RF), and ρ_a , V_a , and c_a are the density, volume, and specific heat of the air. Equations (2.4) and (2.7) account for the thermal loads, q_{sf} and q_{rf} , of the motors in the air stream in Btu/h. The controllers discussed in Section 2.4 provide positive values of q_h and q_{rh} , and negative values of q_c .

The initial conditions for the system of equations are

$$\text{at } t = 0, T_i = T_i(0) \text{ for } i = 1 \text{ to } 6 \quad (2.11a)$$

$$\text{at } t = 0, T_{rh,i} = T_{rh,i}(0) \text{ for } i = 1 \text{ to } n \quad (2.11b)$$

$$\text{at } t = 0, T_{z,i} = T_{z,i}(0) \text{ for } i = 1 \text{ to } n \quad (2.11c)$$

$$\text{at } t = 0, T_{w,i} = T_{w,i}(0) \text{ for } i = 1 \text{ to } n \quad (2.11d)$$

where $T_i(0)$ are initial temperatures for the components of the AHU (HC, CC, SF, and RF), $T_{rh,i}(0)$ are the initial temperatures for the reheat coils, $T_{z,i}(0)$ are the initial temperatures for the Zones, and $T_{w,i}(0)$ are the initial temperatures for the walls inside each zone.

2.3 IAQ Model

This report focuses on the levels of carbon dioxide (CO_2) in building zones. For purposes of the model design, the CO_2 concentration is examined as a pollutant in the system. This pollutant is measured in parts per million (ppm). Referring to Fig. 2.2, a conservation of mass balance for the air flow mixer, gives

$$\dot{m}_{p,sa} = \dot{m}_{p,oa} + \dot{m}_{p,rc} \quad (2.12)$$

where p represents the pollutant, in this case CO₂. The process of converting from mass to concentration is given in the Appendix. From the Appendix, Eq. (2.12) is expressed in terms of flow rate and concentration as

$$Q_{sa} C_{sa} = Q_{oa} C_{oa} + Q_{rc} C_{rc} \quad (2.13)$$

The supply air volumetric flow rate is

$$Q_{sa} = Q_{oa} + Q_{rc} \quad (2.14)$$

At the exhaust and recirculated air splitter, the recirculated concentration is

$$C_{rc} = C_{ra} \quad (2.15)$$

Substituting Eqs. (2.14) and (2.15) into Eq. (2.13) and solving for C_{sa} give

$$C_{sa} = \frac{Q_{oa} C_{oa} + (Q_{sa} - Q_{oa}) C_{ra}}{Q_{sa}} \quad (2.16)$$

The supply air is distributed to each zone where the entering concentration for zone i is

$$C_{z,i,e} = C_{sa} \quad (2.17)$$

Attention is now directed to the zones. Mass transfer of this pollutant is described by the conservation of mass equation of the transient form

$$\frac{dm_p}{dt} = \dot{m}_{p,i} - \dot{m}_{p,o} + \dot{m}_{gen} \quad (2.18)$$

where $\dot{m}_{p,i}$ and $\dot{m}_{p,o}$ are the mass flow rates of the pollutant entering and leaving the zone. The addition of pollutant generation rate, \dot{m}_{gen} , is to account for organisms, such as humans or animals, that generate the pollutant. Items such as plants that absorb CO₂ are represented as a subtraction term, but are neglected for this study.

Using the relations from the Appendix, Eq. (2.18) is applied to a multi-zone model and transforms to

$$\frac{dC_{z,i}}{dt} = \frac{Q_{z,i,e} C_{sa} - Q_{z,i,o} C_{z,i,o} + G_{z,i}}{V_{z,i}} \quad (2.19)$$

where Eq. (2.17) has been used. $Q_{z,i,e}$ and $Q_{z,i,o}$ are taken to be equal to $Q_{z,i}$ because there is no exfiltration and infiltration, the contribution of pollutant is small compared to the air flow rate that does not change due to the addition of the CO_2 in the zone, and there is no build up of air within the zone. A zone effectiveness is incorporated in the $C_{z,i,o}$ term to indicate how well the pollutant is removed from the zone. Hence

$$C_{z,i,o} = m_i C_{z,i} \quad (2.20)$$

where m_i is the “effectiveness” (Knoespal et al., 1991) for each individual zone. The effectiveness is defined as the return air concentration divided by the average concentration in the zone and accounts for the fact that the pollutant may not be fully mixed in the return air (Knoespal et al., 1991). Essentially, m_i is governed by how well the supply air mixes with the air in the zone (Stanke, 1998). A value of $m_i = 1$ implies a fully mixed zone. A value of m greater than one implies that the generation source is too close to the return duct and the generated pollutants are being directly exhausted instead of allowing to be mixed within the zone (Knoespal et al., 1991).

Combining Eqs. (2.19) and (2.20) results in

$$\frac{dC_{z,i}}{dt} = \frac{Q_{z,i} C_{sa} - Q_{z,i} m_i C_{z,i} + G_{z,i}}{V_{z,i}} \quad (2.21)$$

where $i = 1$ to n .

As the air leaves each zone it is mixed with the air from the other zones to form the RA. The RA concentration is

$$C_{ra} = \frac{1}{Q_a} \sum_{i=1}^n Q_{z,i} m_i C_{z,i} \quad (2.22)$$

The initial conditions for the system of IAQ equations are

$$\text{at } t = 0, C_{z,i} = C_{z,i}(0) \quad (2.23)$$

where $C_{z,i}(0)$ is the initial pollutant concentration in the zone.

2.4 Controllers

2.4.1 Introduction

The system is described by a thermal and IAQ model, however, a control scheme must be implemented to govern the system variables to control heating, cooling, and indoor CO₂ levels. Control algorithms are used to modify q_{h} , q_{c} , and q_{rh} over time. The implementation of these control algorithms provides a dynamic system that has changing inputs while maintaining a scheduled setpoint temperature for the individual zones. This study focuses on two different type of control algorithms, a proportional-integral (PI) feedback (FB) control and a feedforward (FF) control, and how they are used in combination to create feedback and feedforward control. The IAQ pollutant levels are not actively controlled.

2.4.2 Feedback control

The PI controller is used in a wide variety of HVAC applications. A PI controller provides more control than a proportional (P) controller because it is coupled with an integrator. This integrator acts as “memory” where the error is summed up over the simulation time while it approaches zero and the offset of the error is removed. The form of a PI algorithm is (Hittle, 1997)

$$u_{\text{fb}}(t) = K_p \left[e(t) + \frac{1}{T_c} \int_0^t e(\tau) d\tau \right] \quad (2.24)$$

where $u_{fb}(t)$ is the controller output or control signal at time t , K_p is the proportional gain coefficient, T_c is the integral time, τ is the variable used for time over the simulation time, and $e(t)$ is the error representing the deviation of the setpoint temperature from the measured output. Both the AHU and the zones are controlled using the FB control. Each unit has a different form of the error. The error for the HC and CC for the AHU is

$$e = T_{sp,sa} - T_4 \quad (2.25)$$

where $T_{sp,sa}$ is the setpoint temperature of the supply air to the zones. A FB controller is used to regulated each zone, thus each zone has error. The error measured for each zone is

$$e = T_{sp,i} - T_{z,i} \quad (2.26)$$

where $T_{sp,i}$ is the setpoint temperature of the zone.

The values of K_p and T for the HC, CC, and the zones are different and come from a process of “tuning” the controller for the system. The tuning process changes the reaction time of the system to become a responsive system. A non-responsive or “sluggish” system reacts too slowly and requires a longer period of time to reach a setpoint temperature. On the other hand, and an over-responsive or “aggressive” system responds to quickly and often “over-shoots” the setpoint temperature by a wide margin. This study focuses on a responsive PI controller. More information regarding the choices used for tuning the system is explained in the results and discussion section.

2.4.3 Feedforward control

The FF control is a method proposed by Salsbury (1998) to anticipate changes in parameters that affect the system operation. For example, a change in T_{amb} is not acted upon by the FB control until after the air passes through the AHU. Successful

implementation of Salsbury's feedforward control scheme was not possible, but a modified version is implemented. The modified version is

$$u_{ff}(t) = K_1(T_{sp,sa} - T_{amb}) - K_2(T_6 - T_{amb}) \quad (2.27)$$

where $u_{ff}(t)$ is the FF control signal at time t ; K_1 , and K_2 are FF proportional gain coefficients; $T_{sp,sa}$ is the setpoint temperature of the supply air, and T_6 is the return air temperature. This modified FF control anticipates a change in control signal by sampling air "forward" of the AHU and compares this to the ambient air temperature. The difference is then multiplied by a proportional constant to adjust the control signal. Since this algorithm samples only the "forward" air, large changes to the control signal may occur during times of rapid changes in ambient temperatures. This effect is accounted for in the first term in Eq. (2.27) where the difference between the setpoint and ambient temperatures is multiplied by K_1 . As seen by Eq. (2.27) a high value of $u_{ff}(t)$ indicates a large deviation from the setpoint temperature, resulting in a higher demand for either heating or cooling.

Determining values or "tuning" of the signal for the FF proportionality gain coefficients is done in a similar manner as the PI controller. Values for K_1 and K_2 are substituted into the equations and the system is examined to analyze the results. Minor increments in the values of K_1 and K_2 are solved as well to determine which coefficients perform better than other coefficients. The ideal scenario for the control coefficients are determined from the coefficients that show the most rapid change or largest slope in the temperature change over time in the RA during a setpoint change while still maintaining control. This study investigates the an ideal scenario for the values of the FF proportional gain coefficients selected.

2.4.4 Feedback and feedforward control

The combination of both control schemes discussed in Sections 2.4.2 and 2.4.3 is implemented in only the HC and CC control of the system. The individual zones are controlled by a FB controller for each reheat coil. The combination of the FB and FF control schemes used in the AHU may allow for better control of the system. This combination is shown by

$$u(t) = u_{fb}(t) + u_{ff}(t) \quad (2.28)$$

The PI control dominates the control through periods of time where the setpoint temperature remains fairly constant. During periods of rapid changes of the setpoint temperature, the FF control adds additional signal to change the zone temperature faster. When the two methods are combined, the control coefficients must be tuned again. The same techniques are used to tune the system to find the appropriate values for K_p , T_i , K_1 , and K_2 that are used when the coefficients are separated in Eqs. (2.24) and (2.27).

2.4.5 Performance merits

Performance is determined once the system is simulated to decide which system control scheme is better than another for given system parameters. In the case of two systems achieving their desired goals, it becomes difficult to evaluate which system performs better than another. Cost calculations provide evaluative factors or quantitative information about the performance of the controllers. These calculations are made in real time during the simulation. The calculations refer to the cost of heating, cooling, comfort, maintaining supply air temperature, and pollutant level are based on the following expressions:

$$J_{\text{htg}} = \int_0^{t_f} q_h^2 dt + \int_0^{t_f} \left(\sum_{i=1}^4 q_{\text{rh},i}^2 \right) dt \quad (2.29)$$

$$J_{\text{clg}} = \int_0^{t_f} q_c^2 dt \quad (2.30)$$

$$J_c = \int_0^{t_f} \left[\sum_{i=1}^4 (T_{\text{sp},i} - T_{z,i})^2 \right] dt \quad (2.31)$$

$$J_{\text{sa}} = \int_0^{t_f} (T_{\text{sp,sa}} - T_4)^2 dt \quad (2.32)$$

$$J_p = \int_0^{t_f} \left[\sum_{i=1}^4 (C_{z,i} - C_{\text{max}})^2 \right] dt \quad \text{when } C_{z,i} > C_{\text{max}} \quad (2.33)$$

Quadratic forms of the cost functions are used for Eqs. (2.29) to (2.32) to ensure that all values, positive or negative, are cumulatively added over the simulation time. Eqs. (2.29) to (2.32) quantitatively measure which simulation is better than another by measuring costs of heating, cooling, or comfort within the system. Thus a lower value of merit indicates lower cost. The merit in Eq. (2.33) describes a way to quantitatively test how uncomfortable the system is over the simulation time. The summation term in J_p is only computed if $C_{z,i}$ is greater than C_{max} . C_{max} is defined as the maximum level of CO_2 in a zone for occupants to feel comfortable. At levels of 600 ppm and above, complaints from occupants in the zone will occur, denoting that the amount of outdoor air will need to be increased (Grot, 1991). These equations are compared once a simulation is completed to another simulation with different parameters. The comparison shows which modifications in system parameters affect a change in the system performance factors.

2.5 Summary

An HVAC system is composed of two systems, the AHU and the conditioned zones. The AHU provides conditioned air to the zones as well as maintaining IAQ. A system of equations is written to express the thermal interaction through the system. Another system of equations is written to describe pollutant flow through the system. The two systems of equations are combined to form the HVAC system. Once these equations are implemented a control scheme is used to maintain a setpoint temperature in the zones in the system and maintain a level of acceptable IAQ. Once the system is properly defined, an analysis can be done to evaluate the performance merits of the system. The merits can be compared between simulated systems to determine which system performs better for a given set of system parameters.

CHAPTER 3

ICON-BASED SOFTWARE IMPLEMENTATION

3.1 Introduction

With the system defined in Chapter 2, focus is given to how the system of equations are implemented and solved in a software package. As mentioned in Chapter 1, there are several software packages available to solve this type of system. This study uses a method of simulating a system based on an icon-driven software package. A method such as this has advantages as previously mentioned. The icon-based software package chosen for this study is Easy5 (Easy5, 1996). Easy5 is available on a wide variety of platforms including the Hewlett-Packard Unix workstation that was used for this study. Chapter 3 focuses on the implementation of the physical model and equations into the icon-based software general descriptions of the software and how to perform basic tasks within the software are discussed. A procedure is then given on how the Zones and AHU are formed and combined to create the overall system in the Easy5 software.

3.2 Basic operations

The Easy5 software uses a GUI interface providing easy access to the function and menu options during model building. A library bin is located on the left side of the screen. Inside the selected library, a number of different functions are available. Once a desired function is found, the user clicks on the words of the function and moves the mouse over the screen to place the icon in its desired location on the workspace. Once in place, the icon can be opened to input the parameters necessary to define the system. The

variables that the icon outputs can be changed to a more user-oriented name describing the function of the icon. The process of dragging icons from the library to the workspace and inputting system parameters continues until the system is configured.

Once the icons are installed on the workspace, the icons are connected together via lines. The lines represent numerical values passed between the icons used to solve the system of equations representing the system. Multiple lines can be drawn to and from the icons either representing the same values from the icon or different variables that are passed to another icon. Adding a number of icons to the screen can easily clutter the workspace making it difficult to work with many icons at once. To keep the workspace clear and, more importantly, to group icons according to functionality, submodels are created to contain multiple icons or other submodels to be represented by a single icon. A detailed procedure on creating submodels is described in Section 3.3. in creating submodels for the AHU.

Once the system is constructed with icons and interconnected, the model is ready to be built. Building of the model compiles the FORTRAN code generated by the software by converting the icons and connection lines into a FORTRAN code. This conversion and building process is performed as a background process. A successfully built model is ready to be simulated. Depending on the type of system, the model is either solved for a steady-state value or evaluated as a function over a specified simulation time. This study focuses on the transient solution of thermal and pollutant transport throughout the system.

3.3 Model implementation

Easy5 was used to implement the model that is diagramed by Fig. 2.1. Figure 2.1 shows an AHU with four zones connected in parallel. A diagram showing the Easy5 representation of Fig. 2.1 is presented in Fig. 3.1. The relationship between the physical

model of Fig. 2.1 and the icon model of Fig. 3.1 creates a visual parallelism between the physical model and the icon model. Figure 3.1 represents the model at the least detailed level of view and illustrates the connections of the building HVAC system. More detailed views of the interactions between components are shown later. At this level, it is seen that the connection lines run from the outdoor air parameter submodel to the AHU submodel. Connection lines then run from the AHU to the zones (supply air) and then back to the AHU (return air). Some of the lines in these figures actually represent multiple connections between two icons. The multiple connections allow more than one value to be passed between each submodel. Submodels for each of the AHU components are generated and coupled together with the connection lines. Once a component is built it is assembled into a submodel where it is labeled and connected with other components, eventually making up the AHU. A similar procedure is used to build the submodels for the zones.

3.3.1 AHU representation

Figure 2.2 is a representation of the AHU and is represented in Easy5 as show in Fig. 3.2. To aide in the visual representation of the model, submodels are introduced to contain individual components and the equations that govern them. Submodels within Easy5 provide a way to condense a group of icons into a single icon. This technique is used in the AHU where multiple submodels represent different components within the AHU. The AHU in Fig. 3.2 is made up of two flow splitters (FS), two flow mixers (FM), HC, CC, SF, RF, controller block, and a cost calculation submodel. Where possible, two lines run between two components to represent the thermal and pollutant information passed from the previous components carried by the air as it travels through each component of the AHU.

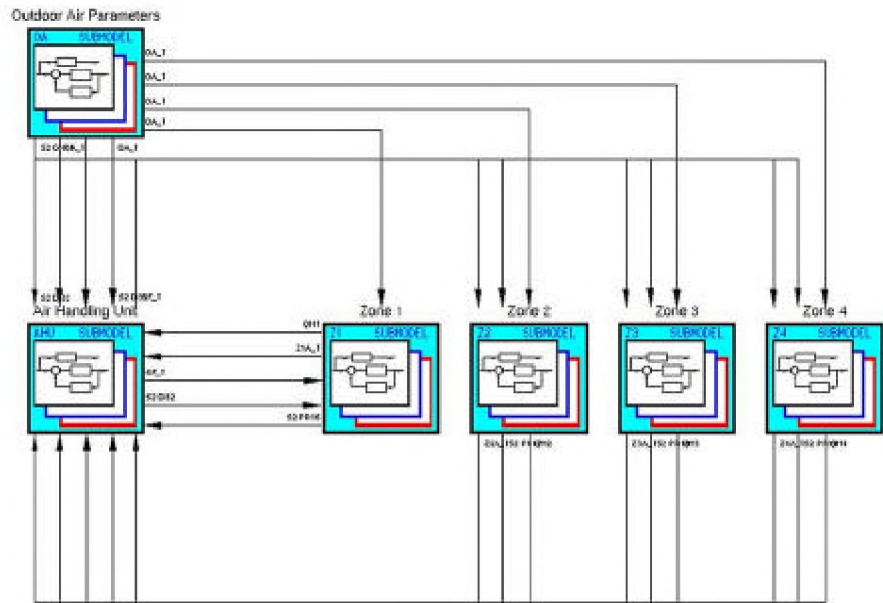


Figure 3.1 Easy5 representation of model.

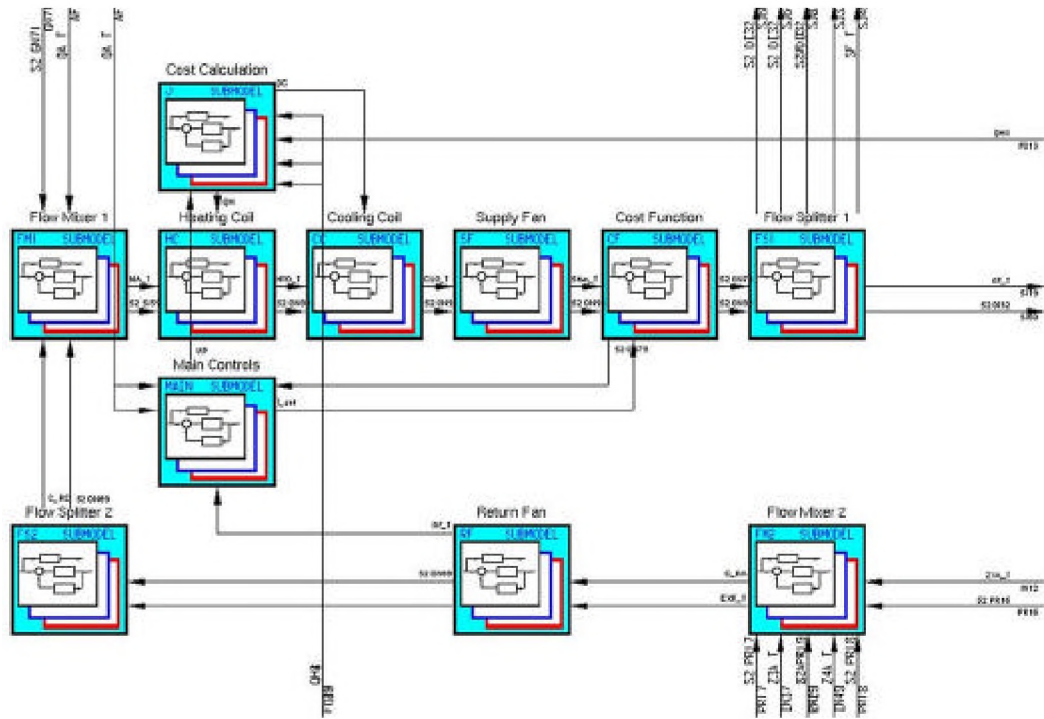


Figure 3.2 Easy5 representation of AHU.

The submodel for the FM 1 is expanded and shown in Figs. 3.3 to 3.5. Within the FM 1, there are submodels for temperature and concentration mixers as indicated in Fig. 3.3. The temperature mixer 1 submodel is expanded and shown in Fig. 3.4, where the mixing of outdoor air and recirculated air is shown to form supply air. Similarly in Fig. 3.5, C_{rc} is combined with C_{oa} to create C_{sa} .

The next component that interacts with the air is the HC in Fig. 3.2. Figure 3.6 represents the HC in Easy5. Concentration is shown to pass directly through the HC because the HC does not effect the level of concentration of the pollutant. The submodels within the HC are expanded and shown in Figs. 3.7 and 3.8. Figure 3.7 represents the air flow conductance of the HC, while Fig. 3.8 is the HC capacitance. The value of q_h that comes from the controller block is then added into the system with a summing junction as shown in Fig. 3.6. The integrator block in Fig. 3.6 is connected to both of the submodels. The function of the integrator is to integrate the ordinary differential equation to obtain values of T_2 in the HC at each time step. Essentially, the integrator is solving for T_2 in Eq. (2.2) for each time step. This temperature result is passed to the CC. The construction of the submodel (not shown) for the CC is the same as the HC except that q_c is subtracted from the model instead of adding q_h .

Similar to the HC and CC, Fig. 3.9 represents the supply fan in Easy5. As in the HC, the concentration of the pollutant is passed through the SF. The submodels for the conductance and capacitance of the SF are identical to those for the HC and CC, only the numerical parameters are different. A thermal load is added for the temperature increase across the fan. After the SF, the air travels to FS 1 that is represented in Fig. 3.10, where lines are drawn from each component to each of the four zones, two lines per zone, one for concentration and the other temperature.

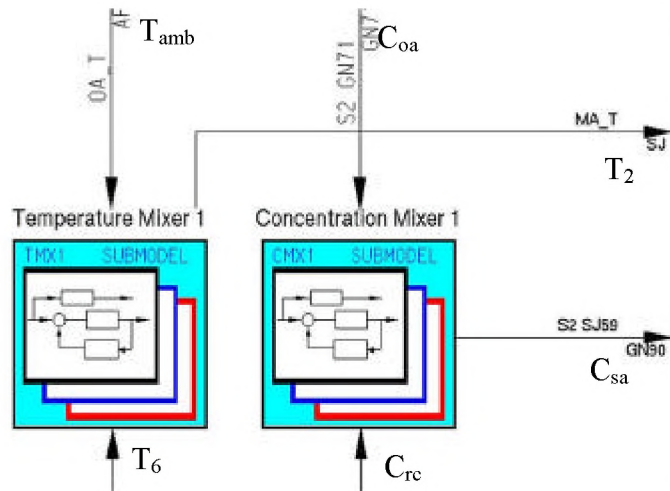


Figure 3.3 Icon representation of FM 1.

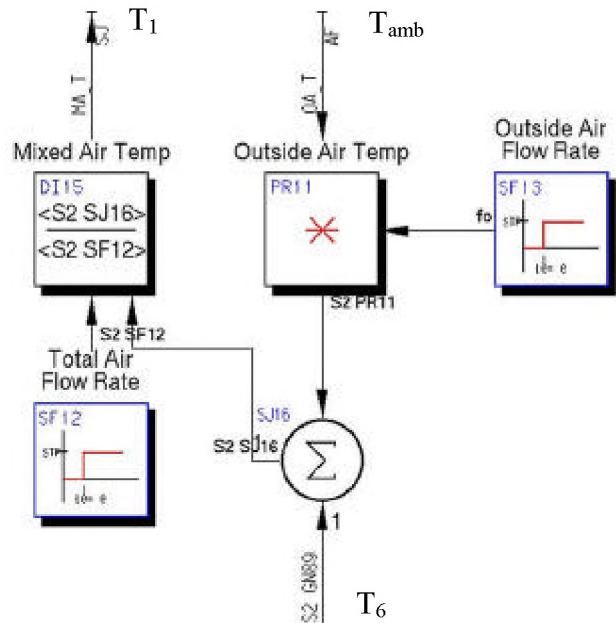


Figure 3.4 Temperature mixer 1.

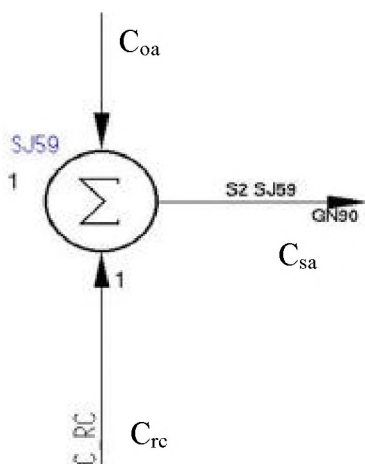


Figure 3.5 Concentration mixer 1.

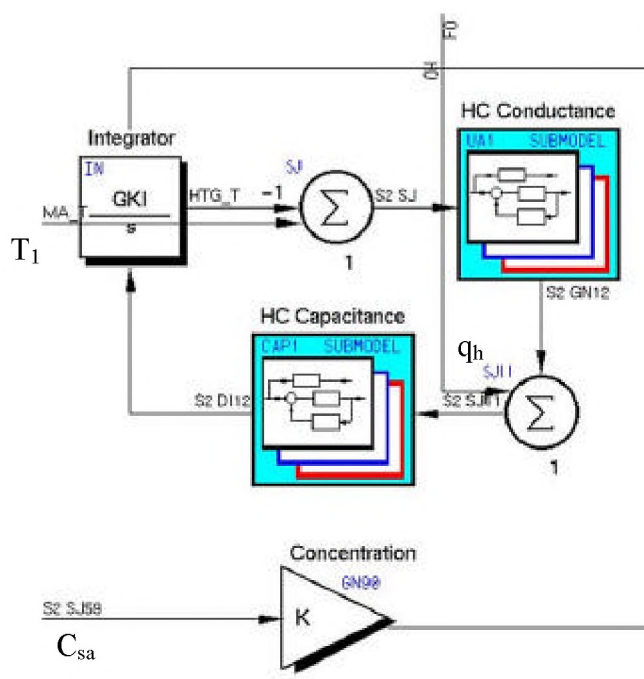


Figure 3.6 Icon representation of HC.

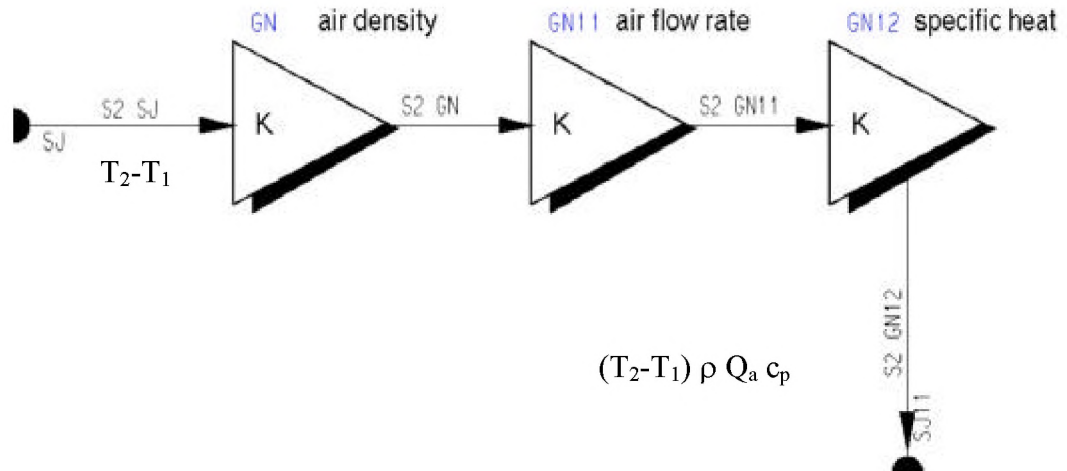


Figure 3.7 Easy5 schematic of HC conductance.

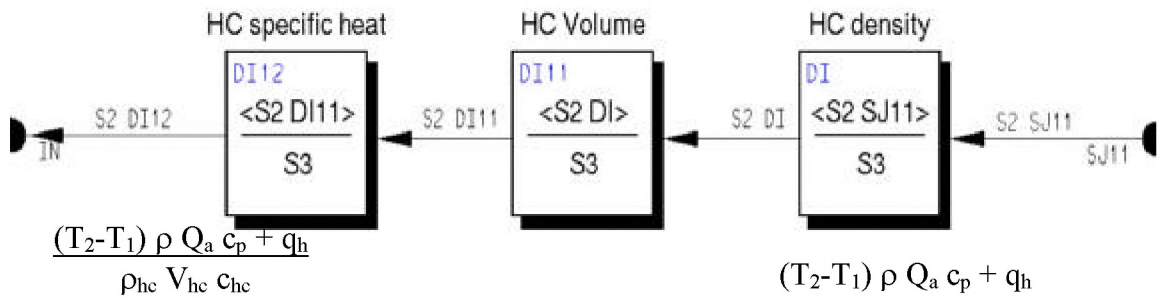


Figure 3.8 Easy5 schematic of HC capacitance.

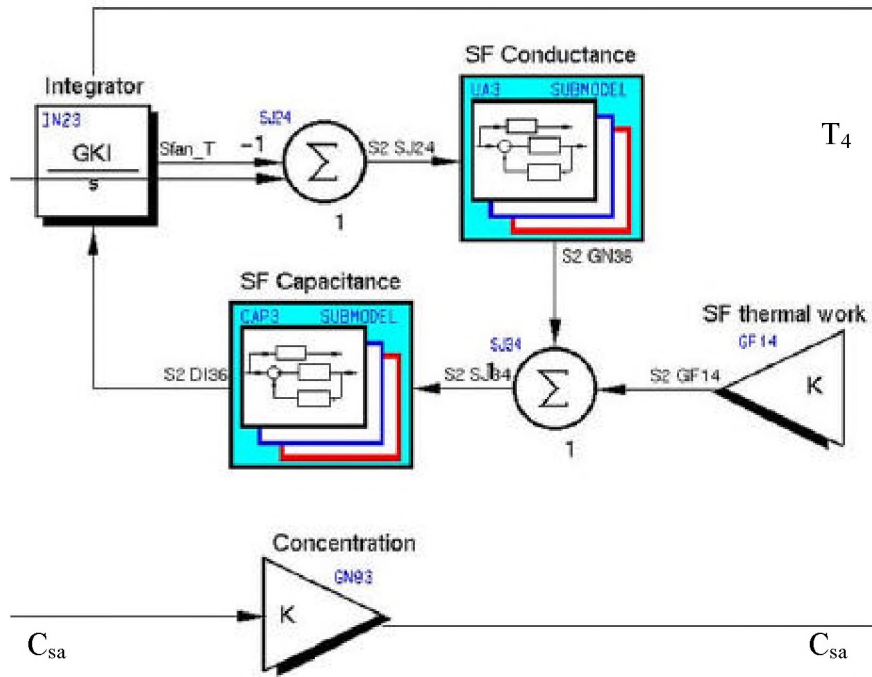


Figure 3.9 Easy5 representation of the SF.

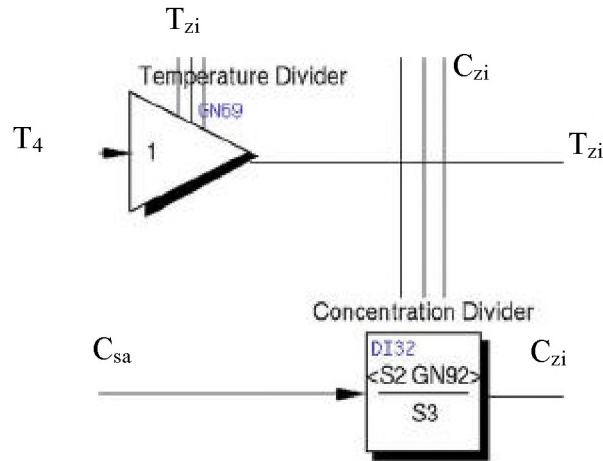


Figure 3.10 Easy5 schematic of the FS 1.

Once the air is returned from the zones, it is combined in the FM 2, illustrated in Fig. 3.11. The submodels for the temperature and concentration are expanded to show the inner workings of the FM 2 in Figs. 3.12 and 3.13. Figure 3.12 show, that each zone temperature is combined with the flow rate, added together, and then divided by the total flow rate to form the return air temperature. Like Fig. 3.12, Fig. 3.13 sums the pollutant concentration leaving a zone and divides by the total air flow rate to obtain C_{ra} . After FM 2 the air enters the RF and FS 2. The model representations of the RF and FS 2 are not shown because they are identical to those for the SF and FS 1 except for the input parameters.

The main control submodel in Fig. 3.1 contains icons that are used to control the HC and CC of the AHU. Figure 3.14 is a representation of this controller. The block labeled Global Input Parameters is an input block that contains assigned numerical values of all variables that could be changed between simulations. This block converts the user defined variable to the actual variable name inside Easy5. For instance, the density of the air could be modified by opening the block and changing its value. The FORTRAN code inside this block references the air density, ρ_a , to the actual Easy5 variable, KGN13. The variable is described with the first letter as the input value, K, an example would be 0.0735 kg/m^3 . The GN represents the notation for gain block and the 13 references the 13th gain block used in the system. The variables are assigned inside the FORTRAN block to correspond with each component in the AHU. Along with the FORTRAN block, the setpoint temperature of the supply air is set with a signal generator block. This value feeds directly into the PI controller which is represented by Eq. (2.24). The inputs to Easy5 are in terms of K_i and K_p , where K_i is given by

$$K_i = \frac{K_p}{T_c} \quad (3.1)$$

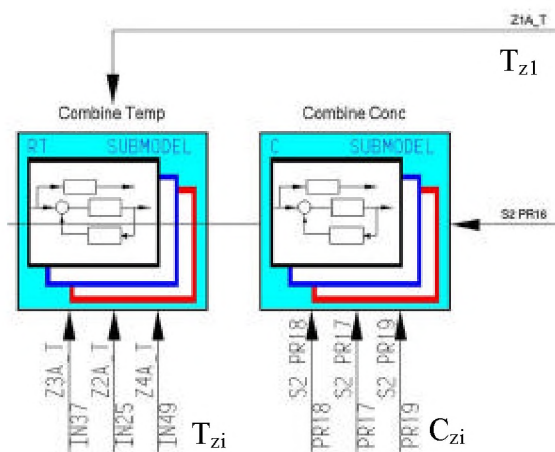


Figure 3.11 Easy5 schematic of FM 2.

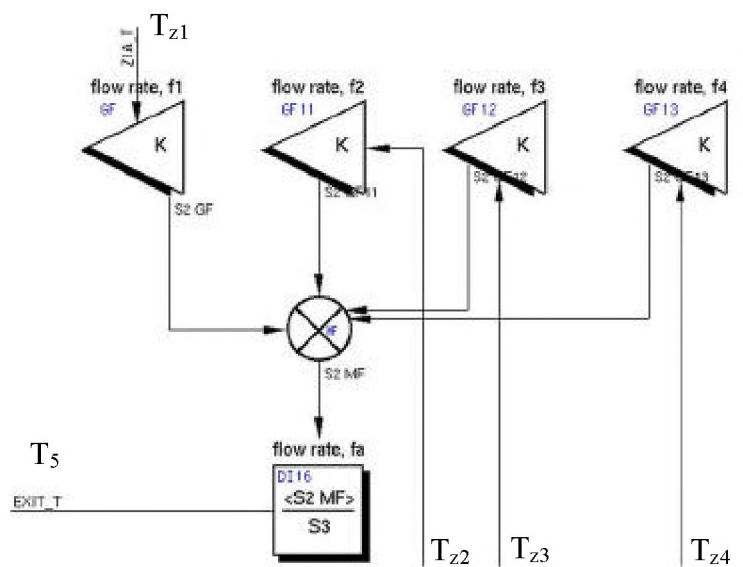


Figure 3.12 Easy5 schematic of combined temperature submodel.

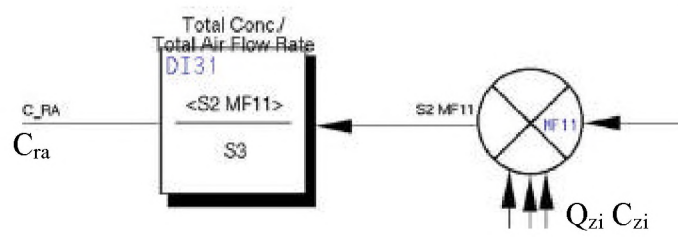


Figure 3.13 Easy5 representation of combined concentration submodel.

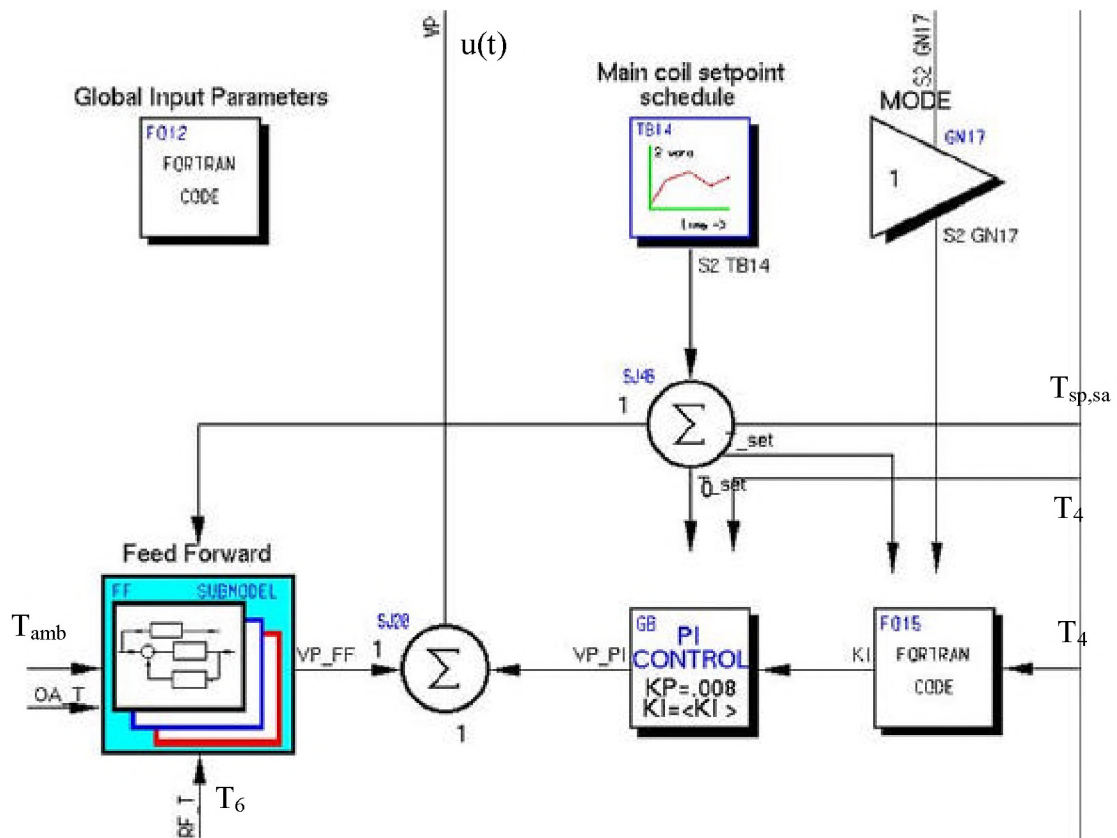


Figure 3.14 Main control submodel.

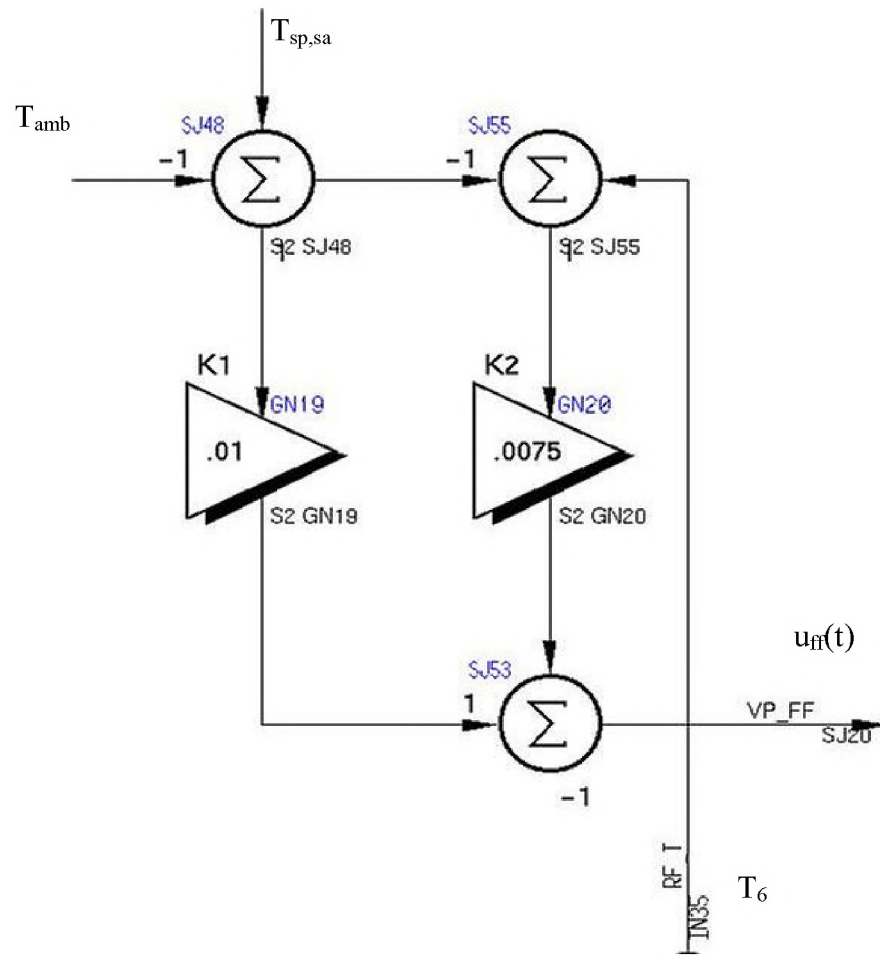


Figure 3.15 Feedforward submodel.

From Eq. (3.1), inputs to Easy5 are assigned in terms of K_i and K_p . This controller is coupled with the feedforward submodel, shown in Fig. 3.15 and described by Eq. (2.27), to create a control signal, C_s , which is expressed by Eq. (2.28).

Finally, Fig. 3.2 shows two submodels that represent the performance merits described in Section 2.5. Figure 3.16 shows the submodel cost function from Fig. 3.2 and represents Eq. (2.32) where the supply air cost function is computed. In a similar format as the cost function submodel, Fig. 3.17 is a representation of the cost calculations submodel from Fig. 3.2 and computes the merit calculations in Eqs. (2.29) to (2.31) and (2.33).

3.3.2 Zone representation

Figure 2.3 is a physical representation of a zone. This diagram is implemented into Easy5 to create one of the four zones. Figure 3.18 is created to correspond with the physical model and has submodels for the reheat coil, zone, and wall. Like the AHU, the zone submodel has a global-input-parameter block to input parameters that govern the individual zone. A PI controller is used to control the amount of reheat energy supplied to the zone. Coefficients input into the controller are “tuned” to modify the controller to produce a desirable response. This “tuning” process is explained in Chapter 4. Different coefficients are chosen for the reheat coils than the HC. This is due to the different capacitances and air flow rates in each unit.

Figure 3.19 represents the interior zone conditions. Similar to other submodels like the SF and HC, the zone submodel is constructed in the same way. The submodels for conductance and capacitance in Figure 3.19 are identical in construction to those Figs. 3.7 and 3.8 except for the input parameters. The wall submodel displayed in Fig. 3.20 shows the interaction with the inside and outside conditions described in Fig. 2.3. Now that the

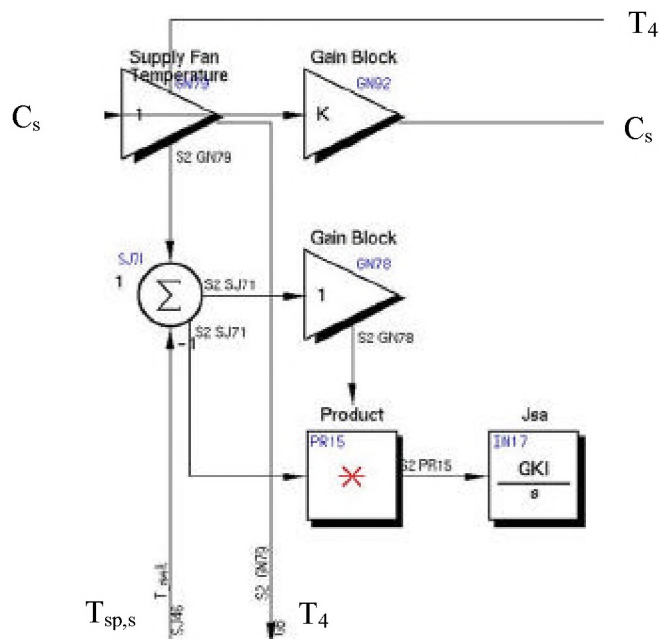


Figure 3.16 Supply air merit calculation.

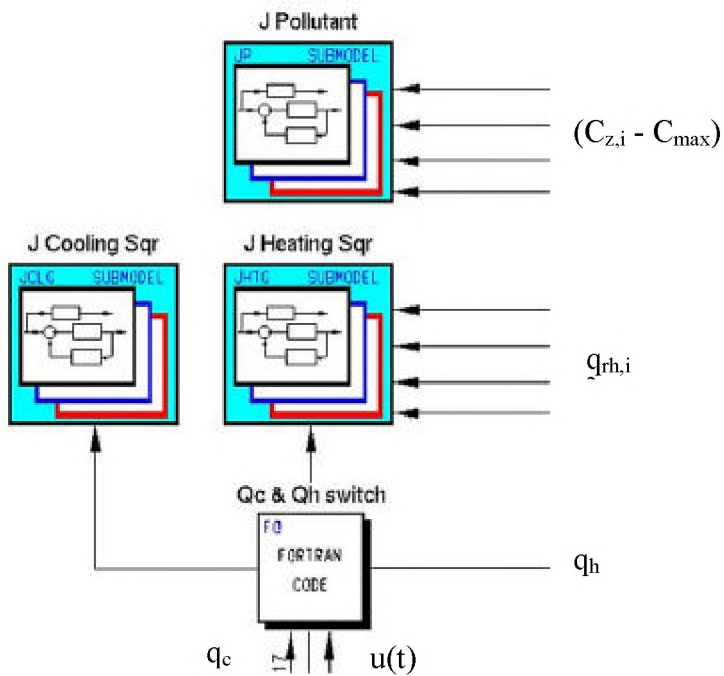


Figure 3.17 Heating, cooling, and pollutant merit equations.

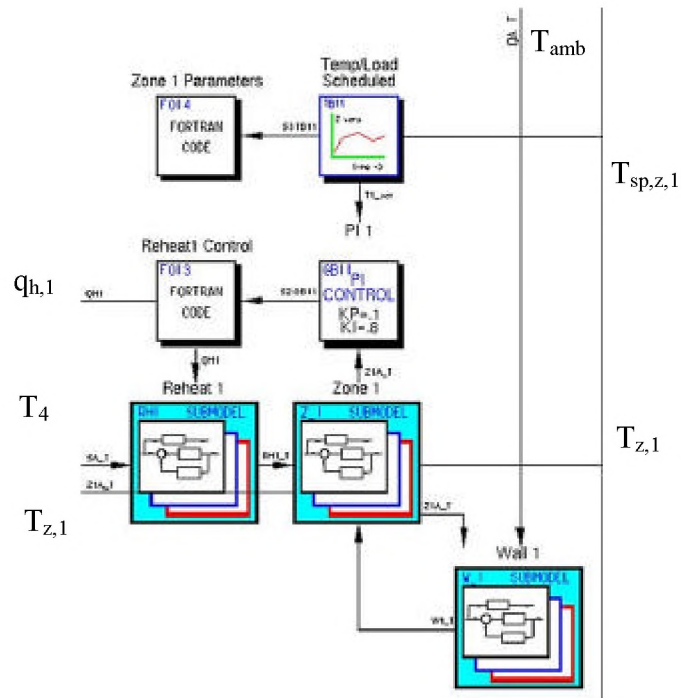


Figure 3.18 Zone representation.

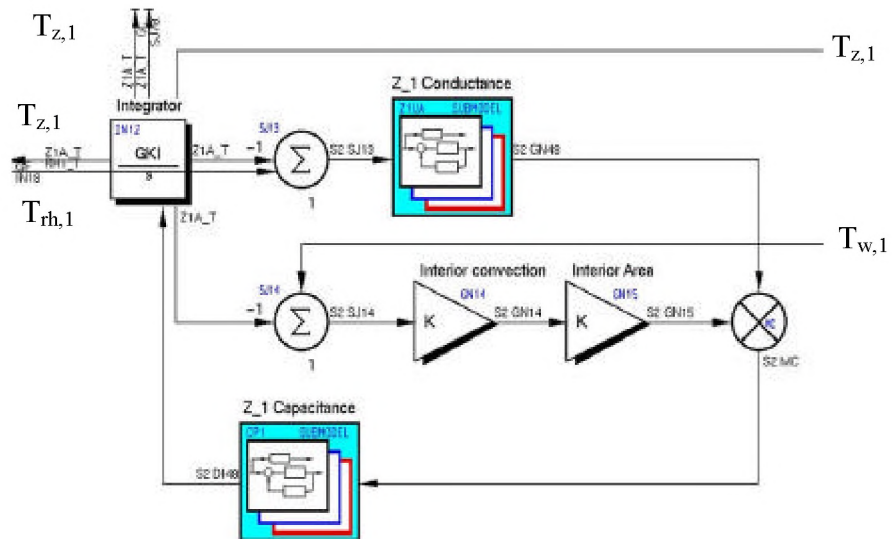


Figure 3.19 Detailed zone representation.

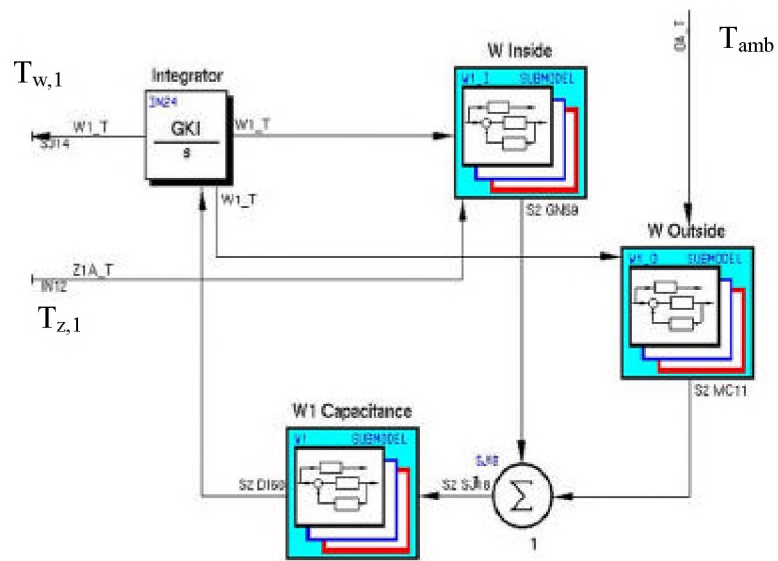


Figure 3.20 Zone envelope representation.

thermal interaction in the zone is explained, attention can focus on the pollutant interaction.

Figure 3.21 shows the Easy5 representation of Eq. (2.21). The integrator block labeled, zone concentration, integrates at every time increment giving a new value of the zone concentration. The zone effectiveness and generation terms are represented by a gain block and a function generator. The sudden concentration change is used to send CO₂ into the zone for a short period of time. This is represented by a pulse-width generator block. Lastly, a calculation performed to determine the merit of each zone is represented by Fig. 3.22. This merit calculation is constructed similar to the merit calculations in the cost function submodel in Fig. 3.17. An integrator block is used to sum all the values from the start of the simulation and obtain a merit value for the zone. Finally, the overall system is governed by outdoor air conditions. The outdoor air conditions contain the flow rate of the air, the temperature, and the concentration of the pollutant as it passes into the first stage of the AHU. These conditions do not show on the physical model, but are necessary to solve the equations in Easy5. A representation of these conditions are shown in Fig. 3.23.

3.4 Numerical solution considerations

As previously mentioned in Section 3.1, Easy5 is executed on a C110 HP-UX workstation operating at 120 MHz with 128 megabytes of memory. The speed of the workstation effects wall clock time for compiling (building), screen redraws, and actual simulation of the model. During simulation of the model, wall clock times are dependent on the amount of output variables. A typical execution time for the model in this study ranges from 10 to 15 seconds. The wall clock times depend on the size of the output file generated by the simulation. Data are stored at every integration step period, which is set

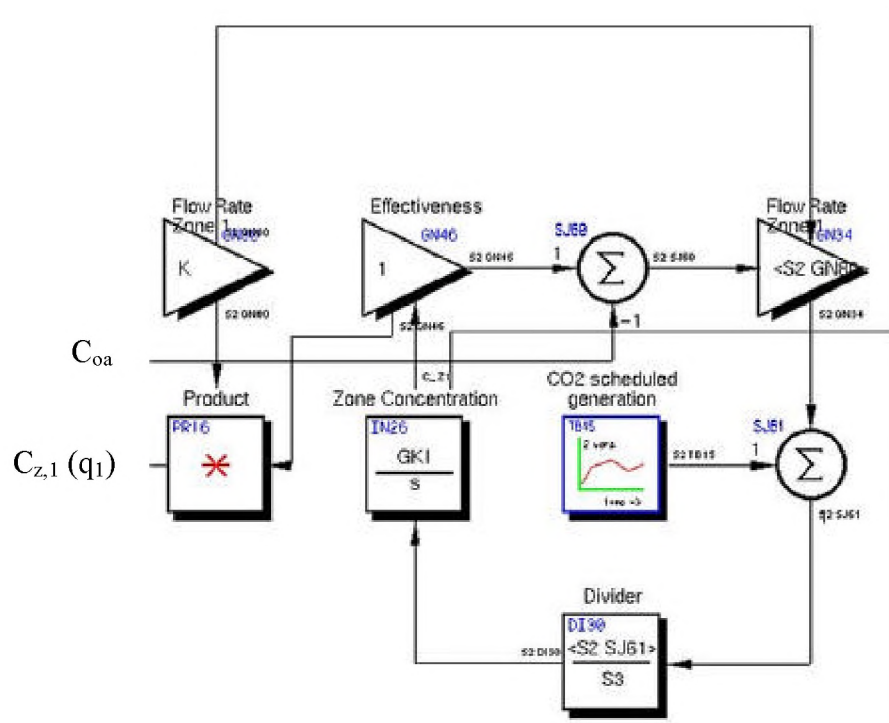


Figure 3.21 Zone pollutant concentration representation.

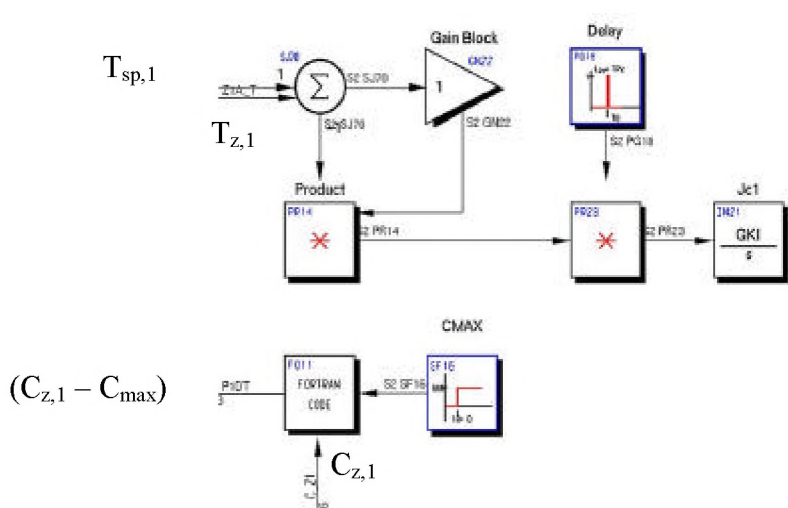


Figure 3.22 Zone merit representation.

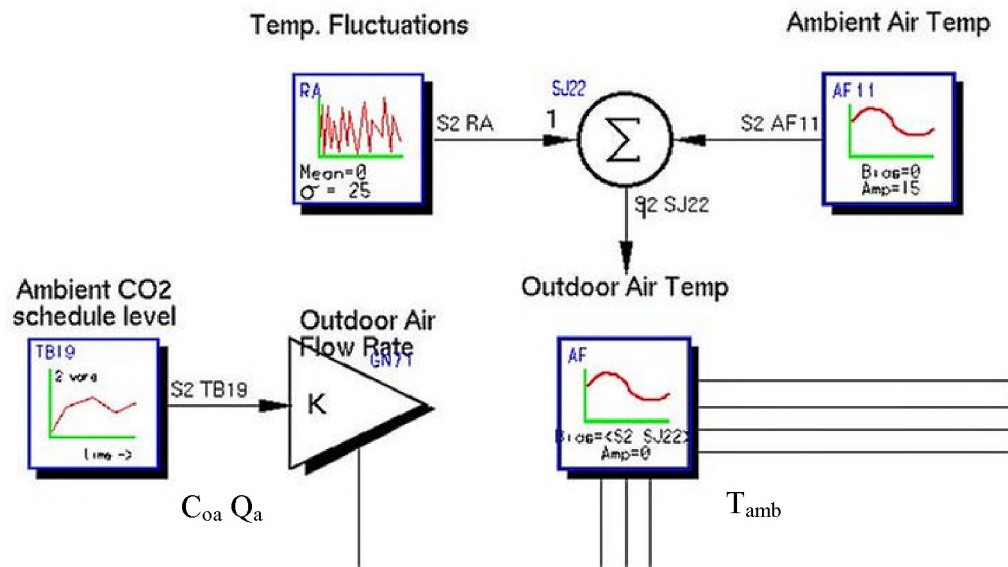


Figure 3.23 Outdoor air parameters.

by the user at the start of the simulation. An integration step size of 0.01 h is chosen to obtain an accurate solution for the integration, and obtain a smooth curve in the data generated by the simulation. Larger step sizes produce fewer data points resulting in staircase looking graphs. Solutions for smaller step sizes are similar to those for the chosen step size but result in longer simulation times. Multiple solution methods to the integration are also available. The integration method for this study is the default method within Easy5, namely, the Boeing Computer Services gear method. This method is a variable step integration method. Comparisons of the results of the numerical integration method to those from an analytical solution show nearly exact agreement (Groszczyk and Smith, 1999).

3.5 Summary

The physical model of the system in Chapter 2 is expressed as a system of icons. Easy5, an icon-based GUI, allows a system like this to be expressed in the form of icons. Using connection lines that pass numerical values between function blocks, a system of equations is implemented. Icons are coupled together to form submodels. Submodels provide visual correlation between the physical and icon models. In this study, icons are connected together via connection lines and then grouped to form submodels. These submodels take the form of the components in the AHU and the zones. This system of submodels is then executed through the Easy5 solving capabilities. The numerical and graphical outputs of this system are discussed in Chapter 4. It should be noted that, due to the number of cases considered in Chapter 4, the Easy5 figures presented here may not contain all the details of the final model.

CHAPTER 4

RESULTS AND DISCUSSION

4.1 Introduction

The simulation model is described in Chapter 2 and implementation is described in Chapter 3 using Easy5. Attention is directed in this Chapter to examining results from the model for several values of the governing parameters and several operating conditions. The model is exercised through various cases to show that each component is working properly. Each test focuses on a different aspect of the model in either the AHU or the Zones. Input parameters are modified for each case to emphasize certain aspects of the system; to verify the ability of the model to work properly; and to obtain results for typical operating conditions. Initial cases show the control aspects of the model. Further applications of the model focus on the comparison of different input parameters to justify which case is “better” than another.

Each case is referenced from the values in Tables 4.1, 4.2, and 4.3 and changes are made according to the case simulated. These tables contain numerical values for the parameters that are similar to those at the ERS (Price and Smith, 1998). This study uses a CAV approach where the flow rate of supply air is fixed at 2400 cfm thereby giving 600 cfm per zone. The CC in the AHU is three times the size of the HC, and is accounted for in the volume of the coils. Because of this, the maximum loads for the cooling and heating coils are set at 210 and 160 kBtu/h respectively. These parameters give a good representation of real world data to show the validity of the model. It is noted that values of ρ , c , and V in combination form the capacitances of the components in the system. The product of these values is the important factor to consider when examining

Table 4.1 Numerical values of model parameters for AHU.

Parameter	Symbol	Value	Units
Air flow rate	Q_a	2,400	ft ³ /min
		144,000	ft ³ /h
Recirculated air flow rate (25%)	Q_r	36,000	ft ³ /h
Outdoor air CO ₂ concentration	C_{oa}	300	ppm
Heating coil: density	ρ_h	556	lb _m /ft ³
specific heat	c_h	0.092	Btu/lb _m -°F
volume	V_h	0.16	ft ³
capacity	q_{hmax}	120,000	Btu/h
Cooling coil: density	ρ_c	556	lb _m /ft ³
specific heat	c_c	0.092	Btu/lb _m -°F
volume	V_c	0.48	ft ³
capacity	q_{cmax}	210,000	Btu/h
Supply fan: density	ρ_{sf}	4.3	Btu/lb _m -°F
specific heat	c_{sf}	0.4	ft ³
volume	V_{sf}	4.0	Btu/h
thermal load	q_{sf}	3,000	Btu/h
Return fan: density	ρ_{rf}	4.3	Btu/lb _m -°F
specific heat	c_{rf}	0.4	ft ³
volume	V_{rf}	4.0	Btu/h
thermal load	q_{rf}	3,000	Btu/h
Ambient air temperature	T_0	variable	°F
Initial temperature: heating coil	$T_{2,0}$	55	°F
cooling coil	$T_{3,0}$	55	°F
supply fan	$T_{4,0}$	55	°F
return fan	$T_{6,0}$	70	°F

Table 4.2 Numerical values of model parameters for Zones.

	Parameter	Symbol	Value	Units
Reheat coil:	density	ρ_{rh}	556	lb_m/ft^3
	specific heat	c_{rh}	0.092	$\text{Btu}/\text{lb}_m\text{-}^\circ\text{F}$
	volume	V_{rh}	0.13	ft^3
	capacity	q_{rhmax}	35,000	Btu/h
Wall:	density (concrete)	ρ_w	123	ft^3
	specific heat	c_w	0.2	$\text{Btu}/\text{lb}_m\text{-}^\circ\text{F}$
	area inside	$A_{z,i}$	160	ft^2
	area outside	$A_{o,i}$	160	ft^2
	volume	V_w	90	ft^3
	Heat transfer coefficient (inside)	h_i	4.0	$\text{Btu}/\text{h}\text{-ft}^2\text{-}^\circ\text{F}$
	Heat transfer coefficient (outside)	h_o	6.0	$\text{Btu}/\text{h}\text{-ft}^2\text{-}^\circ\text{F}$
	Zone thermal load	q_x	0	Btu/h
	Solar radiation	S_o	0	Btu/ft^2
Initial temperature: reheat	zone	$T_{rh,o}$	70	$^\circ\text{F}$
	zone	$T_{z,0}$	70	$^\circ\text{F}$
	wall	$T_{w,0}$	70	$^\circ\text{F}$
CO ₂ generation rates				
	Zone 1	$G_{z,1}$	0	$\text{ft}^3/\text{h}\text{-m}$
	Zone 2	$G_{z,2}$	0	$\text{ft}^3/\text{h}\text{-m}$
	Zone 3	$G_{z,3}$	0	$\text{ft}^3/\text{h}\text{-m}$
	Zone 4	$G_{z,4}$	0	$\text{ft}^3/\text{h}\text{-m}$
Initial concentrations				
	Zone 1	$C_{z,1}$	300	ppm
	Zone 2	$C_{z,2}$	300	ppm
	Zone 3	$C_{z,3}$	300	ppm
	Zone 4	$C_{z,4}$	300	ppm
Air flow rates				
	Zone 1	$Q_{z,1}$	36000	ft^3/h
	Zone 2	$Q_{z,2}$	36000	ft^3/h
	Zone 3	$Q_{z,3}$	36000	ft^3/h
	Zone 4	$Q_{z,4}$	36000	ft^3/h
Zone volume				
	Zone 1	$V_{z,1}$	2400	ft^3
	Zone 2	$V_{z,2}$	2400	ft^3
	Zone 3	$V_{z,3}$	2400	ft^3
	Zone 4	$V_{z,4}$	2400	ft^3
Effectiveness				
	Zone 1	m_1	1	-
	Zone 2	m_2	1	-
	Zone 3	m_3	1	-
	Zone 4	m_4	1	-

Table 4.3 Numerical values of general model parameters.

Parameter	Symbol	Value	Units
Air density	ρ_a	0.071	lb _m /ft ³
Air specific heat	c_a	0.240	Btu/lb _m -°F
AHU			
Proportional gain coefficient	K_p	0.008	1/°F
Integral gain coefficient	K_i	0.6	1/°F-h
Zones			
Proportional gain coefficient	K_p	0.1	1/°F
Integral gain coefficient	K_i	0.8	1/°F-h
Simulation time	t_f	6	h

Table 4.4 Simulation cases.

Number	Testing	Comment
Case 1.0	Zones	Setpoint change
Case 2.0	Zones	Zone load change
Case 3.0	AHU	Heating setpoint change
Case 4.0	AHU	Heating ambient air change
Case 5.0	AHU	Cooling setpoint change
Case 6.0	AHU	Cooling ambient air change
Case 7.0	AHU	PI controller sensitivity
Case 8.0	System	All heating mode
Case 8.1	System	All heating mode – improved controller
Case 8.2	System	Complete simulated system – heating
Case 8.3	System	Setpoint temperature set back
Case 9.0	System	Complete simulated system – cooling
Case 9.1	System	Setpoint temperature set back
Case 10.0	System	Without feedforward stable coefficients
Case 10.1	System	With feedforward stable coefficients
Case 11.0	System	Without feedforward unstable coefficients
Case 11.1	System	With feedforward unstable coefficients
Case 12.0	Zones	CO ₂ generation in zone 1
Case 12.1	System	Scheduled CO ₂ generation in zones
Case 12.2	System	Increased air flow effect on CO ₂ generation

the input values, not the values of the individual terms. Parameters listed in Table 4.2 show values of the input parameters for each of the four zones. Data are given for such items as reheat coil, size of the room, pollutant concentrations, and air flow rates. The maximum load the reheat coils can produce is 35 kBtu/h. Table 4.3 is a listing of general parameters that govern the system. The integral gain coefficient for the AHU is $0.6 \text{ } 1/^{\circ}\text{F-h}$ while the proportional gain coefficient is $0.008 \text{ } 1/^{\circ}\text{F}$. The integral gain coefficient for the zones is $0.8 \text{ } 1/^{\circ}\text{F-h}$ and the proportional gain coefficient is $0.1 \text{ } 1/^{\circ}\text{F}$. Using a trial and error procedure, the values of the gain coefficients were obtained from “tuning” the controller and selecting coefficients that control each unit to minimize overshoot and oscillations in the controlled temperature. The control of the AHU and zones uses only the PI algorithm control for the cases. The addition of feedforward control is investigated at a system wide level in Section 4.4.3.

The number and description of each case is described in Table 4.4. Once the different cases are configured and the simulation executed, the data are plotted using Easy5’s internal graphing program to give an instant feedback on the results from the simulation. However, for graphing purposes, the data are imported into MATLAB, where figures are produced using the graphing capabilities in MATLAB. Graphs are produced for each simulated case and are discussed further in this chapter. The remaining portion of this Chapter discusses different simulation cases that are performed with the model. Each case is unique in showing different working aspects of the components and verification of their functionality. Following each case, a figure that displays the results of the simulation, along with an explanation of the figure and the impact on the system is presented.

4.2 Zone control

To begin the simulations, focus is directed toward showing the temperature control within the zones. Because all of the zones are identical for these cases, only the results of the first zone are examined. Two cases are formed to show zone control, Case 1 and Case 2. In Case 1, the setpoint temperature is scheduled to change during the simulation time from 70 to 75°F over a period of 2 h starting at the end of the second hour of simulation. Figure 4.1 shows the results for Case 1. $T_{z,1}$, T_{sp} , and T_4 are plotted versus time as well as the value of q_{rh} versus time. As seen in Figure 4.1a, control is maintained meaning that there are few oscillations, small peak-to-peak values, and the value decays rapidly during the setpoint change. $T_{z,1}$ follows closely the desired setpoint change. Figure 4.1b shows how the reheat coil responds during the setpoint change. The reheat coil is activated to provide and correct for the temperature change. This is indicated by a rapid increase in energy for the coil. The reheat coil is activated to increase the zone temperature from $t = 2$ to 4 h of the simulation corresponding to the setpoint time change.

Case 2 is simulated to show zone control when an increase in the thermal load in the zone occurs. The setpoint temperature is maintained at 70°F over the simulation time while a sudden load q_{x1} is imposed on the zone for two hours beginning at the second hour of simulation. The value of q_{x1} is changed from 400 to 2400 Btu/h to simulate five people entering the room generating a total of 2 kBtu/h body heat. The value of 400 Btu/h-person is taken as the amount of heat generated for a typical person working in an office environment (ASHRAE, 1993). Figure 4.2 shows the results of this simulation. The insert in Figure 4.2a indicates that the zone temperature is maintained close to the setpoint temperature with only a minor fluctuation when the load is applied and removed. Figure 4.2b shows the reheat and zone thermal loads. The reheat coil reduces the amount of thermal energy applied to the system because the additional heating load provides

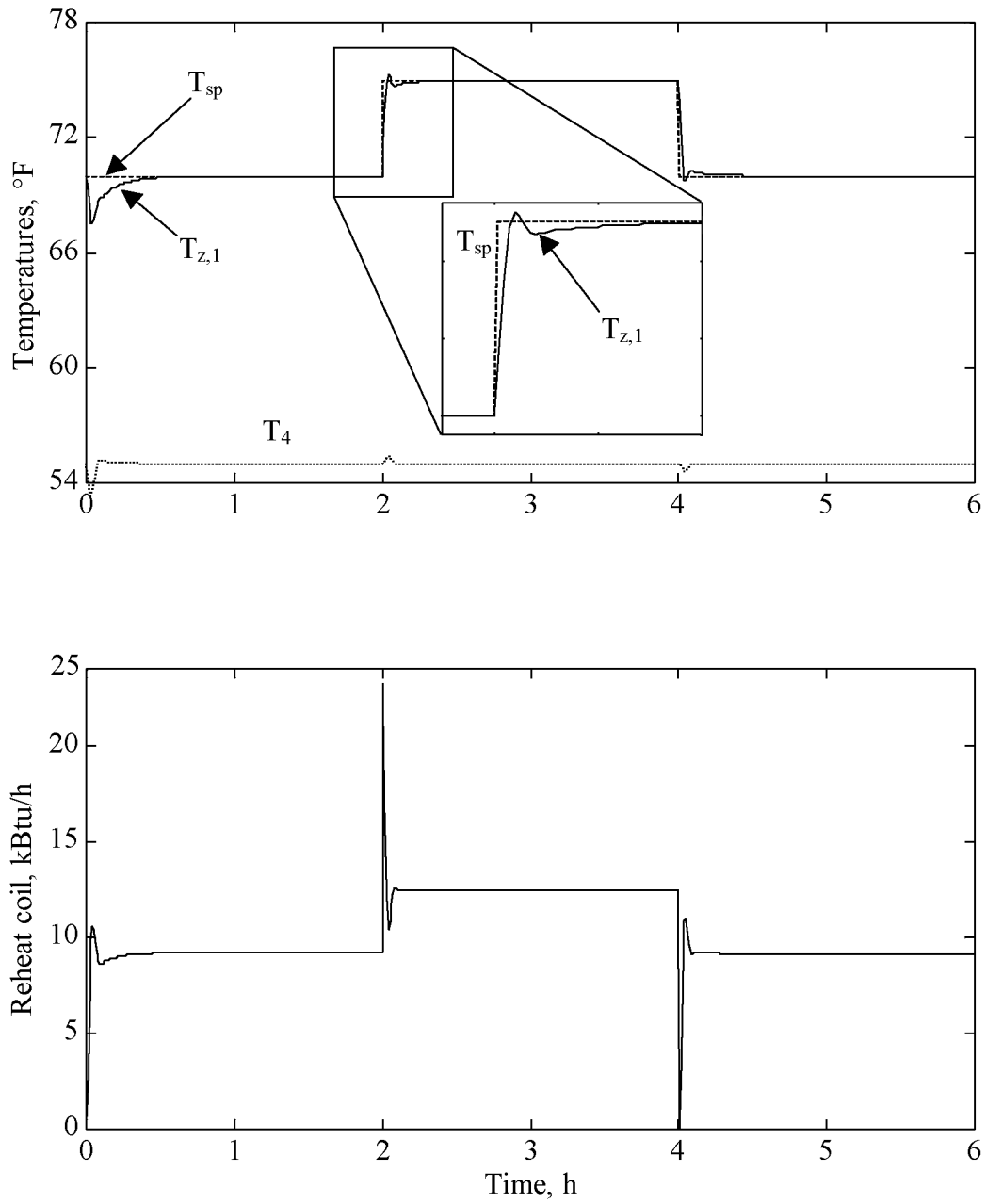


Figure 4.1 Case 1 setpoint temperature change within a zone.

enough heat to maintain the room at the setpoint temperature.

Both Figures 4.1 and 4.2 show that the modeled system controls the zone air temperature during setpoint and heating load changes. The reheat coil responds adequately to maintain the desired setpoint temperature without much overshoot or delay in approaching the setpoint temperature. This is an indication that the zones respond properly to different conditions and examination of other components of the system can be examined.

4.3 AHU control

4.3.1 Heating and cooling coil

Attention is now turned to examining the responses of the AHU unit. The following cases test the AHU for control similar to the control for the zones. In each of these cases, attention is focused on the supply air, T_4 . From Figure 2.2, T_4 is maintained and is fed directly into the control block. The first two cases use only the HC to investigate the control of the supply air. In both Cases 3 and 4, the CC is switched off but the capacitance of the CC is still present. Case 3 is similar to Case 1 in that the setpoint temperature is changed to examine control. The simulation schedules a change in $T_{sp,sa}$ from 55 to 65°F for two hours over the course of the simulation while the value of T_{amb} is set to a constant value of 0°F throughout the simulation period. Figure 4.3 shows the results of the simulation. Figure 4.3a shows that T_4 is a constant before the setpoint change and then quickly adjusts to the new $T_{sp,sa}$ in approximately 0.3 h. Similarly, T_4 adjusts back to the original setpoint after 0.3 h after the change of $T_{sp,sa}$. The trend of T_4 follows closely the setpoint temperature. Figure 4.3b shows the value of the energy load of q_h . As $T_{sp,sa}$ is increased, the load changes to maintain the setpoint temperature, levels

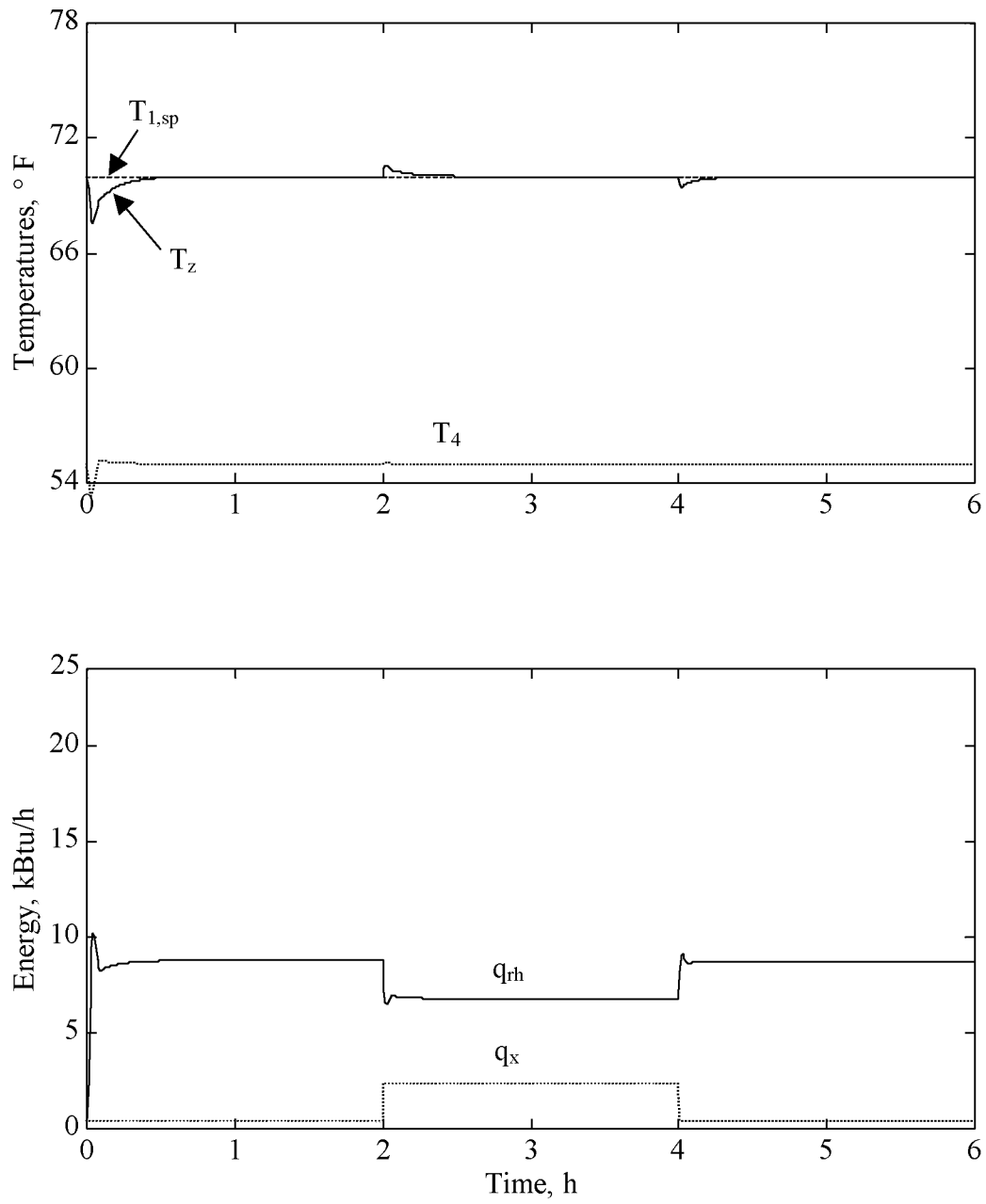


Figure 4.2 Case 2 zone load change.

off at 22.7 kBtu/h once the temperature of 65°F is achieved at $t = 2.05$ h, and then returns to the original value of 0.53 kBtu/h once the setpoint returns to 55°F.

Case 4 examines the change in the load caused by a sudden change in the entering outdoor air temperature. The change in air temperature is reflected by a change in T_1 . The $T_{sp,sa}$ remains fixed at 70°F and T_{amb} fluctuates from 0°F to -10°F for two hours over the course of the simulation. Figure 4.4 shows the results of the simulation. Figure 4.4a shows the temperature fluctuations over the simulation time of 6 h. During the period of T_{amb} change, T_4 changes very rapidly, but is quickly adjusted by the increase in heat as seen in Figure 4.4b. Once T_{amb} returns to 0°F at $t = 4$ h, T_4 “jumps” past the setpoint but quickly returns to 55°F after the heat load is adjusted to compensate for the change in outdoor air temperature. This small “jump” is acceptable since the amount of change is small, 1°F.

Similar to Cases 3 and 4 where the HC is examined, Cases 5 and 6 test the CC. In these two cases, the HC is switched off but the capacitance of the HC is still present. T_{amb} is set at a constant value of 90°F. The setpoint of the supply air is changed in the simulation for Case 5 from 55 to 65°F at hour two and changed back to 55°F at hour four. Figure 4.5a shows the results of Case 5, where T_4 , $T_{sp,sa}$, T_1 , and T_{amb} are plotted versus time for a simulation period of 6 h. The results of Case 5 in Figure 4.5a show that T_4 follows closely to the change in setpoint ($T_{sp,sa}$). The results show good control of the supply air temperature without large oscillations and small peak-to-peak changes and with a smooth curve for transition of temperature. Figure 4.5b shows the value of q_c over the simulation time. The load requirement on the CC remains fixed near -54.6 kBtu/h while $T_{sp,sa}$ remains at 55°F and changes to -32.4 kBtu/h in 0.6 h of the setpoint change to 65°F. The increase in the setpoint temperature indicates that the requirement for cooling decreases, which is shown in Figure 4.5b. During the second setpoint change, q_c returns

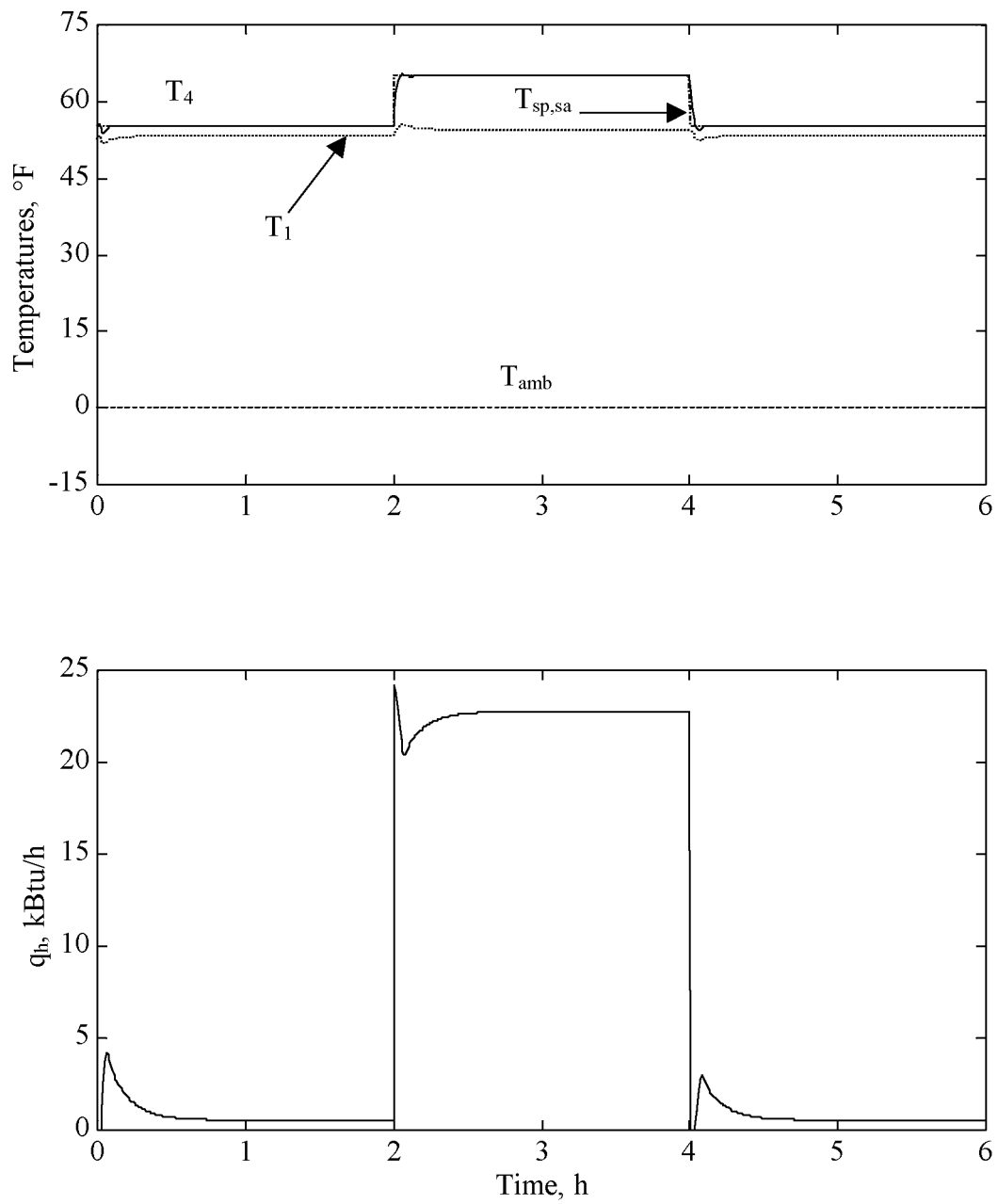


Figure 4.3 Case 3 AHU heating setpoint change.

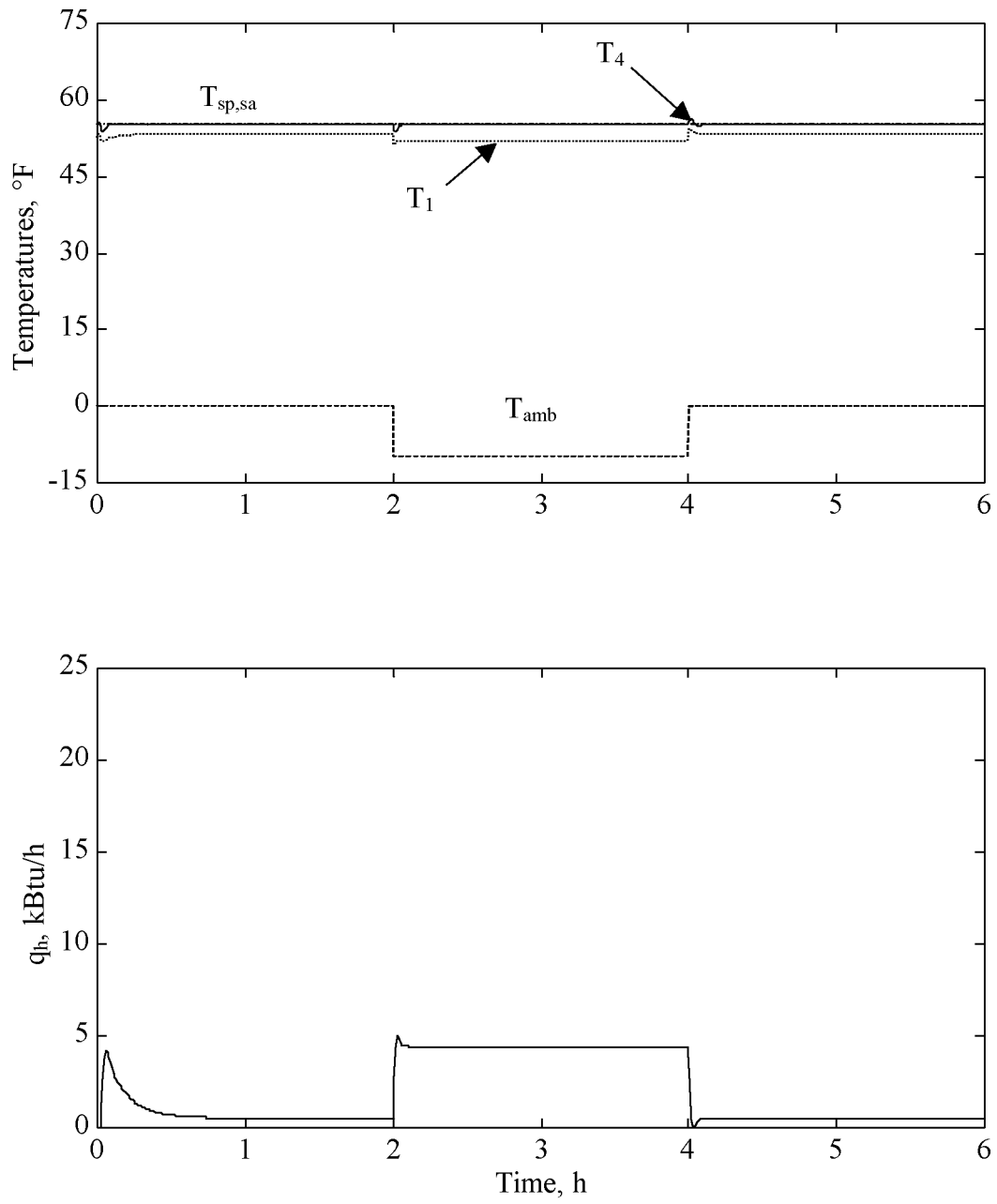


Figure 4.4 Case 4 AHU heating ambient air change.

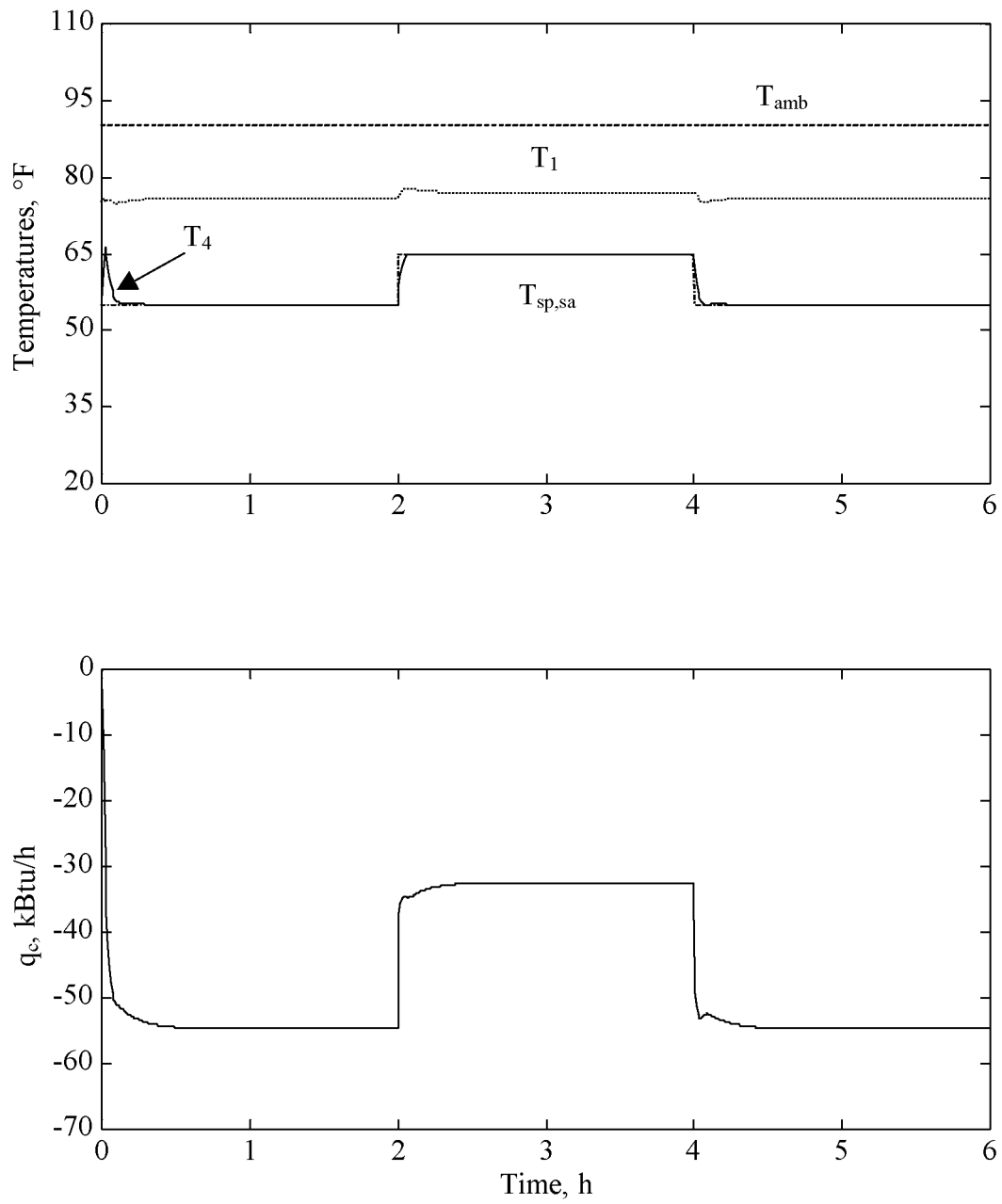


Figure 4.5 Case 5 AHU cooling setpoint change.

to -54.6 kBtu/h within 0.6 h to account for the increase in load change.

Analogous to Case 4 with the HC, Case 6 examines the control of the AHU CC during ambient air temperature change. $T_{sp,sa}$ for the CC is fixed at 55°F. T_{amb} is steady at 90°F for the first 2 h of the simulation and then changes from 90° to 100°F at $t = 2$ h, remains at 100°F until $t = 4$ h, and returns to 90°F for the remaining of the simulation. Figure 4.6a shows the results for T_4 , $T_{sp,sa}$, T_1 , and T_{amb} plotted versus time for a simulation period of 6 h. As seen in Figure 4.6a, the graph of T_4 remains constant at 55°F throughout the simulation with only slight variations during the transition time of the T_{amb} change. While T_4 in Figure 4.6a remains constant, q_c in Figure 4.6b changes to maintain T_4 nearly constant. During the first 2 hours of the simulation, q_c has a steady-state value of -54.6 kBtu/h. During the transition period, q_c adjusts to keep T_4 constant, q_c changes to -63.1 kBtu/h within 0.6 h. Once T_{amb} returns to 90°F, q_c returns to -54.6 kBtu/h within 0.6 h. Both Cases 5 and 6, show that the CC controls the supply air temperature without large oscillations and with a steady transition from one temperature change to another.

4.3.2 Sensitivity to gain coefficients

Now that it has been demonstrated that the PI control algorithm for both the heating and cooling coils of the AHU can control the system around a setpoint temperature, a case is investigated to show the importance of selections of the gain coefficients for the proportional and integral terms. The importance of tuning is mentioned in a study by Salsbury (Salsbury, 1998). The study suggests that even though coefficients may work for one mode of the AHU control, they may not work equally as well in another mode. This suggests that there is an intermediary value of the coefficients that would benefit the system in both a heating and cooling mode. The process of “tuning” a controller for a

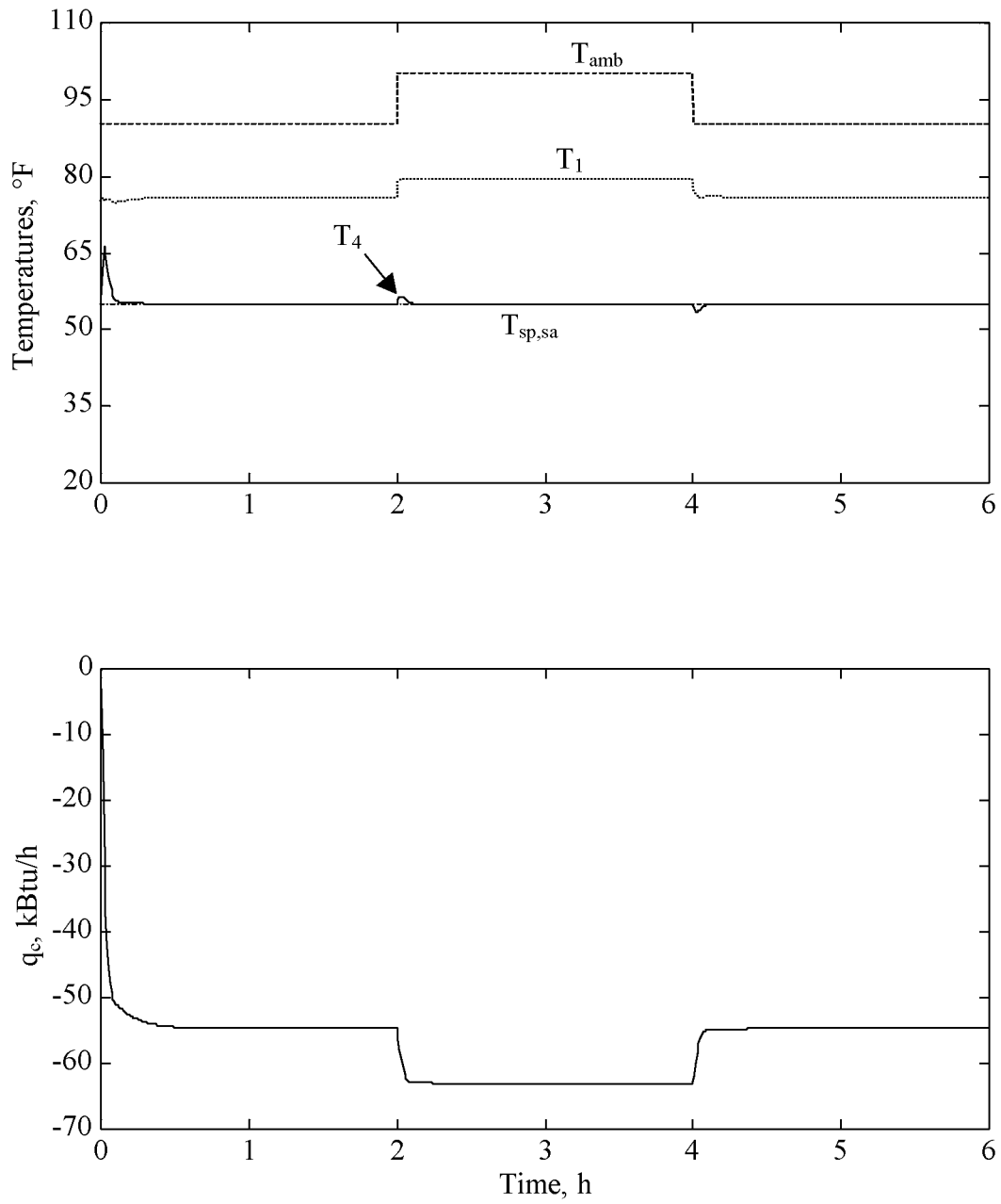


Figure 4.6 Case 6 AHU cooling ambient air change.

particular system obtains values for K_p and K_i in both the heating and cooling mode. The study shows the results of a tuning process when the system is properly “tuned” for only one mode. When only tuned for one mode, the system performs satisfactory for one mode, but not the other mode.

Case 7 examines a simulation in which the same gain coefficients are chosen to control the PI controller in the AHU. During the simulation, $T_{sp,sa}$ is changed from 55 to 65°F at $t = 2$ h until $t = 4$ h. To induce an all heating situation, T_{amb} is set to 0°F while in the all cooling situation, T_{amb} is set to 90°F. Both cases are plotted in Figure 4.7a, where $T_{sp,sa}$, $T_{4,heating}$, and $T_{4,cooling}$ are plotted versus time. It is noted that $T_{sp,sa}$ and $T_{4,cooling}$ are shifted upward by +20°F in Figure 4.7a so that both heating and cooling can be displayed on the same figure. Also, in Figure 4.7b, the absolute value of q_c is taken so both q_c and q_h can be plotted for comparison. For Case 7, $K_i = 0.46$ 1/°F-h and $K_p = 0.2$ 1/°F for the PI control of the AHU. As seen in Figure 4.7a, $T_{4,cooling}$ follows $T_{sp,sa}$ closely without large oscillations and exhibit control. This corresponds to Figure 4.7b, where q_c changes dramatically during the setpoint change, but quickly stabilizes at 32.1 kBtu/h. However, this is not the case when the system enters an all heating mode. $T_{4,heating}$ in Figure 4.7a shows an unstable condition during the setpoint change at $t = 2$ h and reaches 69°F before oscillating around 65°F. The oscillations around 65°F last approximately 0.2 h before decaying and $T_{4,heating}$ reaches 65°F at $t = 1.27$ h after the setpoint change. Figure 4.7b shows the oscillations of the HC during the setpoint change from 55 to 65°F. Values of q_h oscillate between 39.2 and 0 kBtu/h for 0.92 h after the setpoint change. A similar situation occurs when the setpoint changes back to 55°F, smaller oscillations occur before becoming steady, however, they do cause some instability in the temperature between 4.0 and 4.8 h. This case shows the importance of coefficient selection in the “tuning” process to ensure that oscillations do not occur in the output signal.

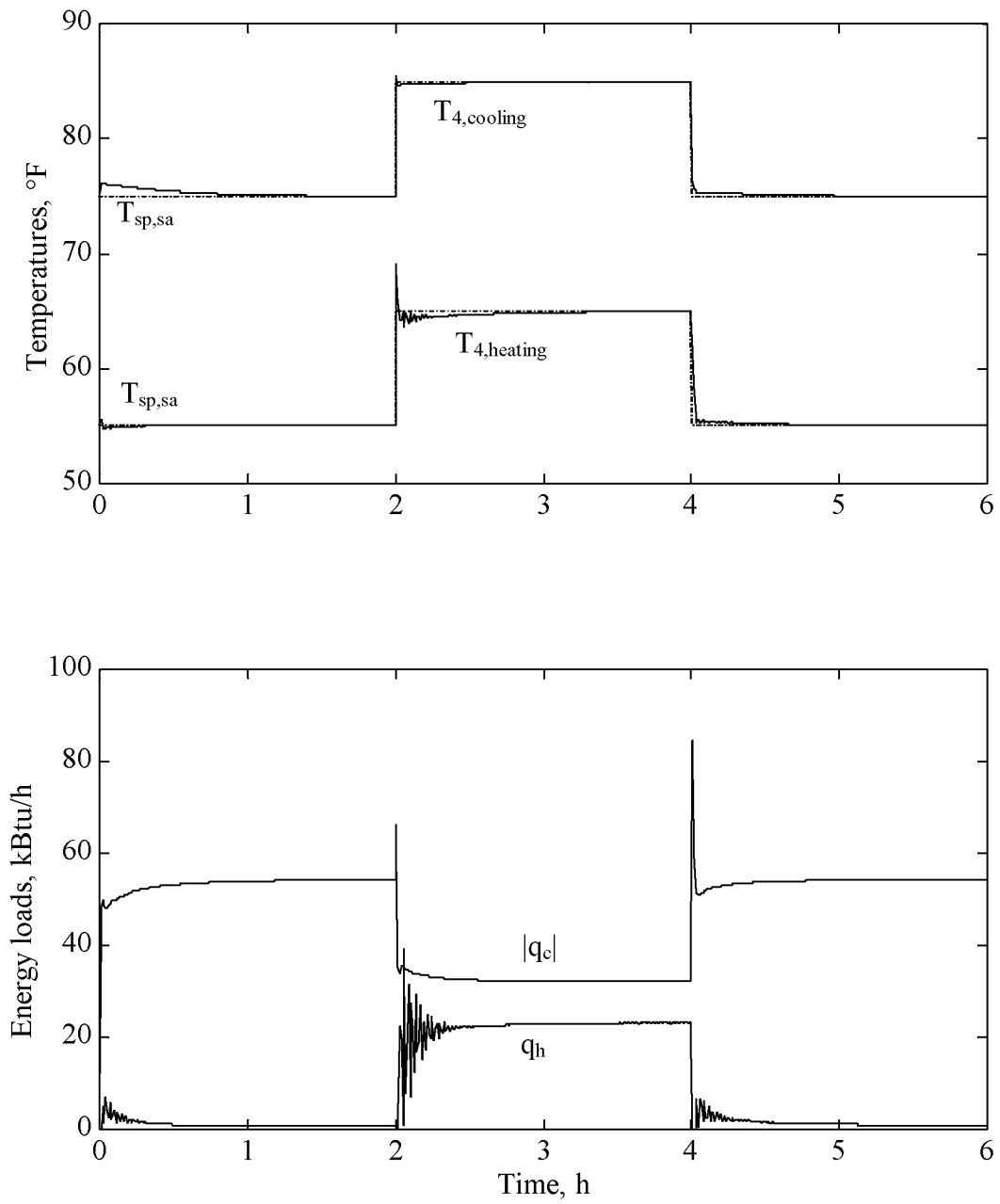


Figure 4.7 Case 7 AHU coefficient sensitivity.

4.4 System control

4.4.1 Heating mode

Now that the component models for the AHU and Zones are shown to function properly and that control can be maintained individually in the AHU and Zones, attention is focused on the combination and interaction between the AHU and the Zones. The system is tested using several different cases to verify a properly operating system. For both the heating and cooling modes, the proportional and integral gain coefficients are 0.008 1/°F and 0.6 1/°F-h for the AHU and 0.1 1/°F and 0.8 1/°F-h for the reheat coils as shown in Table 4.3.

First, the system is tested in an all heating mode. The CC is switched off but the capacitance of the CC is still present. Case 8.0 examines the system with T_4 controlled to a setpoint of $T_{sp,sa} = 55^\circ\text{F}$. To simulate a typical 24 h day during the winter months, T_{amb} is set to a sinusoidal trend with a peak-to-peak value of 30°F centered at 0°F . The lowest temperature of T_{amb} is equal to -15°F at 4 AM and the highest temperature is equal to 15°F at 4 PM. The simulation time, t_f , is 48 h beginning at $t = 0$ h.

Figure 4.8a shows the results of the temperatures of T_{amb} , T_1 , and T_4 plotted over t_f . T_4 is maintained at $T_{sp,sa}$ from $t = 0$ to 11 h and then drifts above $T_{sp,sa}$ because T_{amb} is high and then decreases below $T_{sp,sa}$ as T_{amb} drops. Between $t = 20$ and 30 h, because of the lower value of T_{amb} , T_4 drifts below 55°F to 48°F and then is suddenly returned to 55°F at $t = 30$ h. Figure 4.8b shows that the HC turns off between $t = 10$ and 30 h. However, it would seem that to maintain 55°F , the HC should turn on at $t = 22$ h, but instead the HC turns on suddenly at $t = 30$ h. This finding for the HC displays a characteristic of the PI controller in this mode. Because the system is in the heating mode, during the time when T_4 climbs above $T_{sp,sa}$, the error term in the PI controller is non-zero and the integral term continues to build because of the difference in

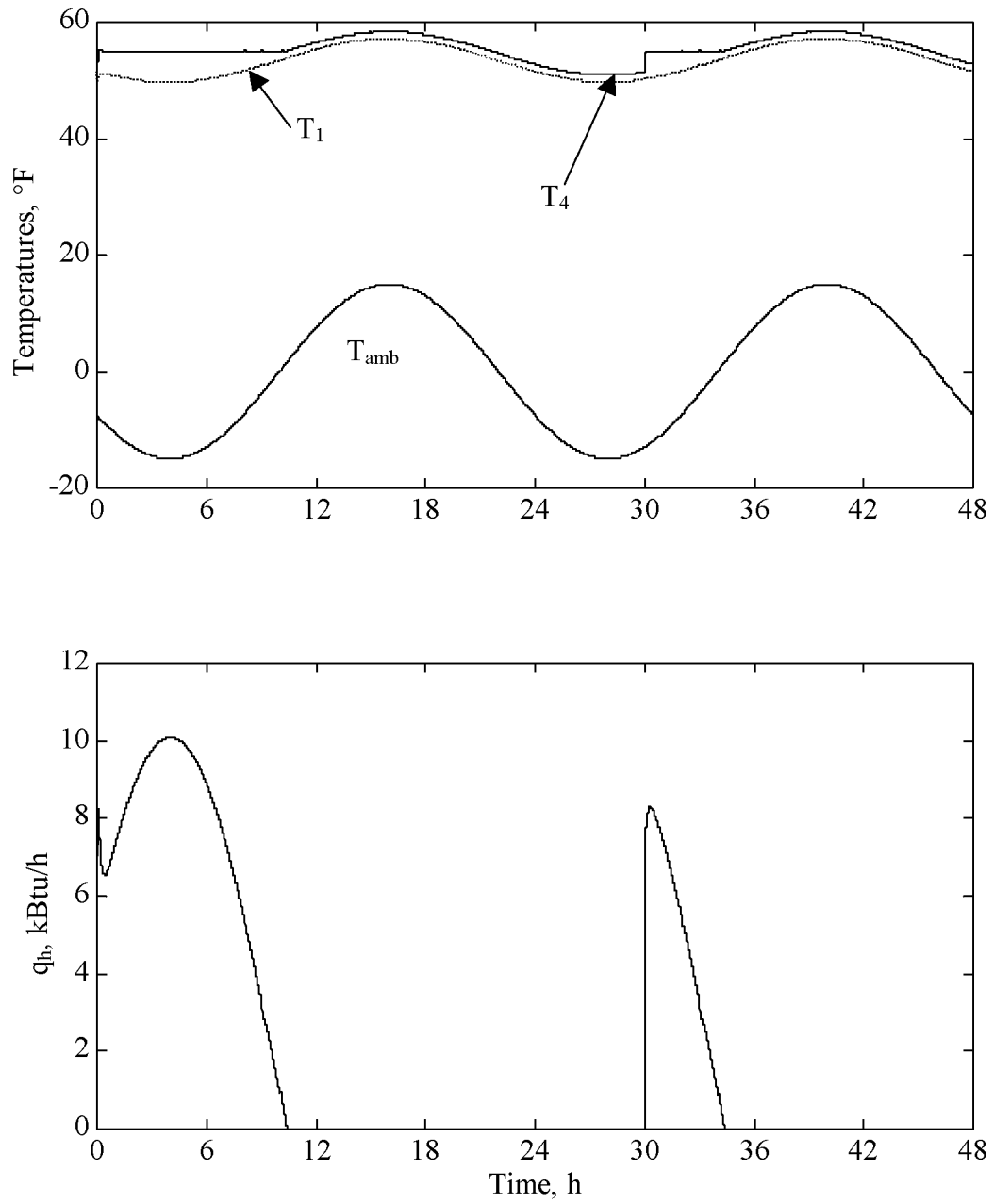


Figure 4.8 Case 8.0 System in all heating mode.

temperature between T_4 and $T_{sp,sa}$ as seen in Eq. (2.25). The integral term is continuously calculated over the simulation time to regulate the flow of heat into the system but T_4 cannot be maintained at $T_{sp,sa}$ because the CC is off. The value of the integral term must be reduced before the HC is switched on to heat the air. The integral term decreases in value for the time period from $t = 22$ to 30 h, where T_4 is less than $T_{sp,sa}$. When the integral is zero, the HC is allowed to switch on to return the supply air to the setpoint temperature.

Case 8.1 addresses this problem of the integral term. The parameters for Case 8.1 are the same as those for Case 8.0, except for the PI controller. A modified PI controller is inserted into the system to govern the K_i coefficient. The K_i coefficient controls the integral term being summed over the simulation time. The modified PI controller contains a FORTRAN block to control the value of the integral coefficient. During times where the difference between $T_{sp,sa}$ and T_4 is more than -0.5°F , K_i is set to zero. Once the temperature difference is less than -0.5°F , the tuned value of K_i is set in the PI controller.

The results of Case 8.1 using the modified PI controller are shown in Figure 4.9. The same variables that are plotted in Figure 4.8 are shown in Figure 4.9. As seen in Figure 4.9a, T_4 remains at or above 55°F . A small “blip” in temperature fluctuation is seen near $t = 22$ h, where the temperature drops slightly below 55°F . This occurs due to the constraint of the error to -0.5°F . Figure 4.9b shows that the HC turns on and off in a cyclic fashion to keep T_4 at 55°F . When Figure 4.8a and Figure 4.9a are compared, the time where T_4 falls below 55°F does not exist in Figure 4.9a, which shows that the modified PI controller works properly for the heating mode case. Similar modifications are included in the PI controller to correct the problem during the all cooling mode as well. Further discussions for the cooling mode case are made in Section 4.4.3.

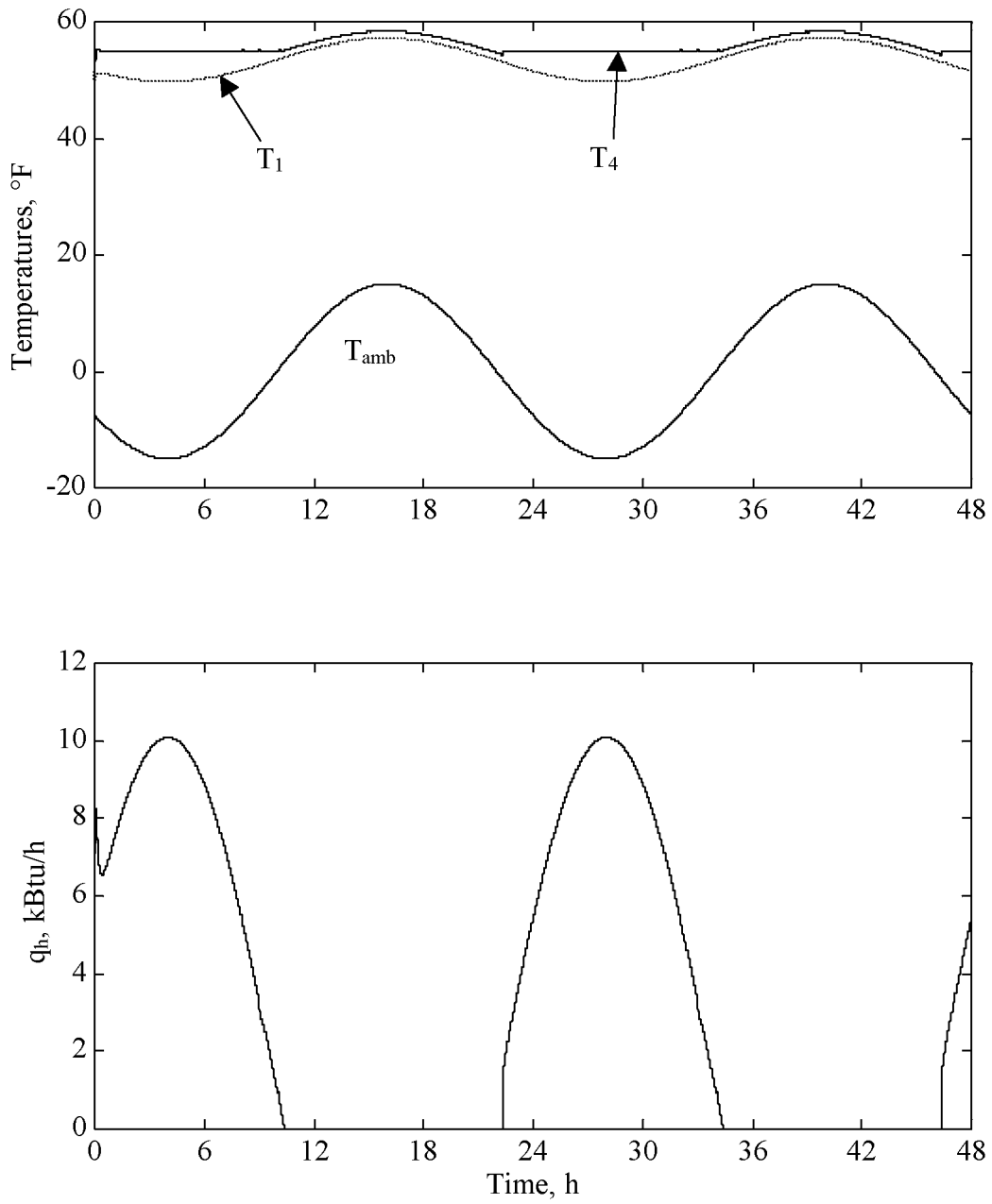


Figure 4.9 Case 8.1 System in all heating mode improved controller.

With the problem of the integral term corrected, a full system simulation in the all heating mode is investigated in Case 8.2. Again, T_{amb} is set to the same condition as in Cases 8.0 and 8.1. However, in this case an element of realism is added by adding minor localized temperature fluctuations to T_{amb} . These minor fluctuations account for the variability obtained in a real world atmosphere and are included to challenge the controllers. Changes in sunlight, cloud cover, and/or wind speed can alter ambient temperatures. To account for these changes, the signal of T_{amb} is expressed as

$$T_{amb} = T_m + A \sin(\omega t + B) + RN(\mu, \sigma) \quad (4.1)$$

where T_m is the temperature the signal is centered about, A is the peak-to-peak amplitude value, ω is the phase equal to 0.2618 rad/h, t is time in h, B is a time shift equal to 3.6652 rad, and RN is a normal-distribution random number generator, where μ is the mean and σ is the standard deviation. The noise is added using a random number generator icon within Easy5. The mean is set to zero and the standard deviation is set to 0.4°F for the inputs to the random number generator inside Easy5. To examine if the random number generator produces random values, a test case is implemented where the random number generator is called several times to produce a distribution. The number of data points used to generate the distribution is 10,000. The random numbers are added to bins with an interval of 0.1°F over the temperature range of -3 to 3°F. The bin values are then divided by 10,000 and 0.1°F to give a frequency of occurrence distribution. The results are given in Figure 4.10. To show that random numbers are generated successfully, the generated random numbers are plotted along with a curve for a normal Gaussian distribution curve. The normal distribution curve is given a mean of zero and a standard deviation of 0.7°F. The independent values for evaluating the normal distribution curve are taken at the upper limit of a bin range. From Figure 4.10, there is an agreement between the mean and standard deviation of the normal distribution curve and the random

number generator. The mean and standard deviation of the bin values are \bar{X} is 0.00375°F and $S = 0.700^\circ\text{F}$. The \bar{X} and S fit close to the normal distribution curve. The discrepancy between the standard deviation of 0.4°F assigned in the icon and 0.7°F computed from the bin data is unexplained at this time.

To further challenge the controllers, scheduled loads to simulate a typical office work day are implemented and are summarized for each of the zones in Table 4.5, where the $T_{sp,z,i}$ is set to 70°F . A base load of 400 Btu/h is selected to represent computers, lights, and other equipment running during the time of non-occupancy. Zone 1 is

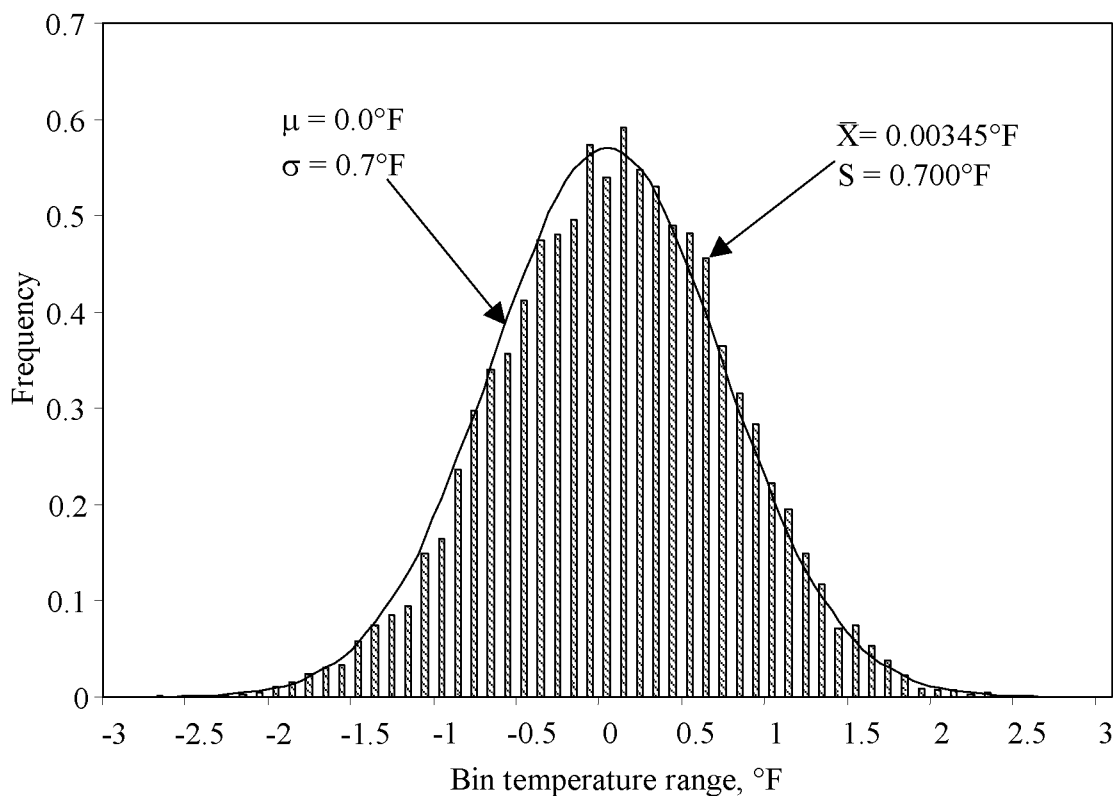


Figure 4.10 Random number distribution.

subjected to a steady additional load of 800 Btu/h during the day time from $t = 8$ to 17 h. The load in Zone 2 is a ramped function over an hour from $t = 8$ to 9 h adding 1200 Btu/h of heat to the zone until it ramps down from $t = 17$ to 18 h. Zone 3 has a load in the morning of an additional 1600 Btu/h, then a load with an hour break from $t = 12$ to 13 h, where the load reduces to the baseline load, and then a load that returns to 2000 Btu/h until $t = 17$ h. Zone 4 simulates a conference room that is occupied for an hour from $t = 9$ to 10 h adding 1600 Btu/h to the zone and again from $t = 13$ to 15 h.

The random noise included in T_{amb} gives a curve as shown in Figure 4.11a. Because the noise signal is added to the system, minor fluctuations are seen throughout the results. The simulation time for Case 8.2 is set at a 24 h period with $T_{sp,sa}$ set to 55°F. It is noted that the true simulation time in Easy5 is 48 h, however, only the results are shown for the last 24 h of the simulation to allow for the system to become stable within the first 24 hours and to reduce the effects of the start-up conditions. The environmental and load conditions are the same for the first and second 24 h periods.

The results for Case 8.2 are shown in Figure 4.11, where the temperatures for each

Table 4.5 Scheduled zone loads.

Time (daily) h	Zone 1 Btu/h	Zone 2 Btu/h	Zone 3 Btu/h	Zone 4 Btu/h
0 – 8	400	400	400	400
8 – 9	1200	ramp to 1600	400	400
9 – 10	1200	1600	2000	2000
10 – 11	1200	1600	2000	400
11 – 12	1200	1600	2000	400
12 – 13	1200	1600	400	400
13 – 14	1200	1600	2000	2000
14 – 15	1200	1600	2000	2000
15 – 16	1200	1600	2000	400
16 – 17	1200	1600	2000	400
17 – 18	400	ramp to 400	400	400
18 – 24	400	400	400	400

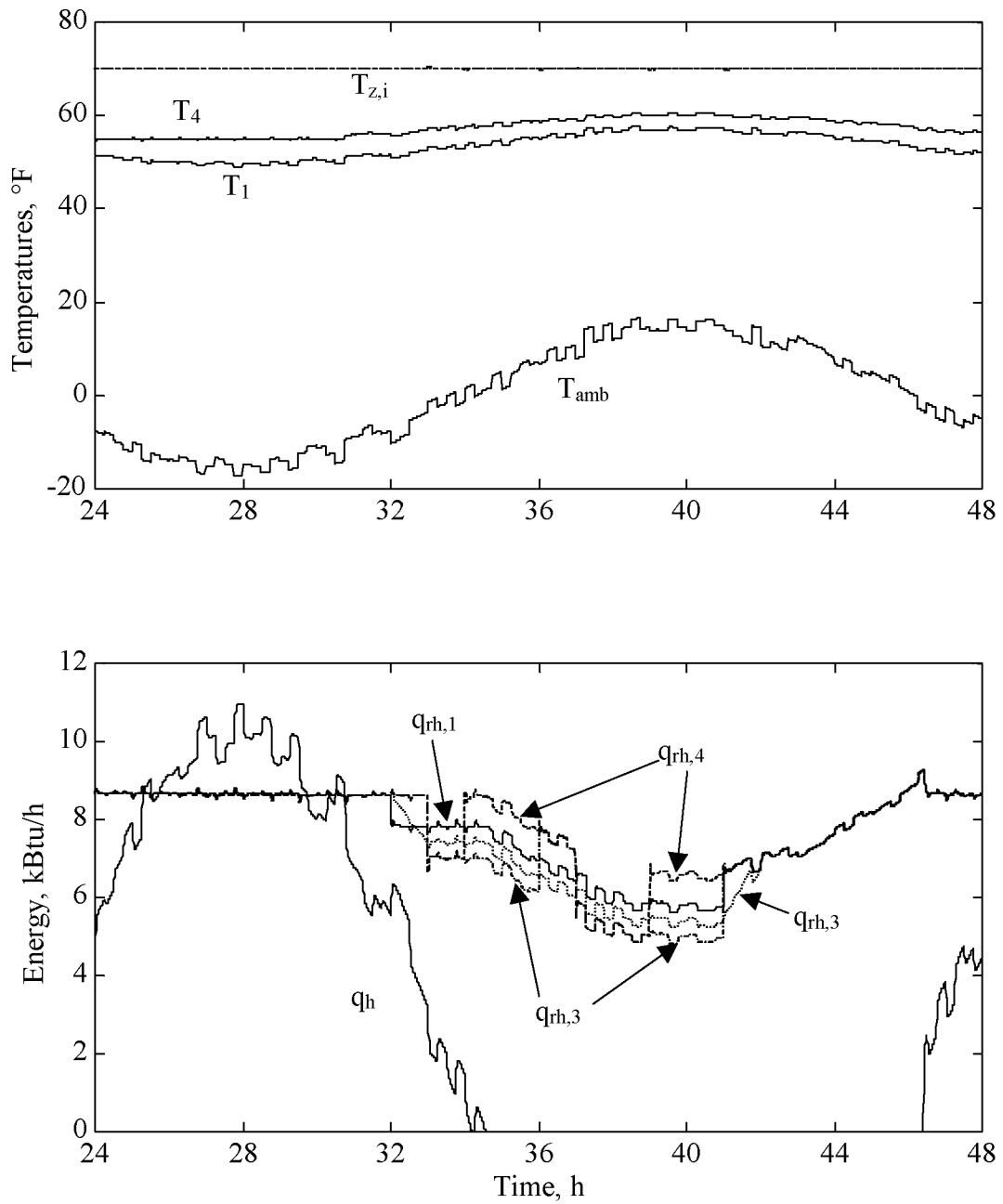


Figure 4.11 Case 8.2 simulated system.

zone are plotted along with T_{amb} , T_1 , and T_4 in Figure 4.11a. Only minor temperature changes occur in each of the zones for brief periods during the load changes as specified in Table 4.5. Figure 4.11b shows the loads for the HC and the reheat coils for each of the zones. As seen by the curves, the HC maintains a profile similar to that of Case 8.1. The reheat coils provide the majority of the extra heat needed to maintain the temperature in each zone. The reheat energy ranges in values between 5 to 8.5 kBtu/h. As seen in Figure 4.11, control is maintained throughout the zones and AHU during the heating only mode.

Case 8.3 investigates the situation of raising $T_{sp,sa}$ to maintain T_4 at a higher temperature so the reheat coils do not use as much energy as when the setpoint temperature is lower. The same parameters that are used for Case 8.2 are used in Case 8.3 except for $T_{sp,sa}$, which is increased from 55 to 60°F to investigate the changes when the setpoint is raised.

Figure 4.12 shows the results of the heating and reheat coils in Case 8.3. Temperatures are not plotted in this result because they are similar to the temperature plot in Figure 4.11a. The results in Figure 4.12 suggest that, by raising the setpoint temperature, q_h increases, and the reheat coil energy is reduced, lowering the load on these components. However, by raising the temperature of the supply air, less energy is used by the reheat coils, but control of the zone temperatures could be lost if a large increase of thermal load energy occurs. If the setpoint temperature is changed to 63°F, the reheat coils at times during the simulation turn off and the zone temperature rise above their setpoint causing a loss of control for the zone temperatures until the load is removed. This could be remedied by using a variable-air-volume (VAV) process to allow more air flow to each zone.

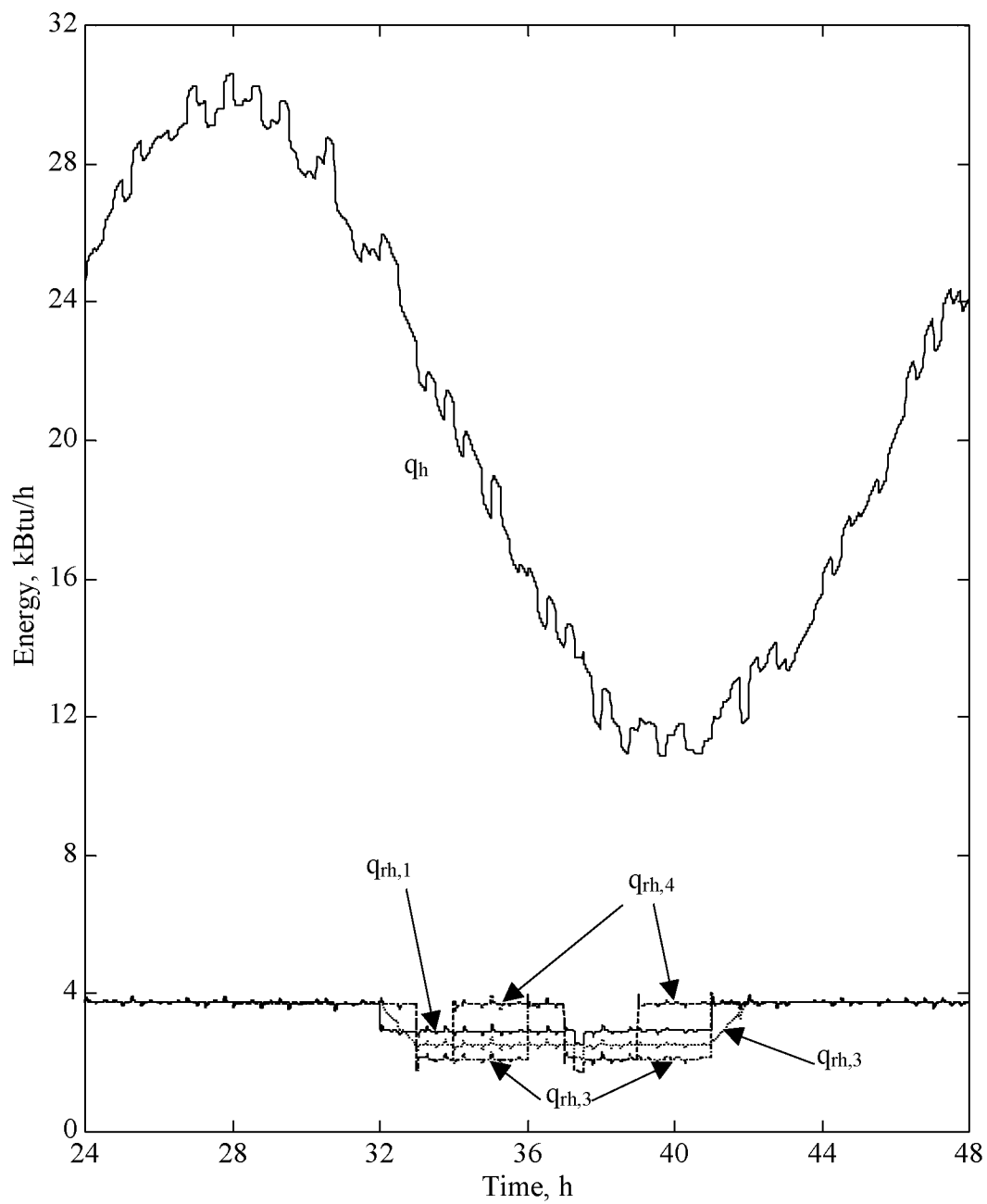


Figure 4.12 Case 8.3 simulated system.

4.4.2 Cooling mode

Like the all heating mode, the system is tested in the cooling mode, where the HC is switched off but the capacitance of the HC is still present. These cases represent the system for a summer operation and the reheat coils in the zones are used to aid in adjusting the temperatures of the zones to a setpoint.

Case 9.0 examines the system in cooling mode, where T_4 is controlled at a constant value of 55°F. T_{amb} is set to act as a sinusoidal temperature range over a 24 h period. The peak-to-peak value of the temperature distribution of 30°F is centered around 80°F. The simulation time is 24 h beginning at $t = 0$ h with the lowest temperature of T_{amb} of 65°F at $t = 4$ h and the highest temperature of 95°F at $t = 16$ h. Random temperature fluctuations are included. It is noted that the true simulation time in Easy5 is 48 h, however, only the results are shown for the last 24 h of the simulation to allow for the system to become stable within the first 24 h. The zones are subjected to the same loads as described in Table 4.5.

Figure 4.13 displays the results of Case 9.0. Figure 4.13a is a plot of T_4 , T_{amb} , T_1 , and $T_{z,i}$ versus t_f . As seen in Figure 4.13a, $T_{z,i}$ represents a steady constant value of 70°F corresponding to the setpoint for the zones. Minor fluctuations in the zone temperatures vary only 1°F peak-to-peak for 0.2 h during the load changes in each zone, but control is still maintained for the zones. The small temperature fluctuations correspond to the energy output of the reheat coils as seen in Figure 4.13b. Figure 4.13b illustrates the energy output of the reheat coils as well as the value of q_c . For graphing purposes, the absolute value of q_c is plotted on the same figure. The sinusoidal behavior of q_c shows that the coil did not shut off during the simulation and the cooling requirement changes as the value of T_{amb} varies throughout the simulation.

Now that the cooling only mode is proven to work in the system, attention is focused

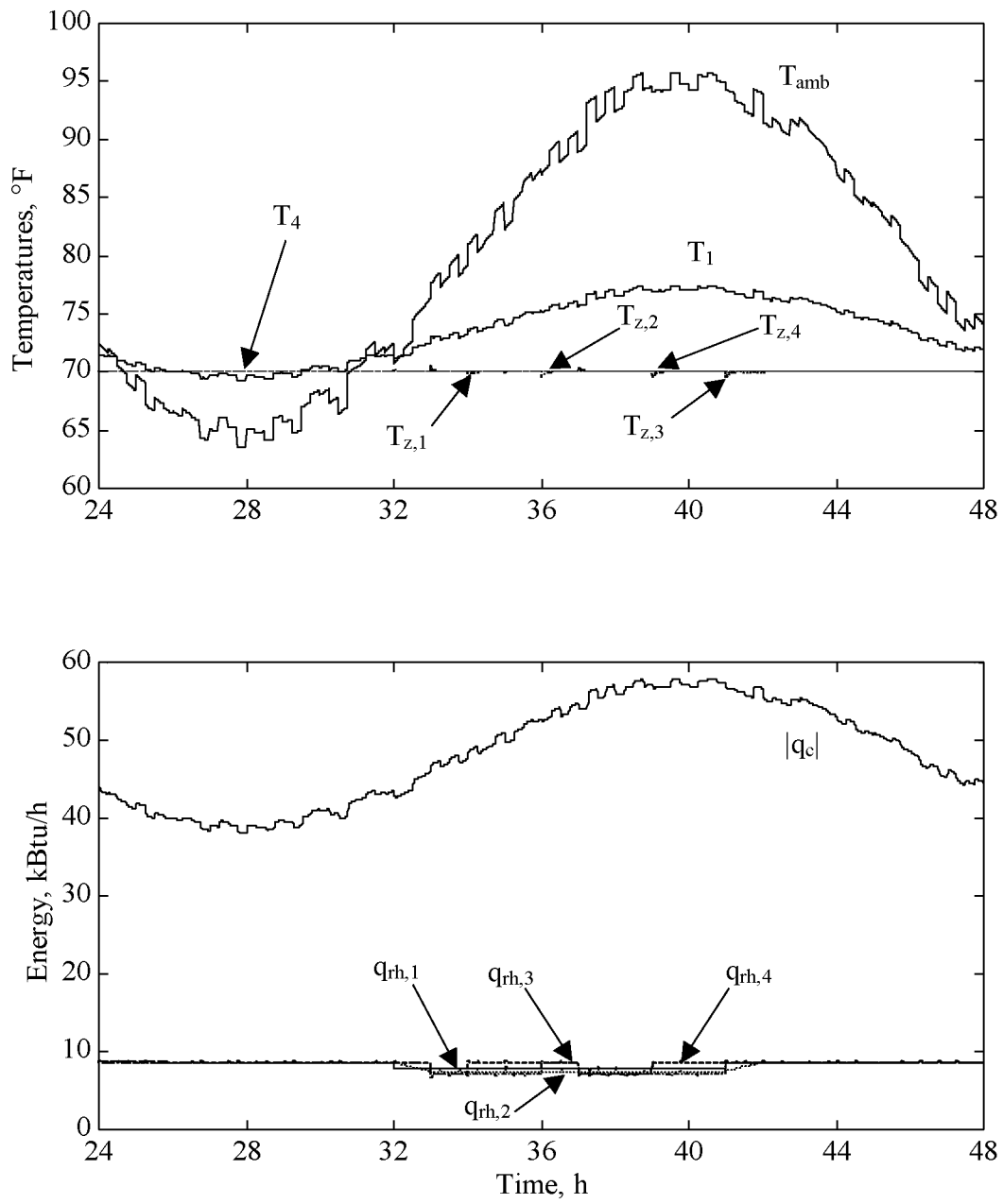


Figure 4.13 Case 9.0 system in all cooling mode.

Table 4.6 Cost function comparison.

	Case 9.0 Btu ² /h	Case 9.1 Btu ² /h
$J_{htg,sqr}$	1.59×10^6	0.416×10^6
$J_{clg,sqr}$	5.67×10^{10}	1.44×10^{10}

on the merit of the system. During the summer, it is desirable to reduce the overall cost of the system by making the system more cost effective. In a paper by Knebel (1999), the question is asked why the setpoint is set at 55°F. Case 9.1 investigates a similar case as Case 9.0 but, to reduce the cost functions, J_{htg} and J_{clg} , T_4 is to be maintained at 65°F instead of 55°F as in Case 9.0. All other parameters remain the same between both cases.

The graphs for Case 9.1 are not shown due to the similarity with those of Figure 4.13. Instead, a comparison is made between J_{htg} and J_{clg} to evaluate the overall merit of the two cases. Table 4.6 displays the results for the cost functions of Case 9.0 and 9.1. As seen in Table 4.6, the value for J_{clg} is reduced from 5.67×10^{10} to 1.44×10^{10} Btu²/h. This shows a reduction in energy consumed in the CC. Likewise, there is a decrease in the energy consumed in the reheat coils from 5.67×10^{10} to 1.44×10^{10} Btu²/h. From this it maybe indicated that, by increasing $T_{sp,sa}$ to $T_{sp,z,i}$, costs are decreased as indicated by lower values of cost functions in Table 4.6. Control, however, may be lost with a large input of thermal load for a zone.

4.5 Feedforward control

As shown in Section 2.4.3, FF control is added to the system to complement the FB control algorithm. Salisbury (1998) reported that FF control reduces the reliance on the feedback loop and how the FF loop complements the feedback loop. Two cases are investigated where to ascertain the characteristics of FF control and its effect on the system.

Cases 10.0 and 10.1 examine the effects of FF control using the stable proportional and integral gain coefficients other than those values cited in Section 4.4. Test parameters for both of these cases are like those of Case 8.3 with a setpoint change of T_4 from 52 to 55°F. During the night-time operation of the building, the setpoint is set back to 52°F to conserve energy in the main HC. The setpoint change occurs in the morning before the occupants arrive when $t = 31$ h. This case focuses on results from $t = 30$ to 32 h to capture only the setpoint change and the resultant behavior of T_4 and the energy required. In Case 10.0, FF control is inactive, relying only on feedback control, and FF is turned on in Case 10.1 to compare the changes from Case 10.0. The proportional coefficients of the FF control are tuned according to the suggested values by Salsbury (1998). The values for K_1 and K_2 are 0.01 and 0.0075 1/°F.

The results of Cases 10.0 and 10.1 are displayed in Figure 4.14, where the temperatures and heat transfer rates in the left column are for only feedback and those in the right column have FF added. In examining Figure 4.14a, two important traits of the curves are observed. First, in examining the curve $T_4 - 10.1$ during the setpoint change, the slope is greater than $T_4 - 10.0$ during the same time period. Hence, for the feedforward case, the setpoint temperature is reached faster. Secondly, the FF control shows a smoother curve in $T_4 - 10.1$ than in $T_4 - 10.0$ indicating that the FF control dampens oscillations in the system, which demonstrates better control. The results reported by Salsbury (1998) for feedforward control display similar characteristics. In comparing both curves in Figure 4.14b, the results appear very similar indicating, for the same amount of energy, the two previously mentioned advantages can be obtained. This is supported by the values of J_{htg} . J_{htg} for Case 10.0 is 1.552×10^8 Btu²/h while J_{htg} for Case 10.1 is 1.559×10^8 Btu²/h a difference of 7×10^5 Btu²/h, which is minor enough to conclude the addition of FF control is valid.

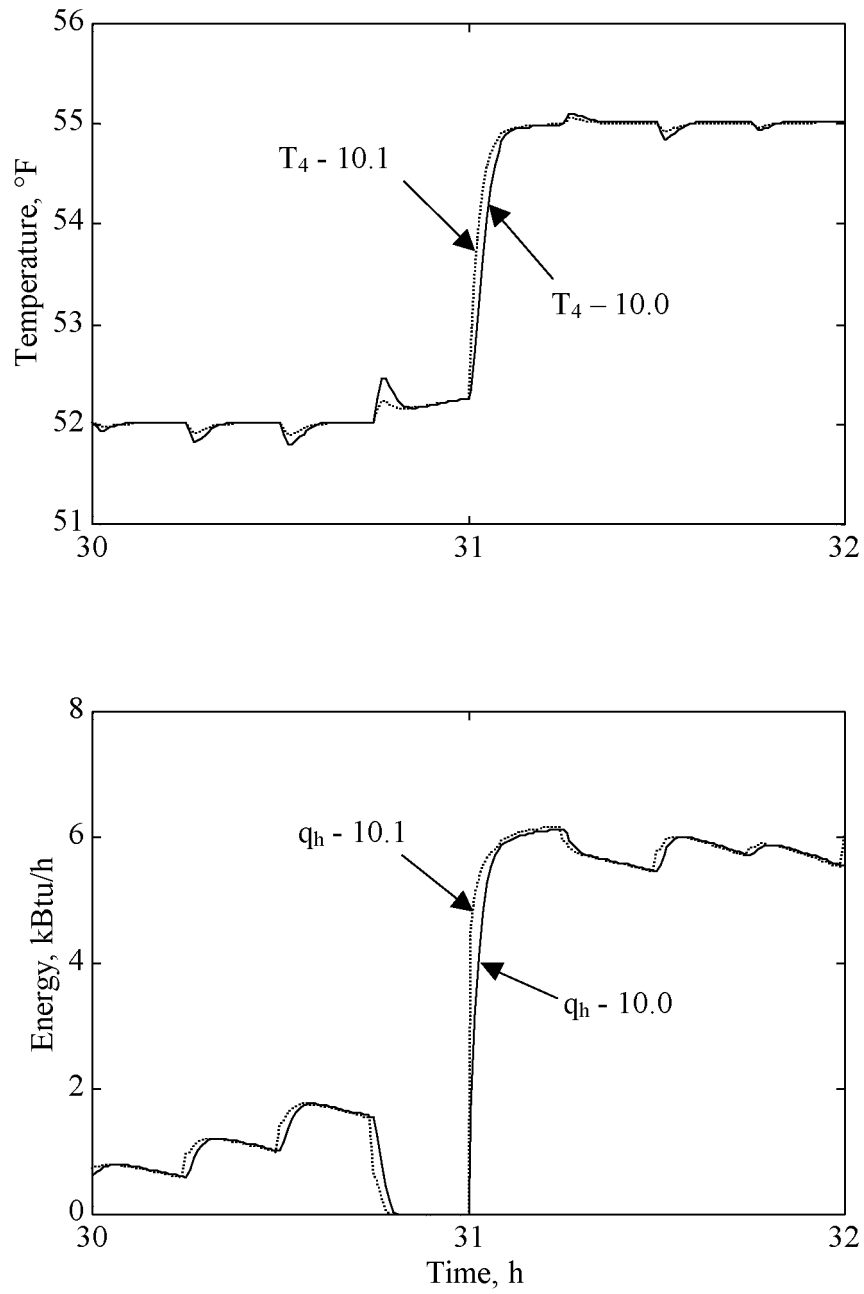


Figure 4.14 Cases 10.0 and 10.1 without and with FF control.

Now that FF is examined using the stable proportional and integral gain coefficients, it is desired to examine the effect of FF control for the system using the unstable coefficients for the PI controller cited in Section 4.3.2. The same system parameters used for Cases 11.0 and 11.1 are those for Cases 10.0 and 10.1 except for the values of the proportional and integral gain coefficients, which are changed to the unstable values from Case 7 of $K_i = 0.46 \text{ 1/}^\circ\text{F-h}$ and $K_p = 0.2 \text{ 1/}^\circ\text{F}$.

The results of Cases 11.0 and 11.1 are shown in Figure 4.15. Again, only the results for the one-hour time periods before and after the setpoint temperature change are examined. Both Figure 4.15a and b show the instability in the system when the setpoint change occurs. When t is between 30 and 31 h, the temperature fluctuations are decreased with the FF control in Figure 4.15b when compared to Figure 4.15a. The FF control slightly dampens the oscillations in the signal producing a more stable signal. This also occurs after the setpoint change when the temperature steadies to 55°F . Case 11.0 steadies approximately 0.33 h after the setpoint change while Case 11.1 steadies approximately 0.19 h after the change. Similarly, examining Figure 4.15c and d, the energy output during $t = 30$ to 32 is dampened somewhat in Case 11.1 when compared to Case 11.0. Examining the merit for both cases finds that J_{htg} for Case 11.0 is $1.706 \times 10^8 \text{ Btu}^2/\text{h}$ while in Case 11.1 J_{htg} is found to be $1.734 \times 10^8 \text{ Btu}^2/\text{h}$ a difference of $2.9 \times 10^6 \text{ Btu}^2/\text{h}$. The additional cost for Case 11.1 is due to the higher values of q_h that occur immediately after the setpoint change. From Figure 4.15d, the large peak in energy when the setpoint is changed is larger than in Figure 4.15c, resulting in higher energy costs. The higher costs could be justified due to the reduced wear on the system by using a more damped and controlled system.

From these cases the use of FF control, though not as drastic a change in control as reported by Salsbury (1998), is an improvement to the system. The findings of this study

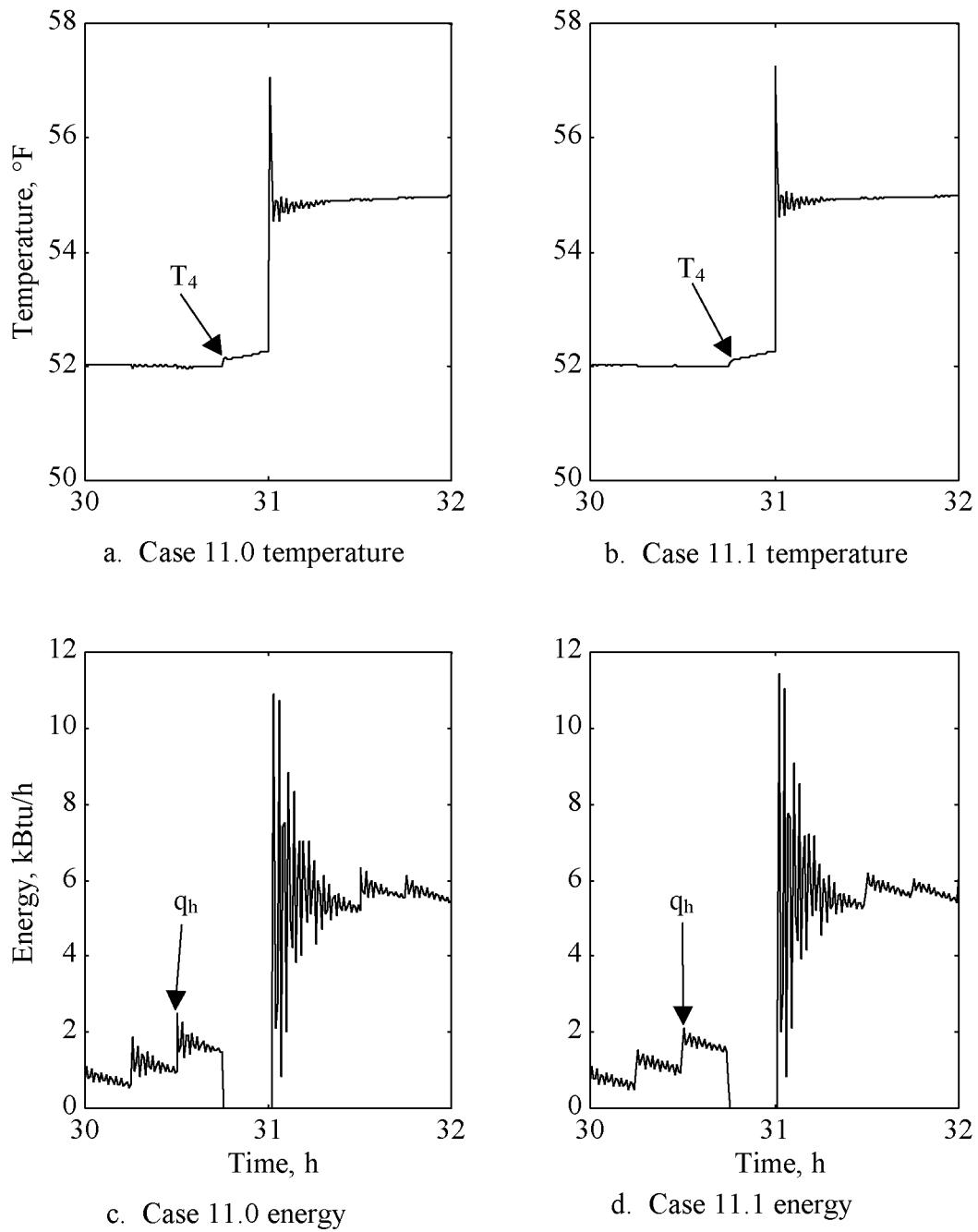


Figure 4.15 Cases 11.0 and 11.1 without and with FF control using instability.

for FF control comply with the results found by Salsbury (1998). Values of the proportional gain coefficients, K_1 and K_2 , could be modified to alter the effect of FF on the system, but are shown in this study to prove that the effect on the system is validated. Although, FF control is not the dominant contributor to the control signal, it does complement the signal where the feedback control signal lacks in control. This conclusion was observed by Salsbury (1998) as well, where he stated that the FF and feedback controllers complement each other, and deficiencies in one controller are compensated for by the other.

4.6 IAQ considerations

After examining responses for the thermal model represented in Section 2.2, the IAQ model of Section 2.3 is tested using the Easy5 simulation. With the thermal model, it is important to control the thermal comfort level of each individual zone. However, in the IAQ model, the monitored comfort level is attributed to the level of CO_2 in the zones. Because the system is a recirculated CAV system, the amount of control to the system is limited to the amount of outdoor air entering the system. Because of this, only suggested outdoor air flow rates can be implemented during the simulation. The IAQ pollutant levels are not actively controlled by changing the percentage of outdoor air. The outdoor air flow brings in a lower concentration of CO_2 to the zones, flushing them of the pollutant. As stated in Section 2.4, levels of CO_2 above 600 ppm produce complaints from the occupants. It is desired, therefore, to maintain levels of CO_2 below 600 ppm to provide adequate IAQ comfort to the zones.

Case 12.0 investigates the effects of a high pollutant generation rate in a single zone. The incoming air CO_2 level is held fixed at 300 ppm which is typical for normal background levels of pollutant in the atmosphere (Walsh, 1984). Like the other

simulations, Case 12.0 is simulated for 48 h, and only the final 24 h are shown. While the other zones are not occupied, Zone 1 receives a large generation rate of CO₂ to simulate a large number of people entering the room at once. This generation rate of 6×10^6 ft³/hr-m of CO₂ occurs from $t = 33$ to 37 h. The unit of “m” for the generation rate refers to million (10^6). This case shows how the pollutant influences the concentration of the other zones and the supply air.

Figure 4.16 illustrates the results from Case 12.0, where concentration in ppm is plotted versus the simulation time where $t = 24$ to 48 h. As seen in Figure 4.16, the generation rate of Zone 1 that increases from zero to 6×10^6 ft³/hr-m at $t = 33$ h results in a new steady state concentration level in Zone 1 of 591 ppm at $t = 34.5$ h. As Zone 1 generates the CO₂, C_{sa} increases resulting in increasing levels of CO₂ in the remaining three zones. C_{sa} , C_{z2} , C_{z3} , and C_{z4} steady at a level of 425 ppm at $t = 36.39$ h. Once the generation rate in Zone 1 is stopped at $t = 37$ h, all zones and supply air return to 300 ppm after 1.38 h. Even with the 6×10^6 ft³/hr-m generation rate in Zone 1, none of the other zones reach the uncomfortable level of 600 ppm. The performance merit J_p is found to be zero for this case.

Case 12.1 examines the pollutant levels and their changing values throughout a work day in the system. Case 12.1 is analogous to Case 8.3 in reference to the load changes. The load changes represent people entering and leaving the room and the levels of CO₂ generation shadow the thermal loads in Table 4.5. Table 4.7 displays the pollutant load generation rates as they change with respect to the thermal loads in Table 4.5. The system is simulated again for 48 h with only the final 24 h being plotted to reduce the influence of the startup conditions. The generation values in Table 4.7 are cycled every 24 h time period. Additionally, to show CO₂ fluctuations with the outdoor air as may occur in the urban environment, C_{oa} in Case 12.1 is ramped up from 300 ppm to

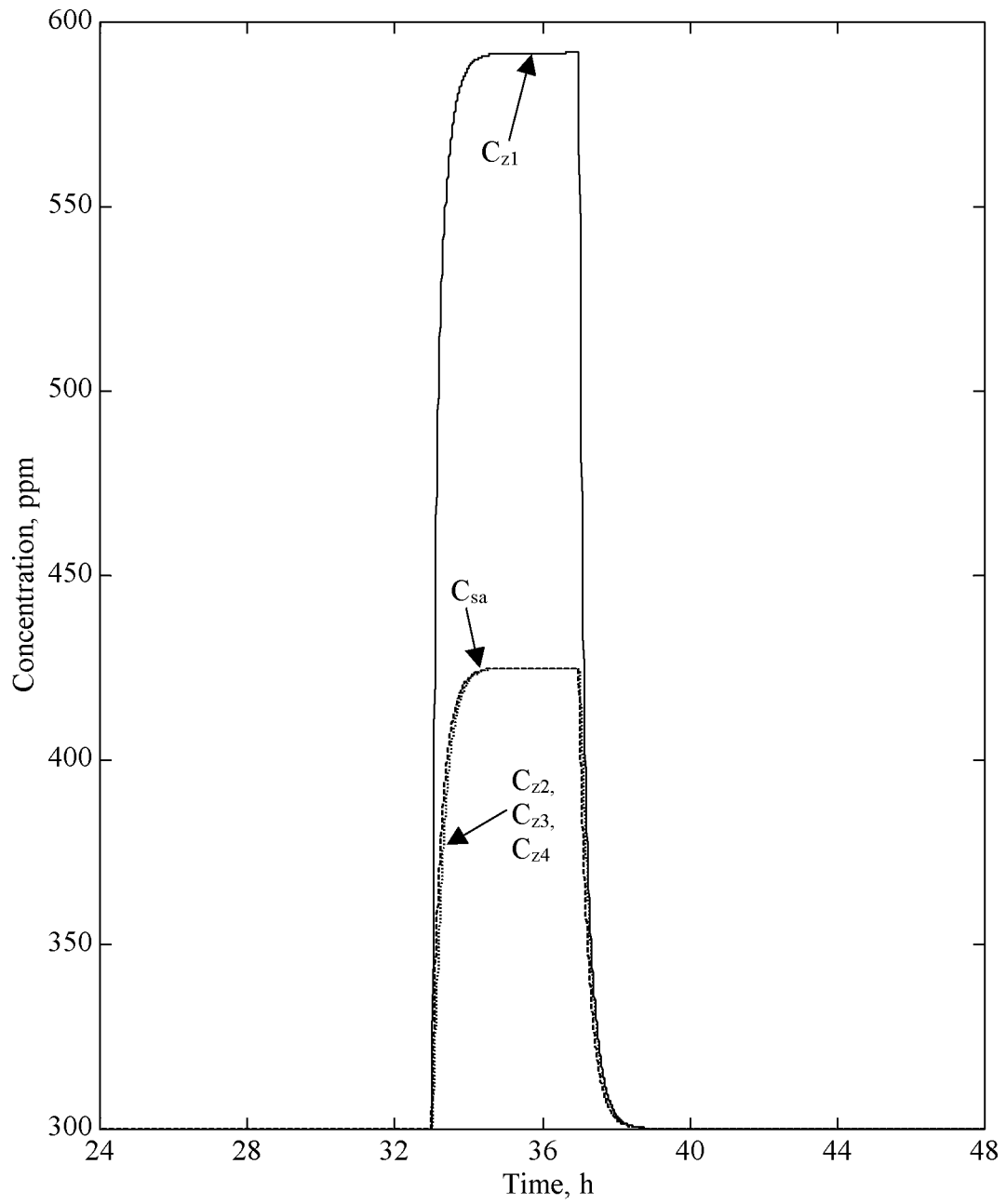


Figure 4.16 Case 12.0 effect of CO₂ generation in Zone 1.

Table 4.7 Scheduled zone CO₂ generation rates.

Time (daily) h	CO ₂ generation rate, ft ³ /hr-m			
	Zone 1	Zone 2	Zone 3	Zone 4
0 – 8	0	0	0	0
8 – 9	1×10^6	ramp to 2×10^6	0	0
9 – 10	1×10^6	2×10^6	3×10^6	3×10^6
10 – 11	1×10^6	2×10^6	3×10^6	0
11 – 12	1×10^6	2×10^6	3×10^6	0
12 – 13	1×10^6	2×10^6	0	0
13 – 14	1×10^6	2×10^6	3×10^6	3×10^6
14 – 15	1×10^6	2×10^6	3×10^6	3×10^6
15 – 16	1×10^6	2×10^6	3×10^6	0
16 – 17	1×10^6	2×10^6	3×10^6	0
17 – 18	0	ramp to 0	0	0
18 – 24	0	0	0	0

400 ppm from $t = 32$ to 33 h then held constant at 400 ppm until $t = 41$ h then ramped down to 300 ppm at $t = 42$ h.

The results of Case 12.1 are plotted in Figure 4.17 where concentrations versus simulation time are shown. As seen in Figure 4.17, the concentrations in each of the zones increase according to the generation rates applied in the zones.. All zones appear to increase in concentration as soon as the first two zones begin to generate the pollutant. Between the time where $t = 32$ and 33 h, Zones 3 and 4 lag behind Zones 1 and 2 where the CO₂ generation occurs for this time period. This trend is confirmed with the fact that no generation is occurring in Zones 3 and 4 during this time and the effect of CO₂ is delayed to these zones as they rely on C_{sa} to supply the zones with the pollutant. However, once Zones 3 and 4 begin to generate the pollutant, levels in these zones quickly increase farther above the other zones. At $t = 34$ h, Zones 3 and 4 obtain a maximum value of 666 ppm. With levels above 600 ppm, complaints of “stuffiness and congestion” could begin, but the levels do not stay at this maximum very long and fall

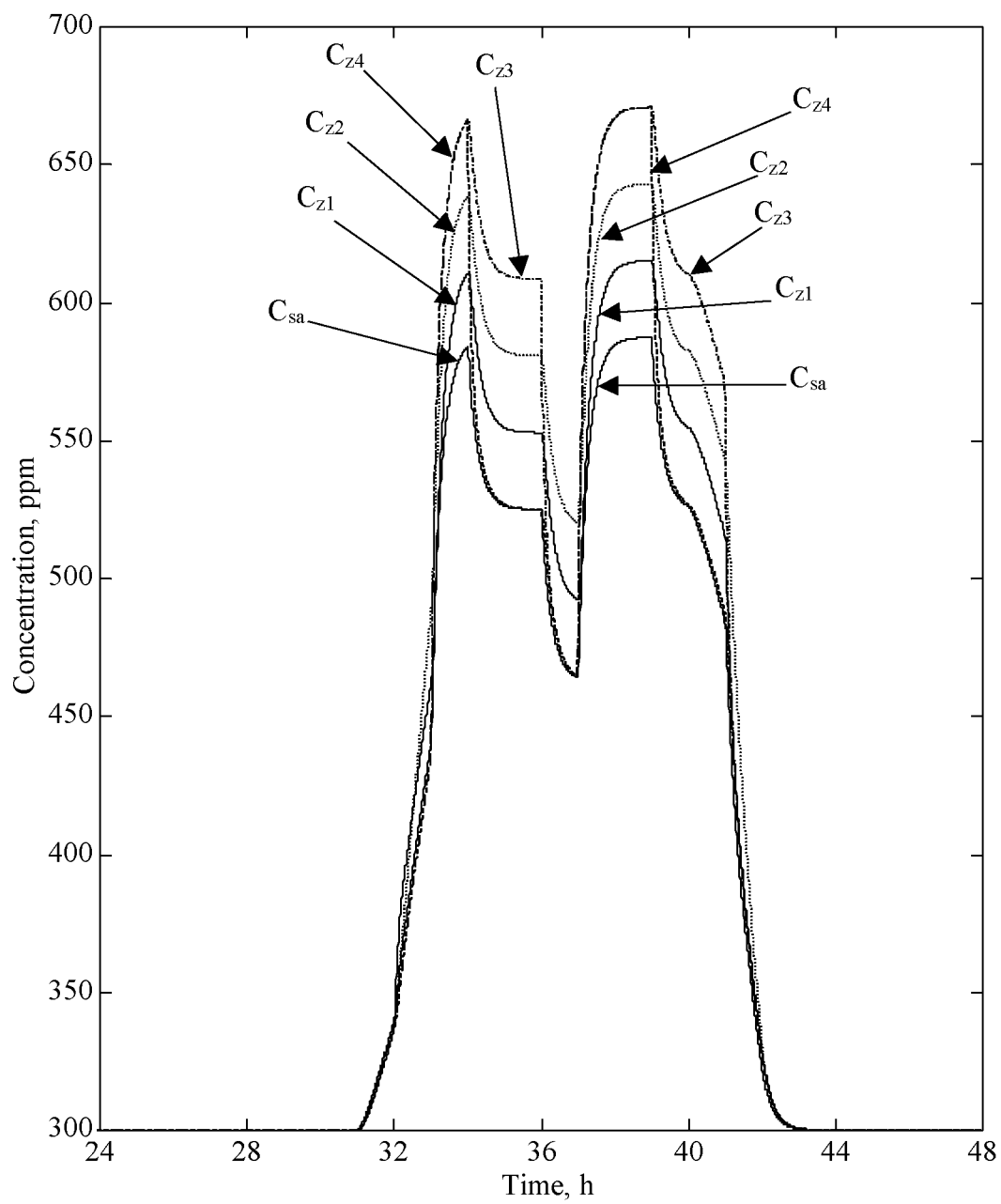


Figure 4.17 Case 12.1 CO₂ distribution throughout zones.

close to or below 600 ppm within 1.34 h. The concentrations falls, becomes steady and then fall again over the lunch hour between $t = 36$ and 37 h. Once work is resumed and the thermal loads are applied again, generation rates increase causing pollutant levels to rise again. Zones 3 and 4 are affected the largest rising above 600 ppm from $t = 37.24$ to 40.38 h. Because of the amount of time where $C_{z,i}$ is above 600 ppm, J_p increases giving a value of 464 ppm-hr.

The value of J_p for Case 12.1 could be considered high. Because the CO_2 levels in the system are not actively controlled or a method for removing CO_2 within a zone, such as an active carbon filter (Hines, 1993) is not present, it is desired to look at an increased outdoor air flow rate through the system. Case 12.2 examines this situation by increasing the outdoor air flow rate where the levels of pollutant are much lower. Test parameters are identical in Case 12.2 to those of Case 12.1, except that outdoor air flow rate is increased to $50,000 \text{ ft}^3/\text{h}$ from $36,000 \text{ ft}^3/\text{h}$. Instead of allowing 25% of outdoor air to mix with the return air, approximately 33% of outdoor air, is mixed with the return air. The outdoor air contains a decreased amount of pollutant which when mixed with the recirculated air provides a decreased overall pollutant level in the supply air.

The results of Case 12.2 are plotted in Figure 4.18 illustrating the concentration levels of each zone versus time. The trend of each curve is similar to those in Figure 4.16, except for the amplitude because the loads applied to each zone are the same as in Case 12.1. By allowing 8% more outdoor air to mix with the return air, the concentrations peak at approximately 600 ppm. J_p for Case 12.2 is found to be 1.44 ppm-h, a reduction of 463.3 ppm-h. However, by increasing the outdoor air flow rate through the system, the performance merits, J_{htg} and J_{clg} , now change for heating and cooling in the AHU and zones. A compromise must be obtained to find an optimal value were all J values are minimized, however, this is beyond the scope of this research study.

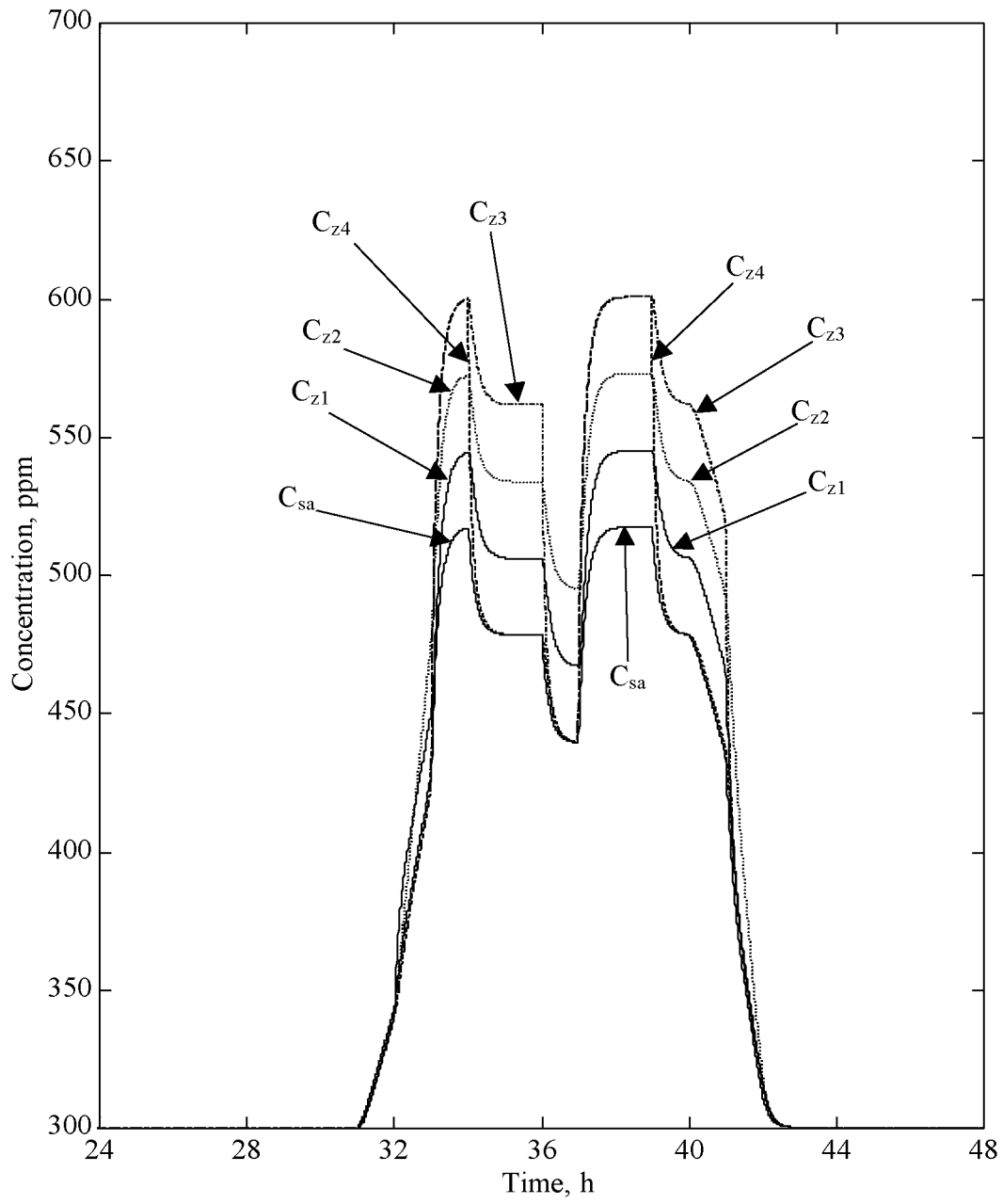


Figure 4.18 Case 12.2 effect of increased outdoor air flow rate.

4.7 Summary

It is shown that thermal control is maintained for both the AHU and zones. The entire system is tested as a whole to show that control is maintained. Results show that, in both the heating and cooling modes, thermal control is maintained when various loads are applied to the system. The addition of FF control shows that FF compliments the feedback control signal, similar results are found by Salsbury (1998).

The IAQ model produced for this study is shown to track pollutant concentration through the system. It is illustrated that increased outdoor air flow rates aides in the reduction of airborne contaminates, resulting in a lower J_p merit value, but with a penalty for the heating and cooling merits, J_{htg} and J_{clg} .

CHAPTER 5

CONCLUSIONS AND RECOMMENDATIONS

5.1 Conclusions

The objectives of this study are (1) to create a model of an HVAC system comprising of an AHU and four zones in an icon-based software package, (2) to couple the multi-zone thermal model with an IAQ model, (3) to introduce a control method to operate the entire system, and (4) to analyze the output from the model given initial conditions and inputs to the system. The motivation of this study comes from the fact that it is attractive to develop such an icon-based model using graphical orientated user interface. EEM's mentioned in Chapter 1 incorporate not only the thermal and IAQ models but the methods of controlling them. Icon-based methods frees the user of solving the coupled equations and allows a visual display of the interconnections from one component to another. In customizing a system, users can add other components, such as IAQ, and combine them with a thermal model, which this study models.

The modules of the components of the AHU and zones are based on equations from statements of the conservation of mass and energy that are applied to a control volume for both the thermal and IAQ models. Once the algebraic and ordinary-differential equations are derived, they are translated into the icon-based software to represent each equation. Modules are built to represent each component of system. Controls are built into the system using a PI controller for the zones and AHU. In addition to the PI controller in the AHU, a FF controller is added to supplement the control signal. To evaluate the performance of the system and to determine which configuration works

better, merit equations are established. These equations give an understanding of performance value for each test case.

Simulations of different scenarios are performed on the zones and AHU to prove that control and thermal setpoint are maintained. Cases 1 and 2 show that control is maintained through each zone. Setpoint temperatures are maintained by the PI controller to adjust the amount of heat supplied by the reheat coils. Cases 3 through 7 show that in either mode, heating or cooling, control and setpoint are maintained. Random temperature fluctuations are then added to the cyclic ambient temperature signal and scheduled loads are applied to each of the zones. Through the different load changes and variable ambient air conditions, control of the system is maintained along with the setpoint temperature of the zones. Cases 8 through 10 use only the PI controller as a feedback control method. Lastly, feedforward control is introduced to compliment the feedback signal. The findings of this system indicate that FF control improves performance of the PI controller by damping disturbances, by producing smaller oscillations, and by allowing the setpoints to be achieved in a shorter period of time. Results in this study are similar, but not as dramatic as those found in by Salsbury (1998).

Using CO₂ as the pollutant in the system, IAQ is simulated. Case 12 investigated the tracking of the pollutant in zones. At anytime when $C_{z,i}$ exceeded the maximum allowable limit, J_p would increase. Though there was not a controlling method to remove the CO₂, the model is successful in tracking the amount of pollutant throughout the system, giving the designer an idea of where build up of pollutant occurs.

5.2 Future work

Future developments and research into this area could include some of the following considerations. Validation of the thermal and IAQ models with experimental data is

necessary in creating a more realistic model. The model could be modified to incorporate a variable air volume (VAV) process. The addition of an auto-tuning module would automatically tune the coefficients of the controllers where optimal values can be achieved more quickly and accurately. The proportional summed derivative (PSD), for maintaining setpoints, controllers could be implemented. Additional control could be added to the outdoor air dampers to allow more or less outdoor air to take advantage of free cooling when possible.

Within Easy5, enhancements can be made on the HC and CC by incorporating a time constant for delay in heating and cooling. Likewise, the wall model representation could be expanded to account for more heat losses and gains for different wall elements. Also, components could be created into a library of Easy5 icons called macros. These macros are user-definable icon function blocks and can be replicated quickly for a multiple system analysis.

To test the system further, different load schedules and setpoint temperatures changes could be examined. To control pollutant levels in the zones, “smarter” controllers could be used to monitor levels of pollutant to allow more outdoor air into the system. Outdoor air could be modeled to be directly fed into a zone instead of traveling through the system before reaching a zone. Along with this, modeling of a passive pollutant absorber could be used to help control levels of CO₂. To obtain a more accurate model of pollutant particle interaction, zones can be divided into an upper and lower region to show with greater accuracy particle or thermal movement within a zone. Expanding even further, a computational fluid dynamics (CFD) subroutine could be used to model zone information such as thermal or IAQ data. These methods would provide more accurate modeling method.

APPENDIX
MASS TO CONCENTRATION CONVERSION

The purpose of this discussion is to derive a relation between the mass of a pollutant and its concentration and to express the conservation of mass of the pollutant in terms of the pollutant concentration. For the discussion, the pollutant is considered as a gas whose properties are described by the ideal gas equation of state and is just one of many gaseous components forming a mixture. The mixture has a temperature of T , has a total pressure of P , and occupies a container with a total volume of V .

There are two methods for describing the state of the pollutant in the mixture. Method 1 is based on the Dalton model (Moran and Shapiro, 1995) and makes use of partial pressures. For this model, the ideal gas equation of state for gaseous component i is expressed by

$$P_i V = m_i R_i T = n_i R_u T \quad (\text{A.1})$$

where, for component i , P_i is the partial pressure, m_i is the mass, n_i is the number of moles, and R_i is the gas constant. R_u is the universal gas constant with a value of $8.313 \text{ kJ/kgmol-K} = 1544 \text{ ft-lb}_f/\text{lbmol-R}$. Now

$$R_u = R_i M_i \quad (\text{A.2})$$

where M_i is the molecular mass of component i . The total pressure of the mixture is the sum of the partial pressures of all components that make up the mixture and is evaluated from

$$P = \sum_{i=1}^J P_i \quad (\text{A.3})$$

where J is the number of components forming the mixture. Method 2 is based on the Amagat model (Moran and Shapiro, 1995) and uses the partial volume. For this model, the ideal gas equation of state is given by

$$P V_i = m_i R_i T = n_i R_u T \quad (\text{A.4})$$

where V_i is the partial volume of the component. The total volume of the mixture is

$$V = \sum_{i=1}^J V_i \quad (\text{A.5})$$

By equating Eqs. (A.1) and (A.4), the relation between partial pressure and volume and total pressure and volume is

$$\frac{P_i}{P} = \frac{V_i}{V} \quad (\text{A.6})$$

With these basic relations, the relation between the mass of a pollutant and its concentration can be examined. Using Eq. (A.4), the pollutant mass is given by

$$m_p = \frac{P V_p M_p}{R_u T} \quad (\text{A.7})$$

where V_p is the volume occupied by the pollutant with molecule mass M_p . Equation (A.7) is multiplied and divided by the mixture volume V to yield

$$m_p = \frac{V_p}{V} \frac{P M_p}{R_u T} V \quad (\text{A.8})$$

The volume ratio in Eq. (A.8) is defined as the concentration expressed as parts per million

$$C = \frac{V_p}{V} 10^6 \quad (\text{A.9})$$

In terms of C, the pollutant mass is given by

$$m_p = \frac{C}{10^6} \frac{P M_p}{R_u T} V \quad (\text{A.10})$$

Equation (A.10) gives the desired relation between the pollutant mass and its concentration.

Applying the conservation of mass equation of the transient form yields

$$\frac{dm_p}{dt} = \dot{m}_{p,i} - \dot{m}_{p,o} + \dot{m}_{gen} \quad (\text{A.11})$$

The relation in Eq. (A.10) is applied to each term in Eq. (A.11) to yield

$$\frac{d}{dt} \left(\frac{C}{10^6} \frac{P M_p}{R_u T} V_z \right) = \left(\frac{C}{10^6} \frac{P M_p}{R_u T} Q_a \right)_i - \left(\frac{C}{10^6} \frac{P M_p}{R_u T} Q_a \right)_o + \frac{G}{10^6} \frac{P M_p}{R_u T} \quad (\text{A.12})$$

where Q_a is the volumetric flow rate of the air and G is the volumetric generation rate in units of ft^3/h per million of the pollutant. The constant common parameters of 10^6 , M_p , and R_u are cancelled in Eq. (A.12). To achieve air flow of the amount found in a zone for HVAC applications, only a small differences in pressure relative to the atmospheric pressure are required. Hence, it is reasonable to assume that the pressures do not vary significantly across the zone so that P can be dropped from Eq. (A.12). Because the temperature variation across a zone is small and absolute temperatures are used, the temperatures in Eq. (A.12) can also be cancelled. After canceling terms, Eq. (A.12) reduces to

$$\frac{dC_z}{dt} = \frac{Q_i C_i - Q_o C_o + G}{V_z} \quad (\text{A.13})$$

Equation (A.13) then serves as the basic relation for further analysis.

REFERENCES

- Ahmed, O., Mitchell, J. W., and Sanford, K. A., "Feedforward-Feedback Controller Using General Regression Neural Network (GRNN) for Laboratory HVAC System: Part I-Pressure Control," *ASHRAE Transactions*, Vol. 104, Pt. 2, 1998a.
- Ahmed, O., Mitchell, J. W., and Sanford, K. A., "Feedforward-Feedback Controller Using General Regression Neural Network (GRNN) for Laboratory HVAC System: Part II-Temperature Control-Cooling," *ASHRAE Transactions*, Vol. 104, Pt. 2, 1998b.
- Ahmed, O., Mitchell, J. W., and Sanford, K. A., "Feedforward-Feedback Controller Using General Regression Neural Network (GRNN) for Laboratory HVAC System: Part III-Temperature Control-Heating," *ASHRAE Transactions*, Vol. 104, Pt. 2, 1998c.
- ASHRAE, *ASHRAE Standard: Ventilation for Acceptable Indoor Air Quality*. Atlanta, 1991.
- ASHRAE, *ASHRAE Handbook: 1989 Fundamentals*, American Society of Heating, Refrigerating and Air Conditioning Engineers, Inc. Atlanta, GA, 1989.
- ASHRAE, *ASHRAE Handbook: 1993 Fundamentals*, American Society of Heating, Refrigerating and Air Conditioning Engineers, Inc. Atlanta, GA, 1993.
- BFRL, <http://www.bfrl.nist.gov/863/iaq.html>, 1999
- Bradley, D., *TRANSYS: Overview*. [Online] Available <http://sel.me.wisc.edu/trnsys/Default.htm>, 1999.
- Building Energy Simulation*, Vol. 19, No. 4, pp. 20-21, Winter 1998
- Bundschuh J. E. and Smith T. F., *Simulation Models For Building-Air Heating and Cooling Components and Systems*, Technical Report: ME-TFS-97-004, Department of Mechanical Engineering, The University of Iowa, Iowa City, 1997.
- Decious, G. M., Park, C., and Kelly, G. E., "A Low-Cost Building/HVAC Emulator", *Heating/Piping/Air Conditioning*, pp. 188-193, January, 1997.
- DOE-Plus, Version 1.1, Innovative Technologies for Energy Management, Berkeley, California, 1992.
- Ellington, K., *SPARK: Building Energy Simulation*. [Online] Available <http://eetd.lbl.gov/btp/spark.html>, January 1999.
- Easy5, Engineering Analysis System, The Boeing Company, Seattle, WA, 1996.

- Fanger, P. O., *The new comfort equation for indoor air quality*, *ASHRAE Journal*, pp. 33-38, October 1989.
- Groszczyk, C. and Smith, T. F., *Development of a Simulation Model for Carbon Dioxide Interaction Using Easy5*, Technical Report: ME-TFS-99-001, Department of Mechanical Engineering, The University of Iowa, Iowa City, Iowa, 1999.
- Grot, R. A., Hodgson, A. T., Daisey, J. M., and Persily, A., "Indoor Air Quality Evaluation of a New Office Building," *ASHRAE Journal*, pp. 16-25, September 1991.
- Hines, A. L., Ghosh, T. K., Loyalka, S. K., and Warder, Jr., R. C., *Indoor Air Quality & Control*, Prentice Hall, New Jersey, 1993.
- Hittle, D.C., "Dynamic Response and Tuning," *Supplement to ASHRAE Journal: Practical Guide to Building Controls*, pp. 40-43, September 1997.
- Kelly, M., "New Directions for the Buildings Division", *Solar Today* Vol. 6, No. 1, pp. 9-10, 1992.
- Knebel, D. E., "Why 55°F," *Engineered Systems*, p. 136, January 1999.
- Knoespal, P. D., Mitchell, J. W., and Beckman, W. A., "Macroscopic Model of Indoor Air Quality and Automatic Control of Ventilation Airflow," *ASHRAE Transactions*, Vol. 97, Pt. 2, pp. 1020-1030, 1991.
- Maple, Maple V Student Version, Maple Waterloo, New York, January 1998.
- Mathematica, A System for Doing Mathematics by Computer, Wolfram Research, Redwood City, California, 1991.
- METASYS, Metasys Product Literature, 1995.
- Metcalf, Ralph, R., *Development Of A Generalized Fan System Simulation For The Building Loads Analysis And System Thermodynamics Program (Blast)*, Department of Mechanical Engineering, University of Illinois, Urbana, Illinois, 1994.
- Nungester, B. and Rhodes, T., "Analysis of flow in a small, multi-zone HVAC systems", *ASHRAE Journal*, pp. 17-23, October 1989.
- Moran, M. J. and Shapiro, H. N., *Fundamentals of Engineering Thermodynamics*, 3rd ed., John Wiley & Sons, New York, 1995.
- Persily, A. K., *Building and Fire Research Laboratory: Indoor Air Quality and Ventilation*, [Online] Available <http://www.bfrl.nist.gov/863/iaq.html>, January 1999.
- Price, B. A. and Smith, T. F., *Description of The Iowa Energy Center Energy Resource Station: Facility Update I*, Technical Report: ME-TFS-98-005, Department of Mechanical Engineering, The University of Iowa, Iowa City, 1998.

- Salsbury, T. I., "A Temperature Controller for VAV Air-Handling Units Based on Simplified Physical Models," *HVAC&R Research*, Vol. 4, No. 3, pp. 265-279, July 1998.
- SIMULINK, Dynamic System Simulation Software. The Math Works, Massachusetts, 1992.
- So, A. T. P., Chan, W. L., Chow, T. T., and Tse, W. L. "A Neural-Network-Based Identifier/Controller For Modern HVAC Control," *ASHRAE Transactions*, Vol. 101, Pt. 2, pp. 14-31, 1994.
- Sparks, L. E., Tichenor, B. A., and White, J. B., *Modeling Individual Exposure from Indoor Sources*. Modeling of Indoor Air Quality and Exposure, Philadelphia, 1993.
- Stanke, D. A., "Ventilation Where It's Needed," *ASHRAE Journal*, pp. 39-47, October 1998.
- TRACE, *TRACE[®] Load Design and Economics Simulation Program*, The Trane Company, La Crosse, Wisconsin, 1990.
- Walsh, P. J., Dudney, C. S., and Copenhaver, E. D., *Indoor Air Quality*, CRC Press Inc., Boca Raton, Florida, 1984.